

THE MEMBRANE, INTERSTITIUM, LYMPHATIC SYSTEM:

A MODEL OF LUNG WATER DYNAMICS

by

David Albert Sebok

B.S.Ch.E. University of Akron
(1976)

M.S.B.E. University of Michigan
(1977)

SUBMITTED TO THE HARVARD-MIT DIVISION OF
HEALTH SCIENCES AND TECHNOLOGY IN PARTIAL
FULFILLMENT OF THE REQUIREMENTS FOR THE
DEGREE OF

DOCTOR OF PHILOSOPHY

in the field of

MEDICAL ENGINEERING

at the

MASSACHUSETTS INSTITUTE OF TECHNOLOGY

September 1983

© David Albert Sebok

The author hereby grants to M.I.T. permission to reproduce and
distribute copies of this thesis document in whole or in part.

Signature of Author _____

September 23, 1983

Certified by _____

Edwin D. Trautman
Thesis Supervisor

Accepted by _____

Prof. Ernest G. Cravalho
Chairman, Division Committee on Graduate Theses

MASSACHUSETTS INSTITUTE
OF TECHNOLOGY

OCT 28 1983

SCHERING-
PLOUGH LIBRARY

LIBRARIES

ABSTRACT

THE MEMBRANE, INTERSTITIUM, LYMPHATIC SYSTEM:

A MODEL OF LUNG WATER DYNAMICS

by

DAVID ALBERT SEBOK

Submitted to the Harvard-MIT Division of Health Sciences and Technology on September 23, 1983 in partial fulfillment of the requirements for the Degree of Doctor of Philosophy in the field of Medical Engineering

ABSTRACT

Pulmonary edema, defined as the existence of an abnormal quantity of water in the lung, is a common and very serious clinical event. Past experiments and models have been directed toward understanding the individual components of the lung related to lung water, particularly the capillary membrane. However, no adequate model exists for characterizing the clinically encountered "integrated lung water system".

This thesis describes the creation of a lung water model which is directed toward aiding the development and interpretation of clinical measurements of the water-dynamics "state" of the lung. In attempting to define this state, we study the steady-state "lung water function curve" (the so-called "Guyton" curve) which presents lung water volume as a function of vascular pressure. This curve describes both the quantity of water present and the propensity for further accumulation at any pressure. A key feature of experimental plots of this function is a two-part behavior in which water volume is relatively insensitive to pressure changes at low pressures and much more sensitive at pressures above a visual "knee".

Our model includes three structural components: the capillary membrane, the interstitial tissue compartment, and the terminal lymphatic, as well as two transported species: water and protein. The model describes the membrane using a Kedem and Katchalsky approach. The other structures are described in terms of linear relationships. Among these are a linear interstitial compliance and a linear, non-sieving lymphatic conductance. The steady-state formulation of this model is reduced to a single, analytical expression which contains three "system" parameters and which predicts a non-linear, two-part system behavior. At

low pressures, lung water is found to be dependent primarily on protein permeability. At high pressures, lung water is dependent primarily on water permeability. The mathematical transition point occurs at a lower pressure than the visual "knee" indicating that the visual "knee" is in a region in which high pressure behavior is beginning to predominate. Non-dimensional forms of the model equation are derived and employed to characterize relationships among variables. We create perturbations of the basic model which explore the effect of the presence of multiple solutes and the importance of our assumption of a lumped interstitium and show that a single solute, lumped model is, for most purposes, adequate.

A time-varying form of the model is derived which shows that water changes are governed by a short time constant and protein changes by a long time constant. This result indicates that the protein protective effect is time dependent. It implies that experimental determinations of the lung water curve are accurate only if sufficient time (greater than 20 minutes) is provided between system perturbations and measurements.

The importance of our model rests with its ability to reasonably describe the experimentally observed non-linear lung water behavior using a model employing only linear descriptions for the interstitium and lymphatic. It also shows that a single "permeability" parameter is not sufficient to characterize the water-dynamics state of the lungs. The model provides a foundation for use in building clinical measurement methods related to lung water.

Thesis Supervisor: Dr. Edwin D. Trautman
Title: Instructor in Anaesthesia (Bioengineering)
Harvard Medical School

ACKNOWLEDGEMENTS

The support, advice, encouragement, and friendship of Dr. Edwin Trautman were major factors in the success of both my graduate studies and doctoral research. His ideas initiated my quest and his wisdom prevented my going too far astray. The reader of this thesis will be the beneficiary of both his prose and organizational skills.

Professor William Deen was an instrumental component of this research through his extensive knowledge of membrane physics and his familiarity with the literature of cellular-level water dynamics as well as his advice. Professors William Siebert and Ascher Shapiro and Dr. Charles Hales also each provided valuable advice and seemed to have the uncanny ability to quickly get to the meat of issues.

I am especially appreciative to the people of the Departments of Biomedical Engineering and Anesthesia at the Massachusetts General Hospital where this work was performed. The philosophy of Dr. Ronald Newbower and Dr. Jeffrey Cooper were vital components of my education and helped to bridge the gap between engineering and medicine in my research. Nancy Herrig, Paul Grimshaw, Peter Martin, and John Edmonson each served the vital function of acting as a sounding board for me in conducting this research. To each of them I offer my deepest thanks. Finally, I would like to thank my brother, Tom, for providing support in the final days of the thesis.

This work was supported by a HST/MEMP Fellowship, by a Whitaker Foundation Fellowship, and through support from the Department of Anesthesia at the Massachusetts General Hospital.

DEDICATION

To my parents,

RUTH AND ALBERT

who provided a rich environment for my growth
and stood by me in my work

TABLE OF CONTENTS

ABSTRACT	2
ACKNOWLEDGEMENTS	4
DEDICATION	5
TABLE OF CONTENTS	6
LIST OF FIGURES	10
LIST OF TABLES	11
NOMENCLATURE	12
1. INTRODUCTION	13
1.1 Significance of Lung Water	14
1.1.1 Clinical relevance	15
1.1.2 Levels of lung water assessment	15
1.2 Relation of Measurements to Models	16
1.2.1 Permeability and measurements	16
1.2.2 Model formulation strategy	17
1.2.3 Steady-state and transient models	18
1.3 Overview of Thesis	19
2. BACKGROUND AND APPLICATIONS	22
2.1 'Role' of Water in the Lungs	22
2.1.1 Respiration: the lung gas exchange function	23
2.1.2 Issues evolving from the lung's exchange function	25
2.2 Lung Structure Relevant to Water Dynamics	26
2.2.1 Macroscopic structure	26
2.2.2 Microscopic structure	27
2.2.3 Definition and role of the functional subunit	30
2.2.3.1 Possible subunit definitions	30
2.2.3.2 Relationship of measurements to subunit behavior	31
2.3 History and Background of Lung Water Analysis	32
2.3.1 History of membrane analysis	32
2.3.2 Considerations of other components	34
2.3.3 Pulmonary edema	35
2.3.3.1 Role of the membrane	36
2.3.3.2 Defensive role of protein	37
2.3.3.3 Defensive role of the interstitium	37
2.3.3.4 Defensive role of the lymphatics	38
2.3.4 Edema classification	39
2.4 Specific Issues in Lung Water Studies	40
2.4.1 The non-linear 'Guyton' curve	40
2.4.2 Lymphatic cannulation	43
2.4.3 Lung water system transient behavior	44
2.5 An Integrated Approach to Lung Water	45
2.5.1 Basic orientation of our model	45
2.5.1.1 Clinical orientation	45
2.5.1.2 Measurement orientation	46

2.5.2	Integrated model approach: the dynamic system	47
2.5.3	Model formulation: an introduction	49
2.6	Summary	49
3.	COMPONENT DESCRIPTIONS AND ASSUMPTIONS	51
3.1	Qualitative Model Description	52
3.1.1	Description of the zero protein permeability system	53
3.1.2	Description of the finite protein permeability system	55
3.2	Membranes	56
3.2.1	The Kedem and Katchalsky membrane model	57
3.2.2	The pore model	61
3.2.3	Choice of membrane model	63
3.2.4	Other membrane considerations	64
3.3	The Interstitium	65
3.3.1	Interstitial architecture	65
3.3.2	Interstitial compliance	66
3.4	The Lymphatics	68
3.4.1	Lymphatic structure	68
3.4.2	Lymphatic function	69
3.4.3	Lymphatic model	70
3.4.4	Lymphatic valves	71
3.5	The Capillary	71
3.6	Other Considerations	73
3.7	Parameter Values	74
3.7.1	Membrane parameters	75
3.7.1.1	Hydraulic permeability	75
3.7.1.2	Protein permeability of the membrane	76
3.7.1.3	Reflection coefficient for protein	78
3.7.2	Interstitial compliance	79
3.7.3	Other model parameters	80
3.7.4	Summary of Parameter Value Selection	82
3.8	Summary	83
4.	THE STEADY-STATE MODEL	84
4.1	Steady State Model Formulation and Mathematical Solution	84
4.1.1	Model formulation	84
4.1.2	Method of characterizing the steady-state model	87
4.2	Mathematical Analysis of Steady-State Model Equations	92
4.2.1	Alternate equation forms	92
4.2.2	Model limits and their characterization	94
4.2.2.1	The transition zone	97
4.2.2.2	The high pressure region	99
4.2.2.3	The low pressure region	100
4.2.2.4	Physical relevance of limiting behavior	101
4.2.2.5	Transition point: alternative definitions	102
4.3	Physiological Analysis of Steady-state Model Equations	103
4.3.1	Graphical presentation of behavior	104
4.3.2	Limiting behavior	107
4.4	Comparison of Model Predictions to Published Data	108
4.4.1	Fluid flux and accumulation	109
4.4.2	Experimental lymphatic concentration	111
4.5	Discussion	113
4.5.1	General behavior: the knee	113

4.5.2 Clinical implications	114
4.5.2.1 The lung water function curve	114
4.5.2.2 The propensity for lung water accumulation	115
4.5.2.3 Component characterization parameters	116
4.5.2.4 "System" parameters	117
4.5.2.5 Implications of lymphatic concentration prediction	119
4.5.3 Assumptions and considerations	119
4.5.4 The Prichard model	121
4.5.5 Measurements and Dimensional analysis	125
4.6 Summary	126
5. MODIFICATIONS TO THE STEADY-STATE MODEL	127
5.1 Multiple Solutes	127
5.2 Multiple Serial Segments	132
5.2.1 Background to the serial segment model	132
5.2.2 Formulation of the two-segment model and its solution	133
5.2.3 Characterizing the two-segment Model	136
5.2.3.1 General behavior of the model	136
5.2.3.2 "Aberrant" behavior of the two-segment model	138
5.2.3.3 Comparison of water behavior of one and two segment models	140
5.2.4 Serial-segment model discussion and implications	143
5.2.4.1 Specific issues	143
5.2.4.2 General issues and conclusions	146
5.3 Summary	146
6. TRANSIENT BEHAVIOR OF THE LUNG WATER SYSTEM	148
6.1 Background and Rationale for Transient Model	148
6.2 Transient Model Formulation and Characterization	149
6.2.1 Model formulation	149
6.2.2 Method for analyzing transient model equations	154
6.2.3 System behavior predicted by the transient model	155
6.3 Limiting Transient Behavior	160
6.3.1 Short-time limiting behavior	161
6.3.2 Late-time limiting behavior	162
6.3.3 Late behavior after a change in C_c	164
6.4 Qualitative Description of Transient Events	165
6.4.1 Qualitative system response to P_c change	165
6.4.2 Qualitative system response to C_c change	166
6.5 Relevant Experimental Data in the Literature	168
6.6 Discussion: Implications of the Transient Model	171
6.6.1 Suitability of lumped system assumption	171
6.6.2 Implications for the steady-state knee	171
6.6.3 Clinical implications	173
6.6.4 Characteristic system parameters	174
6.7 Summary	175
7. GENERAL DISCUSSION AND CONCLUSIONS	176
7.1 Tracers and Lung Water Dynamics	177
7.1.1 The utilization of tracers	178
7.1.1.1 Tracer background	178
7.1.1.2 The use of indices to characterize tracer behavior	179

7.1.1.3 The use of models in tracer index interpretation	179
7.1.2 Indicator-dilution: a tracer utilization example	180
7.1.3 Implications for lung water modeling	181
7.1.3.1 Tracers used to measure component properties	181
7.1.3.2 Use of traces to assess system behavior	181
7.2 Suitability of Our Modeling Approach	183
7.2.1 Alternate Approaches	183
7.2.1.1 The integrated approach	183
7.2.1.2 Model implementation: selection of components	184
7.2.1.3 Model implementation: characterization of components	185
7.3 Suggestions for Future Work	185
7.4 Significant Results and Implications of Our Model	188
7.4.1 General results	188
7.4.2 Clinical relevance	189
7.5 Conclusions	191

LIST OF FIGURES

Figure 2-1:	Interconnected Layers of the Alveolar Capillary Network	29
Figure 2-2:	Guyton's Plot of Lung Water Versus Vascular Pressure	40
Figure 2-3:	Staub's Prediction of the Behavior of the Protein Protective Effect	43
Figure 3-1:	Diagram of Systems Treated in Thought Model	54
Figure 3-2:	Guyton's Concept of Interstitial Compliance	67
Figure 4-1:	Diagram of Lumped Single Solute Model	85
Figure 4-2:	Behavior of the Fluid Flux Equation	91
Figure 4-3:	Behavior of the Lymphatic Concentration Equation	91
Figure 4-4:	Dimensionless Plot of J_v^* versus ΔP^* With C_c^* as a Parameter	95
Figure 4-5:	Dimensionless Plot of θ^* versus ΔP^* With C_c^* as a Parameter	96
Figure 4-6:	Effects of Various Parameters on Steady-State Plots of J_v versus ΔP	105
Figure 4-7:	Effects of Various Parameters on Steady-State Plots of θ versus ΔP	106
Figure 4-8:	Lung Water Function Curve of Gaar [21]	109
Figure 4-9:	Lymphatic Flux versus Capillary Pressure Plot of Parker et al. [67]	110
Figure 4-10:	Example of Lymphatic Cannulation Experimental Results	111
Figure 4-11:	Prichard's Functions for Interstitial Compliance and Lymphatic Conductance	123
Figure 4-12:	Lung Water Behavior Predicted by Prichard Model	124
Figure 5-1:	Diagram of Effect of Presence of Multiple Solutes	131
Figure 5-2:	Diagram of Serial Two Segment Model	134
Figure 5-3:	Diagrammatic Presentation of Behavior of Serial Two Segment Steady-State Model	137
Figure 5-4:	Plots of J_{vm} versus ΔP for the Serial Two-Segment Model	139
Figure 5-5:	Plots of C_i versus ΔP for the Serial Two-Segment Model	141
Figure 6-1:	Diagram of Lung Water Transient Model	151
Figure 6-2:	Transient System Response to a Step Increase in P_c	156
Figure 6-3:	Transient System Response to a Step Increase in C_c	156
Figure 6-4:	Transient System Response to a Step Increase in σ	157
Figure 6-5:	Transient System Response to a Step Increase in ω	157
Figure 6-6:	Transient System Response to a Step Increase in L	158
Figure 6-7:	Transient System Response to a Step Increase in G_1^p	158
Figure 6-8:	Transient System Response to a Step Increase in V_0	159
Figure 6-9:	Transient System Response to a Step Increase in K_1	159
Figure 6-10:	Experimental Time Behavior of Protein-Like Tracers	169
Figure 6-11:	Experimental Transient Behavior of Fluid Flow	170
Figure 6-12:	Transient Behavior of Water Function Curve	173

LIST OF TABLES

Table 3-I:	Experimental Values for L_p	77
Table 3-II:	Experimental Membrane Permeability Values	78
Table 3-III:	Parameter Set Used For Model Testing	82
Table 4-I:	Equations, Parameters, and Variables of Lumped Single Solute Model	88
Table 4-II:	Single Equation Representations of Steady-State Model	89
Table 4-III:	Implicit and Non-Dimensional Forms of the Model	93
Table 5-I:	Essentials of the Two Solute Steady-State Model	129
Table 5-II:	Mathematical Formulation of Serial Two Segment Model	135
Table 5-III:	Total System Behavior of Serial Two Segment Model	142
Table 6-I:	Essentials of the Lung Water Transient Model	152
Table 6-II:	Differential Equations Representing Transient System Behavior	153

NOMENCLATURE

C_c :	Solute concentration in capillary (gm/cm^3)
C_i :	Solute concentration in interstitium (gm/cm^3)
C_l :	Solute concentration in lymphatic (gm/cm^3)
G_i :	Cross-interstitial conductance ($(\text{cm})/(\text{sec-torr})$)
G_l :	Lymphatic conductance ($(\text{cm})/(\text{sec-torr})$)
J_v :	Steady-state fluid flux across interstitium ($(\text{cm}^3)/(\text{sec-cm}^2)$)
J_{vl} :	Fluid flux into lymphatic ($(\text{cm}^3)/(\text{sec-cm}^2)$)
J_{vm} :	Fluid flux across membrane ($(\text{cm}^3)/(\text{sec-cm}^2)$)
J_v^* :	Non-dimensional interstitial "fluid flux"
K_i :	Interstitial compliance ($(\text{cm}^3)/(\text{cm}^2\text{-torr})$)
L_p :	Hydraulic permeability ($(\text{cm})/(\text{sec-torr})$)
\dot{n} :	Steady-state solute flux across interstitium ($(\text{gm})/(\text{sec-cm}^2)$)
\dot{n}_l :	Solute flux into lymphatic ($(\text{gm})/(\text{sec-cm}^2)$)
\dot{n}_m :	Solute flux across membrane ($(\text{gm})/(\text{sec-cm}^2)$)
N_i :	Interstitial solute content (gm/cm^2)
P_c :	Hydrostatic pressure in capillary (torr)
P_i :	Hydrostatic pressure in interstitium (torr)
P_l :	Hydrostatic pressure in lymphatic (torr)
P_c^* :	Non-dimensional capillary "hydrostatic pressure"
Rf :	Gas constant, temperature product ($(\text{torr})/(\text{gm}/\text{cm}^2)$)
V_i :	Interstitial volume (cm^3/cm^2)
V_0 :	Interstitial volume at zero pressure (cm^3/cm^2)
α :	System parameter giving slope of lung water function curve at high pressures ($(\text{cm})/(\text{sec-torr})$)
β :	System parameter giving information about location of the knee ($(\text{cm}^3)/(\text{sec-cm}^2)$)
γ :	System parameter giving information about slope of lung water function curve at low pressures (cm^3/gm)
θ :	Dimensionless capillary solute concentration
θ^* :	Non-dimensional capillary "solute concentration"
π_c :	Osmotic pressure in capillary (torr)
π_i :	Osmotic pressure in interstitium (torr)
π_l :	Osmotic pressure in lymphatic (torr)
σ :	Membrane reflection coefficient
ω :	Membrane solute permeability (cm/sec)

Subscripts:

- 1, 2: Represents compartments one and two in the two compartment model
 Represents solute one and two in multi-solute model

Chapter 1

INTRODUCTION

Lung water is a concern of both clinicians and physiologists. Pulmonary edema, which is defined as an excess accumulation of fluid in the lung [96], is a very common clinical occurrence. It is often a precipitating factor leading to death. Although many clinical measurements are directed toward indirectly assessing the water state of the lung, the concepts of edema and the mechanisms of its production are not well defined. In general, treatment of pulmonary edema is chosen empirically using improved function as the only evaluation criterion.

Lung water has been a concern of physiologists for many years. Various studies have attempted to determine how changes in the rest of the body can affect lung water and, conversely, how lung water affects the body. Implicit in each of these studies is some assessment of the water "state" of the lungs. Yet, nowhere is the concept of lung water state adequately addressed. Further, most of these studies have concerned themselves with individual and isolated components of the lung and not with the integrated system.

The primary objective of this thesis is to propose an integrated model of the lung water system that can serve as a framework for future experimental studies, but more importantly, can provide clinicians with a mental framework for pulmonary edema allowing more rational treatment.

As will be shown, our integrated model provides a number of specific benefits. First, the two-part behavior of the so-called "Guyton curve [29]" which describes the relationship between lung water volume and

pulmonary vascular pressure, can be adequately explained without assigning non-linear behavior to any of the lung's functional components. Further, this curve can be expressed in a non-dimensional form in which the general form of the curve is characterized by a single parameter. Secondly, the integrated approach gives a model in which pulmonary edema can exist in the steady state, something not possible with traditional approaches. It also makes it possible to explore the transient nature of lung water changes. Finally, this approach permits interpretation of the popular pulmonary lymphatic cannulation experiments.

A particular interest of this thesis, in fact the interest that sparked the work, is in the measurements used to characterize the water state of the lungs. It will be shown in the succeeding chapters that the use of a single "permeability" parameter for this purpose, which is the common practice, provides interpretation difficulties and may, in any case, not be sufficient.

1.1 Significance of Lung Water

Water makes up 57% of the human body mass [30]. Its presence is vital for proper body functioning. Yet excessive or improperly distributed water can seriously impair various functions. In no organ is proper regulation of water more important than in the lung whose primary function, gas exchange, depends on the maintenance of a water-free, air-filled compartment.

1.1.1 Clinical relevance

Pulmonary edema is a very common clinical event. Many of the diagnostic tests and procedures involving the lungs have as their goal some assessment of the 'water state' of the lungs [89, 78]. The list of tests related to pulmonary edema includes but is not limited to: chest radiology, blood-gas tests, pulmonary wedge pressure measurements, and various signs elicited from physical examination such as chest palpation, vocal fremitus, and breath sounds.

Pulmonary edema is not a disease entity in itself but rather is a serious complication of a wide range of diseases and syndromes. The list of diseases and agents which have been known to cause pulmonary edema includes: congestive heart failure, proteinuria, endotoxemia, smoke inhalation, oxygen toxicity, and head trauma [77, 89, 92, 11, 44]. It is also a primary finding in adult respiratory distress syndrome. In itself, pulmonary edema is usually not fatal. However, because it almost always appears in a seriously compromised patient, it is often the precipitating factor leading to death.

1.1.2 Levels of lung water assessment

In considering attempts to assess the water state of the lungs, three levels of complexity can be defined. On the simplest level, degradations in the functional performance of the lung are identified and quantified. These may or may not be the result of excess water. The second level is to recognize the existence of excess water and quantify its amount. Finally, the third and most complete level of assessment is to identify and quantify the causes of excess water.

Whether or not the concepts of edema are well defined, people clinically develop pulmonary edema and must be treated. With only a functional assessment of the lung available, treatment can be chosen empirically using improved function as the evaluation criteria. If excess water is known to cause the degraded function, treatment would still be empirical but can then be evaluated in terms of its effect on total lung water. The most rational treatment can only be selected when the probable causes for the excess water are known and can be treated directly.

1.2 Relation of Measurements to Models

1.2.1 Permeability and measurements

Many measurements exist to assess wet lungs. Most try to measure the degree of wetness. Some, however, are geared toward measuring the cause of wetness. As an example, Brigham and Harris use an indicator-dilution injection of labeled urea for such a purpose [9, 35]. The shape of the output concentration curve is said to be related to the "permeability" of the lung toward urea. Further, the lung urea permeability is said to be related to the water state of the lung. The assumption is that, the more permeable the lung is to urea, the more likely it is to be wet.

A possible correlation between the urea indicator-dilution curve and the amount of lung water might be sought using purely empirical methods. However, Brigham believed that a theoretical relationship should exist between urea permeability and total lung water.

The key to this discussion is the word, "permeability". In the common treatment, lung water is considered to be caused by either increased capillary pressure or by increased "permeability". Yet, what

exactly is meant by permeability and how do changes in it affect lung water? Is lung water related to water permeability or to protein permeability or to some combination of both? Perhaps both need to be measured to adequately characterize the lung? Or perhaps urea permeability alone gives sufficient information about both water and protein behavior? Other questions also arise. Can permeability measurements be quantitatively related to lung water? Are the permeability state of the capillary membrane and the capillary pressure all that are needed to exactly characterize the water state of the lungs or are other lung parameters important? These questions can only be fully answered with an understanding of the mechanics of lung water formation, that is, a model of lung water dynamics. The proper interpretation of a lung water measurement cannot be totally clear until the system being measured is understood.

1.2.2 Model formulation strategy

Our goal was to create a model or models which are appropriate for interpreting measurements meant to provide information about water related characteristics of the lung. Such characteristics include extravascular lung water and "permeability". Unfortunately, many factors influence such measurements besides the lung characteristic intended to be measured. Thus, while these measurements can be used to test potential system models, they are of little use in the initial model formulation. Instead, anatomical information must be used to determine the components appropriate for inclusion in the model and functional descriptions of these components must be used for the model's mathematical implementation. However, most of the components are not well described. One must rely on

a critical analysis of available information. In model formulation, it is appropriate to strive for simplicity, as long as the resulting model is capable of describing important system behavior.

The components we chose to incorporate in our model include the capillary, the capillary membrane, the interstitium, and the lymphatic. This choice of components represents a significant departure from traditional models which consider only the capillary membrane in isolation. As will be shown, many of the behavioral features predicted by our model are independent of the exact expressions chosen to characterize the behavior of the components. Nevertheless, whenever possible, the components are described with established component models.

1.2.3 Steady-state and transient models

Almost all discussions of lung water behavior are concerned with steady-state behavior. This parallels much of the rest of medicine in which emphasis is more on the state of the disease than on the time course of events leading to this state. Much of this thesis will be devoted to exploring the steady-state behavior of the lung. However, the transient case will also be examined. There is a natural interest in exploring the time course of edema development. Transient models are also relevant to measurements in that they allow an assessment of when measurements may be said to represent steady-state.

1.3 Overview of Thesis

The approach taken in this thesis is different from previous modeling approaches which concern themselves with water in the lung. We do not intend to place emphasis on any particular measurement or component. Rather, we define and explore the concepts of the "lung water state". In following this different approach, it becomes necessary to use non-traditional ways of looking at the lung and its water. Defining these new concepts represents a key step in the formulation and analysis of our models and therefore represents a significant portion of this thesis.

The chapter by chapter organization of the thesis is as follows. Chapter 2 provides general background on the lung and lung water. We start by taking a thoughtful look at this subject. Why is there water in the lung? What structures are in any way related to lung water? In discussing such structures, we present a general anatomical overview of the lung. A brief history and background for the current approach to lung water studies is then presented. Next, we look at several facets of water behavior which are difficult to address using the current approach.

In Chapter 3, we assemble the parts needed for our integrated approach to lung water modeling. First we show qualitatively the expected behavior produced by assembling the key components into a systems model of lung water dynamics, showing how the interplay of the components can explain certain important behaviors of the lung. Then, by careful examination of available lung structural and functional information, appropriate simple mathematical models for the behavior of these components are chosen. Particular attention is paid to three components: the capillary membrane, the interstitium, and the lymphatic.

Chapter 4 represents the key chapter of this thesis. In it, we assemble the component descriptions to form a simple, mathematical single-solute steady-state model which can be solved analytically. This model is then characterized in various ways. It is used to predict both membrane flux and interstitial protein concentration behavior. Two dimensionless forms are also derived which represent particularly suitable forms for exploring the general character of the model. We then look at limiting behavior and show that three system parameters are sufficient to characterize key behavior of the model. Plots in dimensional form are presented which show how the system responds to changes in various parameters.

In Chapter 5, two perturbations of the basic steady-state model are presented. First, we show how the system might be expected to behave with the presence of multiple permeable solutes. Then we examine our assumption of lumped volumes by exploring a perturbation of our model which represents a first-order approximation to the steady-state behavior of a distributed system.

Chapter 6 uses our approach to treat the transient behavior of the lung water system. We address ourselves to a simple model involving water and only one solute. The interest here is both in determining when conclusions based on a steady-state model might be valid and in examining the time course of water state changes after various system perturbations.

In Chapter 7 we present a general discussion, suggestions for future work, and our conclusions. In particular, some of the issues involved in using measurements to clinically characterize the state of the lung are discussed.

Lung water researchers acknowledge the existence of each of the components discussed in this thesis. But in no case has a systematic attempt been made to assemble the components into a mathematical framework that can be used to describe and quantitate the importance of the interaction of the components. Such an attempt is the goal of this thesis and represents a major part of its significance. Every effort has been made in our modeling efforts to keep the models as simple as possible, to make any parameters that arise in them be physical quantities, and to try to explain system behavior through an understanding of the interactions of system components.

Our success in predicting the lung water behavior experimentally observed by others and in describing expected lung water transient behavior supports our contention that a proper integrated approach can add insights and understanding to the study of lung water dynamics.

Chapter 2

BACKGROUND AND APPLICATIONS

In this chapter we present the background leading up to the creation of our lung water model. There are multiple parts to this effort. First we discuss lung water in very general terms in an attempt to determine the role of water in lung function. Next we present a macroscopic and microscopic anatomical overview of the lung in order to define terms and present a foundation for the rest of the thesis. Here we introduce the concept of the functional subunit. In the third section, the history and background of lung water analysis is presented. First we discuss general background concerning various anatomical components of the lung and then concentrate specifically on pulmonary edema.

In the fourth section we address ourselves to the background for specific issues this thesis will cover. These include the "Guyton" curve, lymphatic cannulation experiments, and lung water transient behavior. Finally we present the features of our modeling approach. This section includes a discussion of our clinical and measurement orientations and material on our integrated approach.

2.1 "Role" of Water in the Lungs

In attempting to understand a process occurring within the lung, one is limited by the observations and measurements that can be made on that organ. These can be conveniently divided into the categories, structural and functional. Structural observations are anatomical and histological

observations made by eye and with the aid of light and electron microscopy, radiography and other imaging aids. Functional measurements include measurements of expired air concentrations of endogenous and exogenous substances, measurements of pressure, measurements of volumes, and any other measurements designed to give information about the functioning of the entire lung or any of its components.

Overall understanding of the lung can also be divided into the categories, structural and functional. These represent parallel paths of research. Each enjoys a certain autonomy from the other. The anatomist may know of the existence of a structure long before its function is known. Similarly, a certain behavior may be observed long before the responsible structure is identified. Of course, these two directions in research complement one another. For example the observance of a certain function can serve to predict the existence of an anatomical structure which can subsequently be sought and found.

In terms of pulmonary edema, structural and functional information represent two different means toward understanding the edema process. We can use these concepts to explore two specific areas pertinent to this thesis: the role of water in the lung and the importance of accurately controlling it.

2.1.1 Respiration: the lung gas-exchange function

The major function of the lung is the exchange of oxygen and carbon dioxide between the blood and the atmosphere. In this sense the lung can be thought of as a "black box" which has inputs and outputs and which in some way processes the inputs. Blood enters through the pulmonary artery and leaves through the pulmonary vein. Air enters cyclically through the

bronchus and leaves through the same path. The blood enters with low oxygen and high carbon dioxide concentrations and leaves with increased oxygen and decreased carbon dioxide content. Air enters with high oxygen and low carbon dioxide concentrations and leaves with decreased oxygen and increased carbon dioxide content. In terms of the rest of the body, the structure assumed by the lung to carry out this exchange task is immaterial so long as the function is accomplished. The exchange efficiency is the only parameter of interest to the rest of the body¹.

If an engineer set out to design a system to carry out the gas exchange function of the lung, the following would be part of his list of design criteria:

1. Only the desired substances are exchanged
2. Maximal exchange surface area
3. Minimal separation between blood and air
4. Minimal blood volume
5. Minimal air flow resistance
6. Minimal blood flow resistance
7. Continuous operation for a period of as great as 100 years

Notice that, except for the water contained in blood, there is no reason why the exchange function requires water to be in the lung. Criteria 1 through 6 can and have been met with artificial exchange units that do not have a "lung water" problem [107].

If we are to explore lung water dynamics, it is necessary to look

¹We neglect here the many metabolic functions of the lung such as the conversion of angiotension I to angiotension II

beyond the exchange function of the lung and consider the actual structure employed by the lung to meet the design criteria. Doing so defines additional functions of the lung. Two of these will be mentioned here.

2.1.2 Issues evolving from the lung's exchange function

The lung provides low blood-flow resistance yet maintains adequate exchange by having many (on the order of 250 million [30]) parallel exchange units in which the actual gas exchange occurs. Blood and air entering the lung are apportioned between these units. This structure imposes two additional design constraints. Firstly, the overall functioning of the lung depends on the distribution uniformity of air and blood to these units [61]. Pathologies that disrupt the match can have serious consequences. Mechanisms must be provided to ensure matched flows. Secondly, such a structure means that space must be provided in the lung for a whole network of branching, non-exchanging air and blood vessels to distribute the blood and air to the exchange units. This space presents a potential area for water accumulation.

Meeting the long-functional life design criteria means that the lung must be capable of withstanding assault and repairing itself after damage [101, 7]. The structure assumed by the lung to carry out this function is that of a living tissue capable of repair and regeneration. It incorporates a defense system consisting of cellular and chemical components which can ward off bacterial, viral, and fungal invasions. Water is vital for the survival of this tissue and its defenses. Yet, a conflict exists. The additional functions imposed on the lung to support this structure can interfere with the fundamental lung exchange function. For example, inflammation, in which a local area is flooded with water,

may provide a better environment for defense against infection yet can locally completely prevent gas exchange.

In summary, water, except for that in the blood, is not essential for gas exchange. In fact, it impedes it. But its presence is essential for maintaining a viable tissue environment. Its control is thus a vital additional function of the lung.

2.2 Lung Structure Relevant to Water Dynamics

Before exploring in more detail the function of lung water control, we first take a structural "tour" of the lung [7, 101, 105]. This will both provide the terminology needed for future discussion and attempt to discern anatomical structures that play a functional role in lung water dynamics.

2.2.1 Macroscopic structure

The normal human has a left and a right lung which are composed of a total of 5 lobes. Each lobe is pierced by a single artery, vein, and bronchus. The bronchus divides an average of 18 times leading finally into a bronchiole. The bronchiole itself divides an additional 4 times and leads into the last non-exchanging duct, the terminal bronchiole. The terminal bronchiole leads to the acinus, the lung's exchange structure. The acinus starts with the respiratory bronchioles which divide into alveolar ducts which in turn finally terminate in the alveolar sacs. In the progression from the respiratory bronchioles to the alveolar sacs, the walls are studded at increasing frequency by air-filled outpouchings called alveoli. The alveolar sac is little more than a tightly packed

cluster of alveoli.

The arteries and veins are closely allied with the air ducts and branch in parallel with them. The artery and vein both lead, after multiple branching, to the smallest blood vessel, the capillary.

In addition to the air and blood transport systems, a third transport system exists, the lymphatic system. Its structure has been much more difficult to define [89]. It is known that it normally contains a plasma-like fluid which flows from small capillary-like vessels into a branched structure that empties into several vessels leaving the lung. These vessels lead to the right or left thoracic duct which eventually empty into the systemic venous system. Functionally the lymphatics play an important role in lung water dynamics which will be discussed in detail chapter 3.

2.2.2 Microscopic structure

We now address the microscopic structure of the lung [73, 23, 97, 39, 22]. There are two key microscopic structural regions [94]. The first is a structure separating adjacent alveoli known as the alveolar septum. It is a thin sheet with a thickness on the order of 10 μm . and is the region where gas exchange occurs. There is within this septum a highly branching capillary network. If gas exchange function was the only concern, it would be most efficient to have each capillary directly adjacent to both alveoli on either side of the septum. EM micrographs of tissue sections actually show that the capillary is in an eccentric position in the septum [19]. On one side, the basement membrane of the alveolar epithelium is fused producing a separation between blood and air of 200-500 \AA . This is known as the "thin" side. The

other side of the capillary has a non-fused basement membrane and usually some tissue space separating it from the alveolar wall. This is known as the "thick" side. The capillaries are surrounded by a space called the perialveolar interstitium which contains water, collagen, elastic fibers, various cells including fibroblasts and leukocytes, and a high density amorphous material made of glucosaminoglycans [72].

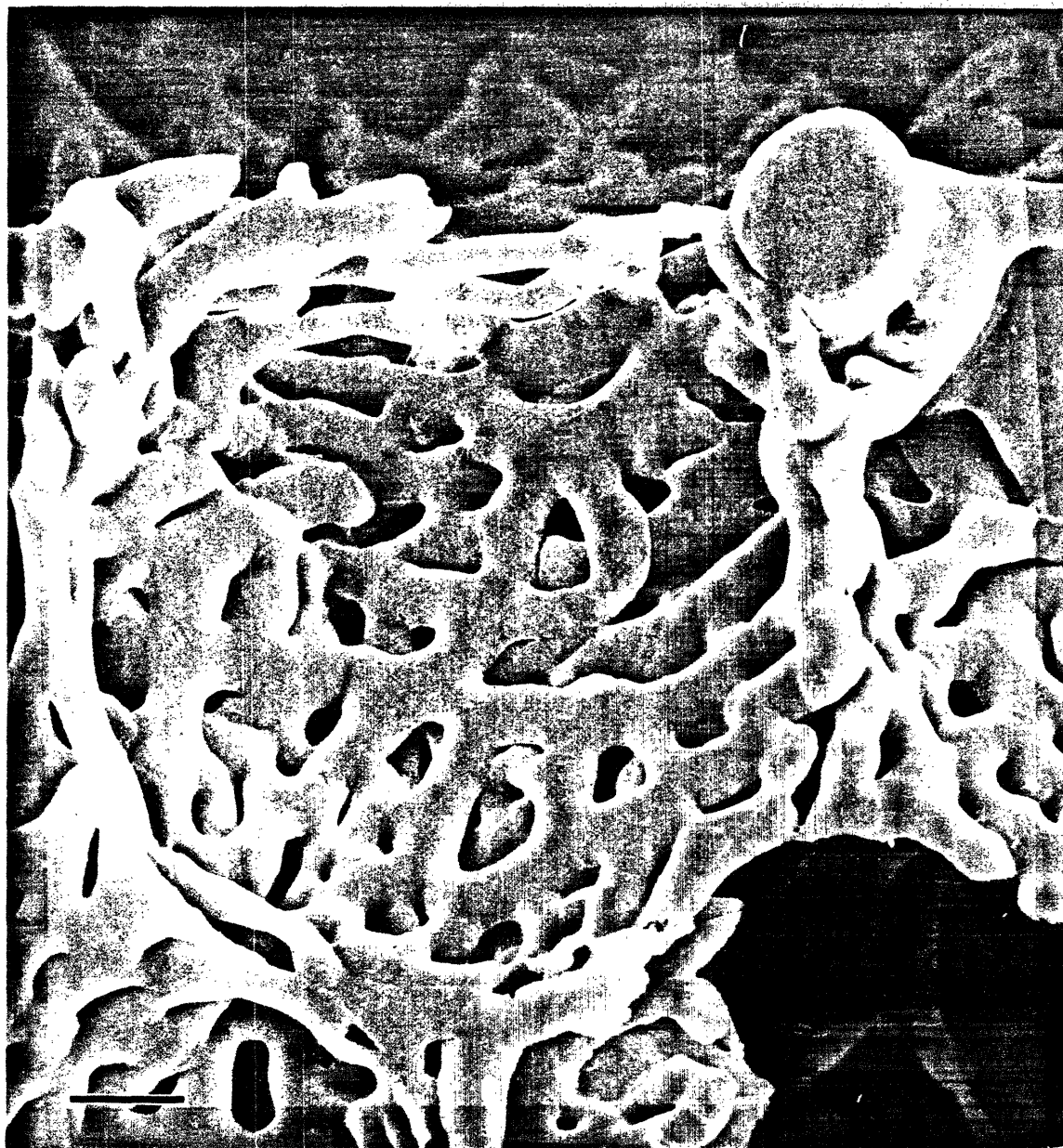
Recent scanning EM micrographs of resin casts of the perialveolar capillary network provide a better sense of its structure and show it actually consists of two highly interconnected layers with each layer tightly adherent to separate sides of the septum. (Figure 2-1) [28] There is so much branching within this network that it is often treated as a sheet of blood interrupted by posts [28, 20].

Vessels delivering blood to the perialveolar network are contained within junctions between three or more septa called septal junctions and in alveoli free areas. These areas are distinguished by the presence of larger vessels, much fewer capillaries, a new type of vessel called a lymphatic, and a much greater amount of interstitial space. These areas are referred to as the "perivascular interstitium". One study has shown the possibility that this space may be structurally separated from the perialveolar interstitium space by cells [25].

The two important points to note from this structural description are: first, a third space besides the blood vessels and airways exists called the interstitium and, secondly, perialveolar interstitium and the perivascular interstitium are quite different.

Figure 2-1: Interconnected Layers of the Alveolar Capillary Network

(from Guntheroth - 1982)



2.2.3 Definition and role of the functional subunit

We will present most of the details of our approach to understanding lung water behavior in the succeeding chapters. But here we present one initial simplification based on anatomical considerations. The lung is like the kidney in that its function is the result of the function of millions of similar subunits. Because of this, it makes sense to try to understand overall function by studying the function of an individual subunit.

2.2.3.1 Possible subunit definitions

At issue here is the definition of the subunit appropriate for this thesis. A common simple definition of a subunit is to consider a single capillary and a cylinder of surrounding tissue as comprising the system. Such a definition was proposed by Krogh [57]. Unfortunately, it neglects the highly branching architecture of the lung capillaries discussed above and does not include structures important to water dynamics such as the lymphatics. Another possibility is to consider the subunit as consisting of a single alveolus and its associated structures. This has the advantage that most of the important structures are included. However the complexity of this structure tends to obscure fundamental principles.

A third approach is to define an idealized subunit whose structure is based on anatomical observations, being careful to include those elements needed to functionally explore lung water dynamics. This is the approach we choose to take. In the succeeding chapter we will explore this functional subunit in great detail, examining each of its constituent components to determine what further simplifying assumptions can be made. For now we just state that the four important structures of our subunit

are the capillary, the capillary membrane, the perialveolar interstitium, and the lymphatic.

2.2.3.2 Relationship of measurements to subunit behavior

There are two issues complicating an approach of exploring overall lung function by studying the behavior of functional subunits. First, the interplay of these subunits is very important to overall function. Secondly, it is very difficult to make direct measurements on the subunits. This last issue deserves some discussion.

Structural measurements provide information on the general ways the fundamental components of the lung are assembled to create the subunits and on the general way these subunits are assembled to create the whole organ. It is possible to make functional measurements on many of the individual components or on analogous structures. For example, many measurements exist on the behavior of artificial membranes [74]. Similarly, many measurements exist to give information about the functional behavior of the entire lung or of individual lobes. The structural information and component functional measurements should permit the creation of reasonable subunit functional models. In fact, this is a primary tenet of this thesis. But the large number of subunits, their heterogeneity, and the existence of structures outside of the subunits greatly complicates any attempt to make detailed conclusions about the behavior of individual subunits based on overall lung measurements. Regarding this thesis, this means that global lung measurements are not very satisfactory for validating the correctness of specific features of our model. Our model must be built using only anatomic information and information on the function of the components. Global measurements are

then only suitable for insuring that the model predicts reasonable general behavior.

2.3 History and Background of Lung Water Analysis

2.3.1 History of membrane analysis

Much of the history of lung water analysis is a history of the study of membranes. Staub gives an interesting review of this history [91]. In the middle 1800's, it was generally accepted that membranes were responsible for restricting the transport of fluids out of the capillary [86]. It was also held that capillary pressure was a moving force for water egress. But a major controversy raged because some of the behavior of water could not be explained using just hydrostatic pressure as a driving force and the membrane as a passive resistance. Many thought that the membrane actively transported water. Ernest Starling carefully analyzed his own and other's experiments and summarized his observations in two landmark articles written in 1894 and 1895 [86, 87]. He showed that, in all cases examined, membrane water movement could be explained by assuming a passive membrane resistance with two types of driving forces, hydrostatic pressure and osmotic pressure, the later being a force created by the difference in solute concentration across the membrane.

With the hydrostatic pressure difference equal and opposite the osmotic pressure difference, there would be no flow. This equilibrium relationship was first published in equation form by Iverson and Johansen in 1929 [43]. Pappenheimer and Soto-Rivera did extensive tests with non-equilibrium conditions and concluded that a linear relation existed between membrane flow and the force imbalance [65]. They expressed this

relation in the form of an equation which is now known as the Starling Equation of fluid flow:

$$J_v = L_p((P_2 - P_1) - (\pi_2 - \pi_1)) \quad (2.1)$$

where P_1 , P_2 , π_1 , and π_2 are the hydrostatic and osmotic pressures respectively on either side of the membrane and L_p , the hydraulic permeability (also widely known as the filtration coefficient), expresses the linear conductance of the membrane. Later work added a coefficient σ before the osmotic pressure term to account for less than maximal osmotic force caused by a membrane leaky to solute.

As people began to consider the flow of protein across the membrane, an expression was developed for protein flow in which two coefficients characterize the membrane, one for its resistance to protein diffusion and one for its resistance to protein convection. Protein transport was considered to be completely independent of water transport [58]. But, in another landmark paper [51], Kedem and Katchalsky pointed out certain inconsistencies that result from the assumption of independence. They used the concepts of an emerging field, non-equilibrium thermodynamics [47, 95, 56] to show that a theoretical relationship exists between an osmotically active solute such as protein and water flow that is independent of the physical model.

The Kedem and Katchalsky approach makes few assumptions about the physical structure of the membrane. It uses thermodynamics to determine what is and what is not physically possible. In 1951, Pappenheimer et al. [66] attempted to assign a physical structure to the membrane to explain its behavior. They used the concept of membrane pores, small

holes that pierce the membrane [74]. This approach has since been made more rigorous using the principles of hydrodynamic theory [18, 84, 3, 1]. It has not been until recently with the use of electron microscopes that anatomical correlates to the pores could be sought [82, 45, 46]. Possible pore structures have been found but they consist of tortuous slits instead of the straight, cylindrical pores normally treated by the pore models.

2.3.2 Considerations of other components

Although the membrane has usually been considered the key component, it has also been recognized that it does not exist in isolation. Krogh in 1919 presented what is now considered the prototypical system structure in which a cylindrical capillary is separated from a concentrically surrounding interstitium by the capillary membrane [57]. Since then, there has been debate on whether the interstitium may possess significant resistance to fluid flow compared to the membrane. Schmidt [81], Apelblat et al. [2], and Salathe and An [79] have each created models examining this possibility.

People involved in lung water dynamics have been interested in the lymphatics for two reasons. First, the lymphatics have been considered to play a part in edema formation. This role will be discussed later. Secondly, they have been treated as providing a 'window on the interstitium', that is, a way of assessing certain interstitial variables such as membrane fluid flow and interstitial protein concentration [76]. Based on the potential of this second application of lymphatics an animal model has been developed. It has been improved and widely disseminated in this country by Staub [88]. This model consists of a surgical preparation involving sheep in which the lymphatic output of the lung is chronically

cannulated and lymph conducted to an exterior collection container. Lung lymph can be collected continuously in awake sheep for long periods of time.

The initial application of this technique was to measure the output of lymph over time after various physiological perturbations. But a second application quickly drew more interest. The lymph collected after inducing edema was found to contain protein, the exact concentration of which depended on the method of inducing the edema. The implications of this observation were extended by fractionating the protein into size groupings and noting that the ratios of concentrations of the various sizes changed depending on the underlying edema etiology. Various researchers felt that protein fluxes provided additional information on the lung water system [5, 37] They reasoned that a system model that could explain the protein fluxes as well as the fluid flux would be a better model of water dynamics than one that considered fluid flux alone. One common form that such models have taken is that of a three pore membrane in which the size and number of each pore is adjusted to best fit the observed lymphatic water and protein fluxes.

2.3.3 Pulmonary edema

Although the broad topic under consideration is lung water dynamics, the interest of clinicians is usually water accumulation, that is, pulmonary edema. This is really more of a clinical term than an exact physiological label. It is not clear exactly what physiological state exists in a person clinically declared to be in pulmonary edema. The edema might represent a transient imbalance of forces or might represent a steady-state condition. The current conception of edema is best

understood by recognizing that the presence of water is considered to be an abnormal condition against which the lung attempts to defend itself. This concept was stated by Robin in his review of pulmonary edema:

"(it is) necessary to keep these spaces persistently dry. This necessity called for an elaborate series of structural and functional adaptations to prevent flooding and preserve the integrity of pulmonary gas exchange. Failure of these mechanisms causes pulmonary edema..."

[77].

The current conception of pulmonary edema is that edema occurs when the lung's defensive mechanisms cannot "cope" with an increase in water flow across the membrane. The defensive mechanisms are considered to be a constant of the system. Thus, edema is approached in terms of identifying circumstances that change fluid flow across the membrane. This view explains the key role of the Starling equation in any quantitative review of the principles of pulmonary edema [89] and in turn explains why one of the two clinical classifications of edema is called capillary leak edema (this will be discussed in more detail later in the next chapter). Pulmonary edema is considered to be a membrane dependent phenomenon.

2.3.3.1 Role of the membrane

The rate at which water leaks into the interstitium is given by the Starling equation, equation (2.1). L_p , the hydraulic permeability, expresses how "leaky" the capillary membrane is to water. This parameter has been of intense interest to researchers and clinicians. Crone [14] presents a good review of the various methods that have been used to measure L_p in living tissue. The work done on artificial membranes has also provided useful information about L_p [74].

The amount of fluid that leaks into the interstitium is also

dependent on the net water driving force (the water chemical potential gradient) existing across the membrane. As noted above, there are actually two forces, hydrostatic pressure and osmotic pressure. Many efforts have been directed toward measuring these two pressures on either side of the membrane. Some of these methods will be detailed in the next chapter. Particularly difficult has been identifying the pressure values in the interstitium. But the classical rationale for these efforts is that, if the pressures are known and the membrane is suitably characterized, the edema process is completely defined.

2.3.3.2 Defensive role of protein

Although many studies consider the membrane forces to be static, the lymph cannulation studies have shown that lymph protein concentration decreases with increasing vascular pressure. Such a concentration change would increase the resorptive forces and tend to counteract the pressure increase. People have thus accepted the possibility that dynamic changes in interstitial protein concentration represent a protective mechanism against interstitial water. Staub discusses this possibility in detail in his recent article [92]. A recognition of the dynamic role of protein necessitates consideration of the system dynamics of protein. The interaction of water and protein fluxes is considered in an important model created by Prichard et al. in 1977 [71]. Their approach will be considered in detail later.

2.3.3.3 Defensive role of the interstitium

The defensive role of the interstitium is considered to be that of a volume which stores any water that crosses the membrane until it can be removed by either the capillary or the lymphatic. Although the presence

of the water is considered abnormal, it is assumed to be better to have water in the interstitium than in the alveoli where it would have a much greater detrimental effect on gas exchange. Staub defines a staged sequence of water accumulation in which water in the interstitium is drawn away from the alveolar vessels, where it might interfere with gas exchange, to the peri-vascular space, which has a large capacity for volume expansion with little detrimental effect [89]. It is only with large excesses that this volume is exceeded and water appears in the alveoli. At that point, the defensive role of the interstitium ceases.

2.3.3.4 Defensive role of the lymphatics

The lymphatics are considered to provide a defensive role in the system by serving as a drainage system. The initial lymphatic vessels appear in the extra-alveolar interstitium where, as stated, lung water is considered to accumulate first.

Probably the best description of the relative roles of the components in the lung water system is given in a article by Taylor [100]. In this article, it is assumed that the net force across the membrane is such as to produce a continual outflow of fluid into the interstitium. A rise in capillary pressure tends to increase the rate of water flux which in turn induces a reaction from the defense mechanisms. Taylor describes the relative contribution of each defense mechanism by assigning to it a pressure which represents its share of the total capillary pressure change. For example, in one case a 10 torr capillary pressure increase divides such as to cause a 4 torr osmotic pressure difference increase, a 3 torr equivalent increase in lymph flow, and a 3 torr equivalent increase in interstitial volume. If interstitial water is considered abnormal, the

10 torr pressure change in this case has been buffered such as to produce only a 3 torr equivalent increase in volume.

2.3.4 Edema classification

It is well accepted that a range of mechanisms exist by which the various diseases and agents can cause pulmonary edema. In an effort to guide better treatment, they are usually divided clinically into two major categories: 1.) high pressure edema which is associated with congestive heart failure and 2.) permeability or "capillary leak" edema exemplified by endotoxemia [92]. This classification system is based on the classical explanation for the mechanisms of edema which, as will be shown in this thesis, may not be accurate.

In this thesis, we define and use the two classifications, "intrinsic edema" and "extrinsic edema", which we find preferable. This is a classification scheme somewhat similar to Brigham's two classifications of primary and secondary edema [11]. We feel it is clinically very natural because a major interest in treatment is in deciding whether the lung edema is caused by a change in the lung itself or by a change external to the lung [78]. Although created from a different premise, this classification system closely parallels the classical one with intrinsic edema analogous to capillary leak edema and extrinsic edema analogous to high pressure edema. Yet it makes no assumptions about the mechanisms of edema and fits much better with the integrated approach to be presented in this thesis. Although our model will describe the mechanisms for extrinsic edema, the primary concern of this thesis will be in elucidating the mechanisms of intrinsic edema toward the goal of providing a quantitative assessment of that state.

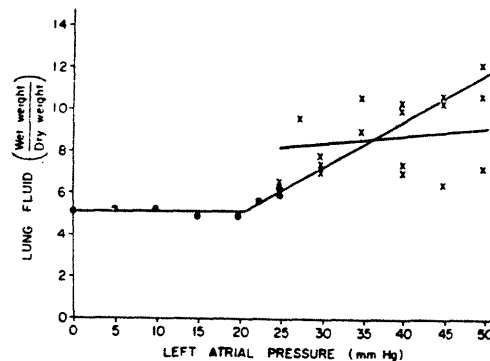
2.4 Specific Issues in Lung Water Studies

After the above discussion, we are in a better position to present the background for specific areas which this thesis will address. A unifying theme is the attempt to characterize the "water state" of the lungs. Such an attempt involves both defining the nature of the lung water system and determining the optimum ways to assess it.

2.4.1 The non-linear "Guyton" curve

In 1959, Guyton and Lindsey published a lung water function curve which was created by elevating left atrial pressure in anesthetized dogs to various levels with an inflatable aortic cuff [29]. The dogs were sacrificed 3 hours after the pressure elevation and the extravascular lung water determined by a wet-to-dry gravimetric measurement. The result is the plot presented in Figure 2-2 in which normalized extravascular lung water is plotted versus left atrial pressure.

Figure 2-2: Guyton's Plot of Lung Water Versus Vascular Pressure
(from Guyton and Lindsey- 1959)



Many dogs did not survive the full 3 hours. These are represented on the plot by x's. Although there is scatter, the general character of the plot

is clear. Subsequent researchers have repeated this work with somewhat cleaner results. These will be presented in the discussion section of chapter 4. The important observation to be made from this plot is that it has a two-part behavior. The amount of water is relatively insensitive to pressure changes until a "knee" in the curve is reached. Above this knee, the sensitivity of water accumulation to pressure changes increases greatly.

If this is indeed the shape of the human lung water function curve, the existence of the knee is clinically very fortuitous. The normal lung vascular pressure is by no means constant. But if the fluctuations are confined to the lower pressure region, these changes will have little effect on the amount of extravascular lung water.

How can the non-linear behavior of this curve be explained? This has been a particularly vexing problem for lung physiologists who use the Starling equation, a linear relation, to describe lung water dynamics. Guyton attempted to circumvent this problem by assuming that the lung normally operates at minimal water volume, a state maintained by a net membrane force normally directed such as to draw water from the interstitium. The knee corresponds to the point at which the capillary pressure is high enough to reverse the direction of the net membrane force. Unfortunately, this approach cannot explain the observed continual net flow of water out of the capillary represented by lymph flow.

The other three explanations of the knee rely on non-linear behavior (saturation) of one of the lung's water defense mechanisms. One of these explanations, called lymphatic saturation, assumes that the lymphatic can remove whatever fluid manages to cross the membrane up to some maximal

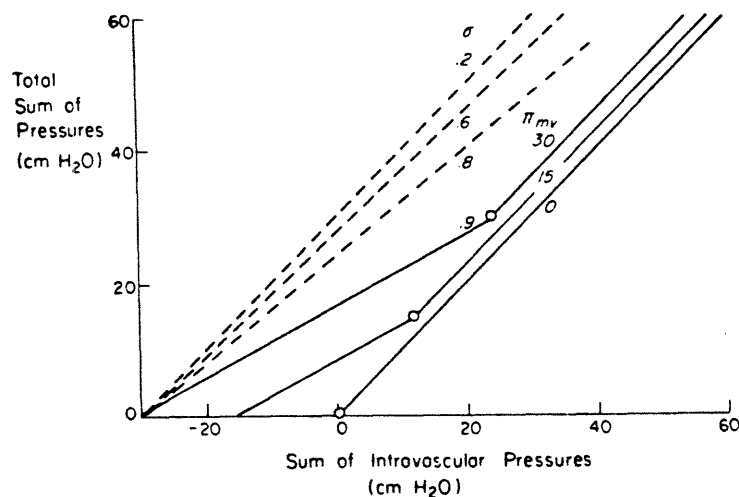
flow rate. Any flow above this maximum will accumulate in the interstitium [10]. This approach has two problems. It assumes a lymphatic saturation phenomena for which there is no good explanation and it predicts an unlimited accumulation of water once saturation is reached. But edema has been noted to exist in the steady-state [17]. Another explanation of the knee relies on the existence of a non-linear compliance. The interstitium is assumed to be relatively non-compliant at pressures below the knee (i.e., volume is insensitive to pressure changes) and compliant above it.

The final explanation proposed for the knee is a saturation of the protein protective effect. This protection is said to occur when interstitial protein concentration drops to counteract capillary pressure increases. A limiting low value of interstitial protein concentration is eventually reached at which point no further protection is possible. Such an explanation is very attractive because it does not rely on the presence of any non-linear component properties.

Staub presented this explanation qualitatively [94] and gave a sketch of how he would expect its effect to depend on membrane parameters which we reproduce in Figure 2-3. In this plot the net Starling force for water flow across the membrane $(P_c - P_i - \sigma\pi_c + \sigma\pi_i)$ is plotted versus the net intravascular force $(P_c - \sigma\pi_c)$. The solid lines represent variations in π_c with a constant σ of 0.9 and the dashed lines represent variations in σ with $\pi_c = 30$. The figure shows that at low pressures, the net Starling force is different from the net intravascular force. This indicates that under these conditions, interstitial osmotic pressure represents a significant though variable system force and that its behavior is very dependent on the system parameters. His article makes no mention of any

Figure 2-3: Staub's Prediction of the Behavior of the Protein Protective Effect

(in Staub - 1980 [94])



mathematical model which served as the basis for his plots.

Prichard et al. [71] also formulated a steady-state model to describe the protective effect of protein. Their's is a quantitative model in which behavior descriptions of the interstitium and the lymphatic are used to create plots of extravascular water versus capillary pressure with L_p , π_c , and membrane protein permeability as parameters. Because this model represents the only model found somewhat similar to ours, we will defer a full discussion of it until our model has been presented in Chapter 4.

2.4.2 Lymphatic cannulation

Although we mentioned the lymphatic cannulation technique above, we did not adequately emphasize its current importance. While suffering several difficulties, it is still considered the best method for gaining insight into the lung water system. The two measurements of importance are lymph flow rate and lymph protein concentration. The flow rate is

used as an indication of impending pulmonary edema. The protein concentration is used either as a qualitative index of lung intrinsic water state or as a quantitative index of capillary membrane state. For this later application, use is made of the hypothesis that, if capillary pressure is raised high enough, lymphatic concentration will reach a limiting low value. A relationship exists correlating this concentration to the membrane parameter, σ $[C_i/C_c = (1-\sigma)/(1+\sigma)]$. σ is then used as the desired index of membrane state.

There are a number of difficulties with this procedure. It is difficult to determine on experimental grounds when limiting behavior is obtained. It is also difficult to determine the effect of falsely assuming limiting behavior. Our lung water model, taking into account as it does the interaction of protein flux, water flux, and capillary pressure, allows us to explore these two issues. We will do so in Chapter 4.

2.4.3 Lung water system transient behavior

The literature is mysteriously quiet about the transient behavior of the lung water system. The only theoretical mention is in models of tracer behavior. But these models do not include equations for water change. The explanation for this lack may possibly be traced back to the use of the Starling equation approach to lung water dynamics. This equation has no term in it for accumulation. It cannot be used by itself to model transient changes. Some authors have come close to formulating a transient model in the form of coupled differential equations describing accumulation of water and protein [6]. But they always simplify these to that of the steady-state case.

We are interested in transient behavior for two reasons. First, all of the experimental data collected to test steady-state models assumes sufficient time for steady-state. The question that arises is: how much time is sufficient for this assumption to hold? Is there important transient behavior that may be occurring over the course of the measurements? Secondly, there is a clinical importance to knowledge of transient behavior because it is useful to understand the time sequencing of the stages of edema pathologies, to understand the delay in effect after treatment, and to understand the length of effectiveness of treatment.

2.5 An Integrated Approach to Lung Water

2.5.1 Basic orientation of our model

Our desire is to create a conceptual framework by which to organize the important details of the above material. That is, we want to create a model of lung water behavior. There are two guiding objectives in this project. First we want the model to be directed, as nearly as possible, towards the clinical perspective. Secondly, we want it to be useful as a tool for interpreting measurements directed toward assessing the water "state" of the lung.

2.5.1.1 Clinical orientation

When clinically considering water dynamics, the concern is usually with water accumulation. Currently, the term, "permeability", is popular as a way of describing the lung. A "high permeability lung" is considered to have more water in it at normal external conditions than a "normal

permeability lung". But, thinking more globally, accumulation may be caused by factors either internal or external to the lung. A change in permeability is only one of many possible changes that may occur within the lung. It simply describes a property of one component of the lung (and does not necessarily describe this component completely at that!). A more general approach based on clinical interests is to speak in terms of the "intrinsic state" of the lung. The goal is to be able to define the state of the lung such that knowing the external conditions, one could estimate extravascular water. In creating a model to do this, we can explore the relative contribution of the various parameters of the lung including those of the capillary membrane.

The shape of the "Guyton" curve is a key feature in the behavior of water in the lung. Describing this shape should thus be a key objective of any clinically oriented model of lung water behavior. We would like to determine the parameters that affect the shape of this curve and the exact nature of these effects. Explaining this shape is a major goal of this thesis.

2.5.1.2 Measurement orientation

Physiologists often speak of measuring the "permeability" of the lung. But what does this term mean? Is there a single "permeability" parameter which can be measured that by itself adequately characterizes the state of the lung?

In terms of physical quantities, when the capillary membrane and water are considered to be the only components of the lung water system, the only system parameter is L_p . Including protein adds at least two more parameters and including the lymphatic adds still more. But what is the

relative significance of each parameter? Which can be ignored? The only way to determine this is to study how they relate to each other in a system model. This was a major reason for the creation of our model. We wanted to determine the number of parameters necessary to characterize the intrinsic state of the lung and to see which of these are most important.

Another issue is that, while L_p etc. may be the physical parameters that determine the state of the system, the parameters actually measured are some complex combination of these. What relationship, for example, does the mean transit time of an indicator-dilution injection of urea have to capillary L_p ? We need an understanding of the system to know how to interpret these clinical and research measurements. An even more intriguing issue is whether some particular clinical measurement might provide a more useful index of lung state than the initial physical parameter which was sought.

2.5.2 Integrated model approach: the dynamic system

While the approach of Taylor described previously explores the relationship between system behavior and component behavior, it suffers from a serious flaw which is symptomatic of the whole field. It effectively considers each component to be independent. The exact division of component contributions in Taylor's work varied depending on the system measured. Yet, his measurements give no hint as to how the relative contributions might change with a given change in conditions. To hope to know this, one needs to understand the interplay of the components.

Traditionally edema is considered in terms of a sequenced chain of events: membrane water flux increases, leading to lymphatic overload,

leading to increased interstitial water, which finally leads to alveolar water and frank clinical edema. But lung water behavior is a dynamic process. Many of the changes occur simultaneously. The components cannot be studied in isolation without some loss of understanding.

The desirability of a dynamic approach is made more clear if one considers the discussion contained earlier in this chapter. The living tissue architecture of the lung makes the presence of water in the interstitium a necessary component. Further, metabolic demands of the interstitial cells necessitate the transport of high molecular weight substances such as glucose from the blood across the capillary membrane into the interstitium. The system must allow this water and substance transport while simultaneously maintaining a suitable environment for gas exchange. Thus, instead of considering lung water to be an unwelcome visitor to be shunned, it is more reasonable to consider the lung to be a system which carefully modulates the amount of water flow, solute flow, and water accumulation. Each of the components plays a role in this modulation process.

There is an inherent attraction to the integrated approach compared with that of considering only the membrane in that the former creates a logical basis by which to evaluate simplifying assumptions. The integrated approach at least considers the potential contribution of each component to the operation of the system rather than ignoring their presence.

2.5.3 Model formulation: an introduction

The intent of this thesis was to create a clinically useful model which could help explain observed phenomena, guide interpretation of measurements, and which could be used to predict clinical behavior under various conditions. With this intent firmly in mind, the model formulation procedure is to:

1. define the system boundaries of the model,
2. determine which physical components to include in the model,
3. determine appropriate descriptions for these components, and
4. decide what assumptions might be reasonable.

We have already partially completed the first step by our previous definition of a functional subunit. We have also partially explored the physical structure of the components of our model. What remains is to develop appropriate mathematical descriptions for each component and search for appropriate assumptions. This will be the task of the next chapter.

2.6 Summary

In the succeeding chapters, we will present a model of lung water dynamics which is particularly oriented toward clinical application and to the interpretation of organ measurements. In the present chapter, we have shown that, while water may impede the gas exchange function of the lung, it is needed to maintain a suitable environment for the living tissue structure of the lung. Water must thus be carefully modulated. We introduced the six important components of the lung water system: water,

protein, the capillary, the capillary membrane, the interstitium, and the lymphatic. Most of the history related to lung water studies was shown to be concentrated on the membrane.

Several specific issues relating to lung water studies were addressed. We presented the "Guyton" curve and indicated that understanding it is a key to understanding water dynamics. We also spoke of the importance of being able to interpret lymphatic cannulation experiments. Finally, it was indicated how little work has been done concerning lung water transient behavior.

In the last part of this chapter, we presented the basic approach of our model. The model should be oriented toward the clinical application of addressing and understanding the concept of the lung water "state". It should also be capable of use in interpreting measurements and guiding the selection of measurements which might help assess the lung water state. This modeling effort differs from previous efforts in its approach of integrating the various components.

Chapter 3

COMPONENT DESCRIPTIONS AND ASSUMPTIONS

In the previous chapter, we presented the material which provides general background and motivation for our modeling efforts. In this chapter, we concentrate more specifically on the model formulation. This is done by examining available information about the functional components of the lung to determine how these components might be best described and what assumptions can be made.

As discussed in the previous chapter, the major components which must be included in our model are: the capillary, the capillary membrane, the interstitium, and the lymphatic. We begin this chapter by presenting two "thought models" which explore qualitatively how the components might interact together in a system. This section represents the key to understanding the basic structure of our model.

A separate section is then devoted to exploring the details of each of the four key components and how they might best be modeled. We discuss the membrane in terms of the two major models which have been created for it: the Kedem and Katchalsky model and the pore model. We discuss the interstitium in terms of its potential roles as a resistance to flow and as a storage element. The lymphatic, the least well understood of the group, is examined with particular emphasis on the lymphatic resistance considering how it might best be modeled. The capillary is discussed with emphasis on its constant nature and on the issue of lumped versus distributed behavior.

We conclude the chapter with a search for appropriate values which to

assign to the parameters that appear in our model. The quantitative formulation and solution of the steady-state form of the model will be presented in the next chapter.

3.1 Qualitative Model Description

In the previous chapter we discussed the concept of the functional subunit and considered the basic components that might make up such a structure. The capillary is the initial source of all lung water. The interstitium is the volume in which lung water accumulates. The capillary membrane separates the water in the capillary from the interstitium. The lymphatic acts as a water drain for the interstitium. We now show how they might interact in an integrated approach to the lung water system.

The general structure used by our models is the following. Water and solutes continually cross the capillary membrane and enter the interstitium. Water flow is driven by a hydrostatic pressure difference and solute concentration differences across the membrane. Solute flows are driven by water flow and solute concentration differences across the membrane. Water entering the interstitium can both change the interstitial pressure and change interstitial solute concentrations (and thus the water and solute driving forces). Likewise, solutes entering the interstitium can change interstitial concentrations and thus change both the water and solute driving forces. Both water and solutes continually leave the interstitium by means of the lymphatic. Water flow is driven by an interstitial-to-lymphatic pressure difference and solute flow occurs by convection. Steady-state exists when water membrane flow equals water lymphatic flow and all solute membrane flows equal the corresponding

solute lymphatic flows. A change in any of the system parameters will cause transient effects based on the interactions of all parts of the system.

3.1.1 Description of the zero protein permeability system

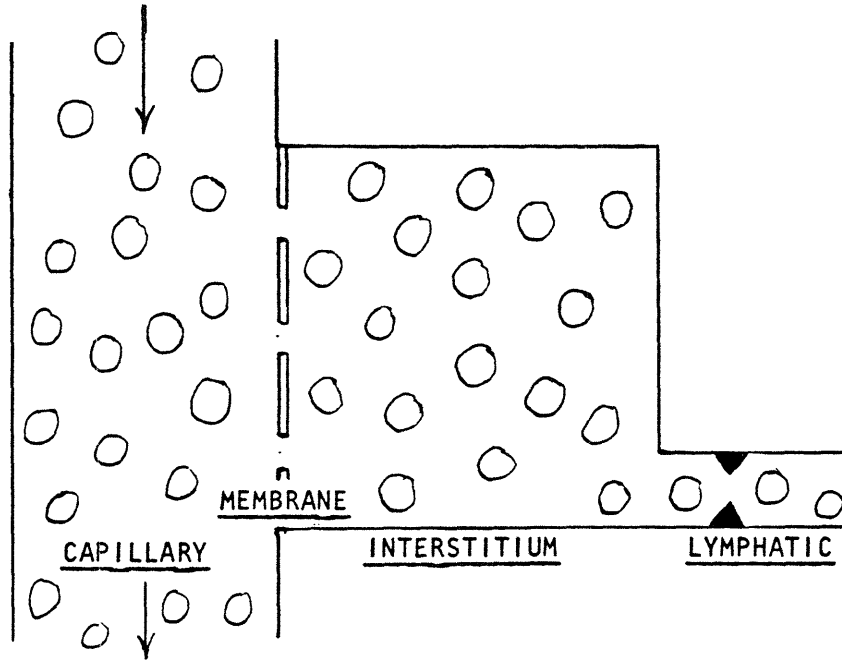
To provide a better qualitative understanding of the interaction of the components in our system, we present the following two "thought" models. Consider the system diagrammed in Figure 3-1a. The interstitium is a well-mixed volume bordered on one side by the capillary membrane and on the other side by the lymphatic. The membrane is permeable to water but completely impermeable to the single solute present, protein. The lymphatic offers a finite resistance to fluid flow but does not sieve protein. The system starts in a state in which capillary, interstitial, and lymphatic pressures are equal, capillary and interstitial protein concentrations are equal, and no flow exists.

What would happen if the capillary pressure is suddenly increased? Water will immediately be driven from the capillary into the interstitium because of the new, non-zero net force across the membrane. This new interstitial water will have the dual effects of raising the interstitial pressure and decreasing the interstitial protein concentration, thus lowering interstitial osmotic pressure. Both these effects will serve to counteract the effect of the increased capillary hydrostatic pressure. However, the increased interstitial hydrostatic pressure will force interstitial fluid containing both water and protein to enter the lymphatic and thus decrease interstitial hydrostatic pressure.

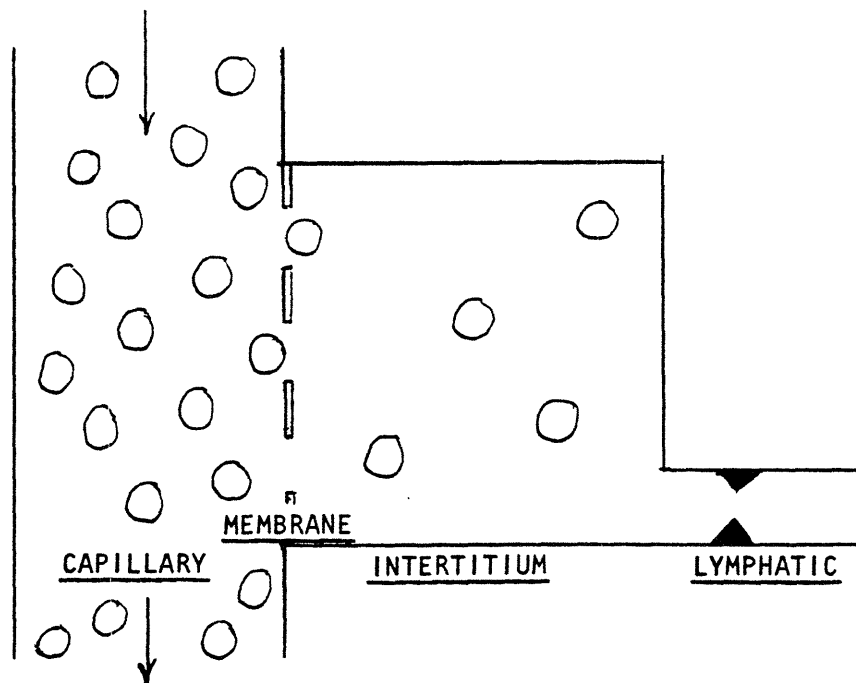
Water will enter the interstitium, water and protein will enter the lymphatic and the protein in the interstitium will be diluted until either

Figure 3-1: Diagram of Systems Treated in Thought Model
Circles represent solute particles

A.) Impermeable Membrane System



B.) Permeable Membrane System



the interstitial protein concentration goes to zero or it decreases sufficiently to cause a decrease in interstitial osmotic pressure exactly equal to the initial increase in capillary hydrostatic pressure. If protein concentration does not go to zero, flow will stop even though capillary pressure is higher than initially. Then the interstitium will be at the same volume and hydrostatic pressure as initially because interstitial pressure must equal lymphatic pressure in order for no lymphatic flow to occur. If protein concentration goes to zero, there will be a steady-state flow of water from the capillary, through the interstitium, into the lymphatic. Interstitial volume is increased because of the increased hydrostatic pressure needed to maintain the lymphatic flow. We have just defined a system having a two-part behavior analogous to the Guyton and Lindsey plot presented in the previous chapter.

3.1.2 Description of the finite protein permeability system

Consider now the system diagrammed in Figure 3-1b. It has the same characteristics as the above system except that it starts at an elevated capillary pressure but is in equilibrium with no flow because osmotic forces exactly counteract hydrostatic forces. What will happen if the membrane suddenly changes so that its protein permeability goes from zero to a finite value? The protein gradient across the membrane will cause protein to diffuse into the interstitium. This flow will change the balance of forces across the membrane and cause water to flow into the interstitium. The water flow into the interstitium will prevent as large a protein rise as might occur otherwise. But the protein gradient would be maintained; protein continues to flow across the membrane. At steady

state, there is now a continual flow of protein and water from the capillary into the lymphatic.

Thus, water follows protein! With no protein permeability, at sufficiently low capillary pressures, there is no water flow. As protein permeability increases, water flow increases (eventually leading to the formation of edema). This is a significant observation. This model shows that water flow, and hence edema, may be related to protein permeability. This dependence does not come out of the Starling equation (which indicates that the only important resistance is given by the hydraulic permeability). It only comes about by including the interstitium and the lymphatic in addition to the capillary membrane in a model of the lung water system.

The conclusion derived from this thought model is that, not only is water flow the result of certain forces, but it can also bring about changes in these same forces. The system is tightly coupled. The steady-state behavior of this system will be explored in a quantitative fashion in the next chapter. With the structure of the thought model providing a framework, we are in a position to examine the individual components of the lung water system and will start with the capillary membrane.

3.2 Membranes

The membrane has been the most extensively studied and modeled component of our system. As we described in the previous chapter, this circumstance is partly the result of attempts to explain water behavior in terms of just the membrane. We concentrate our discussion here on two popular, complementary models of membrane function: the Kedem and

Katchalsky model and the pore model.

3.2.1 The Kedem and Katchalsky membrane model

The importance of the Kedem and Katchalsky approach lies in the fact that, without assuming any particular membrane structure other than that the membrane is homogeneous, it allows selection of the parameters needed to characterize membrane transport behavior [52, 53, 54, 55]. Of additional importance, this approach provides the form of the inter-relationship between water and protein flux across the membrane. It does this using the concepts of thermodynamics. Although no specific physical membrane structure is assumed, many assumptions are involved in the model's derivation. These are often ignored. For this reason, the derivation will be presented here in some detail.

In its simplest form, this model consists of a membrane of unknown physical structure which separates two compartments. Two substances, water and a solute can pass across the membrane. "The starting point of the thermodynamic description of non-equilibrium systems is a calculation of the entropy production during the process" [51]. In this system, the entropy production in compartment 2 is given by:

$$\frac{dS_2}{dt} = \frac{1}{T} (\mu_{w1} - \mu_{w2}) \frac{dN_{w2}}{dt} + \frac{1}{T} (\mu_{s1} - \mu_{s2}) \frac{dN_{s2}}{dt} \quad (3.1)$$

where subscripts 1 and 2 represent the compartments on either side of the membrane, S_2 is the total entropy of compartment 2, μ_w and μ_s are the chemical potentials of water and the solute, and N_{w2} and N_{s2} are the total moles of water and solute within compartment 2. If an ideal solution is assumed, the chemical potential differences can be expressed as:

$$\mu_{w1} - \mu_{w2} = \bar{V}_w \Delta P - RT \Delta \ln(\gamma_w)$$

and:

$$\mu_{s1} - \mu_{s2} = \bar{V}_s \Delta P - RT \Delta \ln(\gamma_s)$$

where \bar{V} is partial molar volume, ΔP is the pressure difference across the membrane and γ is the mole fraction of the component. Using the additional assumptions of a dilute solution and minimal concentration gradient across the membrane allows further simplification:

$$\mu_{w1} - \mu_{w2} = \bar{V}_w \Delta P - RT (\Delta C_s) / \bar{C}_w \quad (3.2)$$

and

$$\mu_{s1} - \mu_{s2} = \bar{V}_s \Delta P - RT (\Delta C_s) / \bar{C}_s \quad (3.3)$$

Here \bar{C}_w and \bar{C}_s represent values averaged over the membrane width. Equation (3.1) may be multiplied by T and normalized to membrane area to produce the dissipation function, ϕ . Substituting equations (3.2) and (3.3) into this function gives:

$$\phi = (\dot{n}_w \bar{V}_w + \dot{n}_s \bar{V}_s) \Delta P + \frac{\dot{n}_s}{\bar{C}_s} - \frac{\dot{n}_w}{\bar{C}_w} RT \Delta C_s \quad (3.4)$$

where \dot{n}_w and \dot{n}_s are molar fluxes of water and solute. Notice that the dissipation function is expressed in terms of the two forces: ΔP and $RT \Delta C_s$ and the two fluxes: $(\dot{n}_w \bar{V}_w + \dot{n}_s \bar{V}_s)$ and $(\dot{n}_s / \bar{C}_s - \dot{n}_w / \bar{C}_w)$. The first of these fluxes, labeled J_{vm} , is the total (water plus solute) volumetric flux across the membrane. The second, labeled J_d , represents the relative velocity of solute to solvent.

The general theory of irreversible thermodynamics assumes that each flux in the system is a function of all forces and the relationship is linear for small forces. Thus for this system:

$$J_{vm} = L_p \Delta P + L_{pD} RT \Delta C_s$$

$$J_d = L_{Dp} \Delta P + L_D RT \Delta C_s$$

where L_p , L_{pD} , L_{Dp} , and L_D are called "phenomenological coefficients". If the law of Onsager is assumed to apply, it requires the equality of the cross coefficients [47, 62]. Thus, with this assumption, $L_{pD} = L_{Dp}$.

These equations are still awkward in that we normally speak of solute flux instead of relative solute velocity. This can be handled by doing a change of basis to give the desired equations:

$$J_{vm} = L_p (\Delta P - \sigma RT \Delta C_s) \quad (3.5)$$

$$\dot{n}_s = J_{vm} \bar{C}_s (1-\sigma) + \omega RT \Delta C_s \quad (3.6)$$

where L_p is the hydraulic permeability, $\sigma = -L_{pd}/L_p$ is termed the reflection coefficient, and $\omega = C_s(L_p L_d - L_{pd}^2)/L_p$ is termed the solute permeability.

Equation (3.5) is the familiar Starling Equation which describes the behavior of water. Equation (3.6) describes the behavior of protein. But notice, and very importantly, the two are coupled. Water flux, J_{vm} , exists as a term in the protein expression. Solute concentration exists as one of the forces in the water expression. σ is in fact a coupling coefficient between the two. It appears in both expressions. This coupling is far too often ignored by others in the field.

An important consequence of this treatment is that, although it gives no information about possible values for the parameters, it does show that just three parameters are sufficient to completely describe this membrane. It must be again stressed that, other than homogeneity, no particular physical structure is assumed for the membrane. In fact, the Kedem and Katchalsky formulation allows the membrane to be more permeable to solute

than to water! (In this case, σ would be negative.)

This approach can be extended to more than one solute. In this case, besides a new parameter for the resistance of movement of each solute through the membrane, there is a coupling coefficient between each solute and water and between any solute pair. But since the solutes are normally dilute, the solute interaction coefficients can be considered to be equal to zero. Thus each new solute will add a solute permeability ω_j , and a reflection coefficient, σ_j .

It must be emphasized that, although the Kedem and Katchalsky model invokes the principles of thermodynamics, there are still many assumptions in its formulation. The important structural assumption is that the membrane is homogeneous. Non-structural assumptions include: the solution is dilute, an ideal solution exists, gradients of pressure and concentration are small, and the law of Onsager holds. Levitt has done experiments with artificial membranes and shown that the Onsager relationship appears to be a reasonable assumption for membranes [62]. The assumption of an ideal, dilute solution is needed to insure a linear relationship between concentration and osmotic pressure. However, protein, our solute of interest, is known to form non-ideal solutions at physiological concentrations [59]. The most critical assumption is that of assuming small force gradients. This is needed to insure that only four parameters are needed to describe the relationship between forces and fluxes (of which two are equal). But both pressure gradients and protein concentration gradients can be relatively large across the membrane.

The term, \bar{C}_s that appears in equation (3.6) is the average of the solute concentration across the membrane. Kedem and Katchalsky considered

this to be a log-mean average. Theoretical derivations of the concentration profile expected within the membrane have shown that a better choice would be a simple arithmetic mean [62]. But the accuracy of this assumption varies depending on the relative fluxes of water and protein across the membrane.

3.2.2 The pore model

The pore model, which is related to the Kedem and Katchalsky model, represents an attempt to attach a physical structure to the membrane. In its simplest form the pore model assumes that the membrane is a flat sheet pierced by multiple, identical, cylindrical pores by which the solvent and a single solute cross the membrane. The two major assumptions are: water can be treated as a continuum and the solute molecules can be treated as a solid spheres. In the presentation given here, it is also assumed that the solutions are very dilute and that the pore is a cylinder perpendicular to the surface of the membrane. For modeling water flow, the pore is treated as a cylindrical conduit with water flow described by the Poiseuille equation. Then the hydraulic permeability is given by:

$$L_p = \frac{D^4 \pi N}{128 \eta L}$$

Here N is the number of pores per membrane surface area, D is the pore diameter, L is the pore length, and η is the fluid viscosity.

The treatment of solute flow is more complex. The solute sphere is assumed to be capable of moving through the pore by either diffusion or convection. The pore imparts three effects which do not exist for solute flow in an infinite medium. First, the solute sphere is not free to flow anywhere within the pore. It is restricted to coming no closer than its

radius to the pore wall. This effect is labeled "steric hindrance". Secondly, the wall adds a certain friction to the diffusion of the sphere. Finally, the effective velocity of the sphere is different from the velocity the fluid would assume at that radial position if the sphere were not there. This effect can be labeled "sphere lag".

Anderson and Quinn [1] have shown how these three effects can be combined with the basic diffusion and convection equations to derive equations for σ and ω :

$$\sigma = 1 - [2(1-\lambda)^2 - (1-\lambda)^4] \bar{G}(\lambda)$$

$$\omega = - \frac{N D^2 RT}{12 N_a d \eta L} (1-\lambda)^2 \bar{K}^{-1}(\lambda)$$

Here λ is the ratio of sphere diameter to pore diameter, N is the number of pores per membrane surface area, D is the pore diameter, d is the particle diameter, N_a is Avogadro's number, L is pore length, and η is the water viscosity. The $(1-\lambda)^2$ factor represents diffusive steric hindrance, the $2(1-\lambda)^2 - (1-\lambda)^4$ factor represents convective steric hindrance, \bar{G} is the sphere lag correction factor, and \bar{K}^{-1} accounts for the diffusive pore wall friction.

Renkin, whose classic formulations are still widely used, assumed that $\bar{G} = \bar{K}^{-1}$, a mistake shown by Anderson and Quinn capable of producing errors in \bar{G} as great as 60%. \bar{G} and \bar{K}^{-1} are both functions of λ . Expressions have been derived for them for small values of λ by assuming that the particle's behavior can be approximated by its behavior at the centerline of the channel:

$$\bar{G} = 1.0 - 0.333\lambda - 0.163\lambda^2$$

$$\bar{K}^{-1} = 1.0 - 2.104\lambda + 2.086\lambda^3 - 1.707\lambda^5 + 0.726\lambda^6$$

However, Anderson and Quinn state that these are only strictly valid for λ less than 0.1. This represents a serious restriction to these equations often not recognized. Protein, to which this approach is often applied, is very close in diameter to those diameters often assigned to pores.

The main advantage of the pore model presented here is that only two parameters, D and N are needed to characterize the membrane. These are experimentally determined indirectly through measurements of any one of the parameters, L_p , ω , and σ . A possible problem with this pore model might seem to be that its hypothetical cylinder-shaped pores do not agree well with the observed tortuous slits of lung capillary membranes. However, the general principles of pore theory are not dependent upon the dependent of straight, cylindrical pores. In fact, hydrodynamic theory is now more thoroughly worked out for parallel plate channels.

3.2.3 Choice of membrane model

As can be seen from the above derivations, neither of the two models can accurately describe the membrane under all conditions. Of the two models, the Kedem and Katchalsky is the more general. With water and protein as the only transported components, it indicates that three parameters are sufficient to characterize the membrane. It gives no information about relationships between these parameters. Each is assumed to be totally independent of the others. The existence of additional solutes will add two new parameters for each solute.

The pore model assumes a physical structure for the membrane and represents a potential subclass of the Kedem and Katchalsky model. It is not a true subclass because, in the forms presented, it represents a differential approach as opposed to the Kedem and Katchalsky's integral

approach. A physical model which was not presented but which represents another subclass of the Kedem and Katchalsky model is the "frictional" or "solute-diffusional" model [51, 85, 3]. In this model, the membrane is treated as a solid structure through which both water and solute diffuse. The integrated form of this model is in fact exactly identical to the Kedem and Katchalsky model.

The pore model provides a relationship between L_p , σ , and ω (this relationship differs from that of the frictional model). It has the major advantage that only two parameters are needed to characterize the membrane. Additional solutes do not entail additional membrane parameters.

In the end, the choice of model to describe the membrane is fairly arbitrary and not very critical. We chose the Kedem and Katchalsky model because of its simplicity and generality. The simplicity is assured by restraining our system to having a single solute. But because of this choice, the behavior predicted by our system model must be interpreted with care. The total independence of the three membrane parameters is probably not a valid assumption even if the pore model does not hold.

3.2.4 Other membrane considerations

There are membrane considerations important to our lung water model besides the membrane model used:

1. There are actually two membrane structures in the lung, the capillary membrane and the alveolar membrane. Although consideration of the alveolar membrane is extremely important when considering alveolar flooding, we are interested in water dynamics before this extreme and will therefore not consider the alveolar membrane.
2. There is controversy over whether "pore stretching" may exist

such that changes in pressure would cause changes in membrane properties [99]. We will consider membrane properties to be constant.

3. There is some evidence that membrane properties might vary along the length of the capillary. We will assume membrane properties to be homogeneous.

3.3 The Interstitium

The interstitium is the second major component of our lung water model. As discussed in the first chapter, it serves no useful purpose in the gas exchange process. Rather, its function is one of housing the feeder vessels for the exchange units and in housing the components needed to support living tissue. It also acts as a repository for water and, for that reason, is of importance to our study.

3.3.1 Interstitial architecture

The lung interstitium is seen structurally to consist of two components, the relatively non-compliant perialveolar space and the relatively compliant perivascular space [89]. Staub includes both spaces in the sequence of pulmonary edema development which he describes [91]. Fluid is said to originate from the capillaries in the perialveolar region from whence it is drawn off into the perivascular region. The nature of the connection between these two compartments is unclear. Gil [25] claims to have observed cells which exist in the regions where the two compartments join which may provide discrete areas of increased resistance. Although the two compartment structure may eventually be found to be significant in terms of lung water behavior, we make an assumption by treating the interstitium in our models as a single

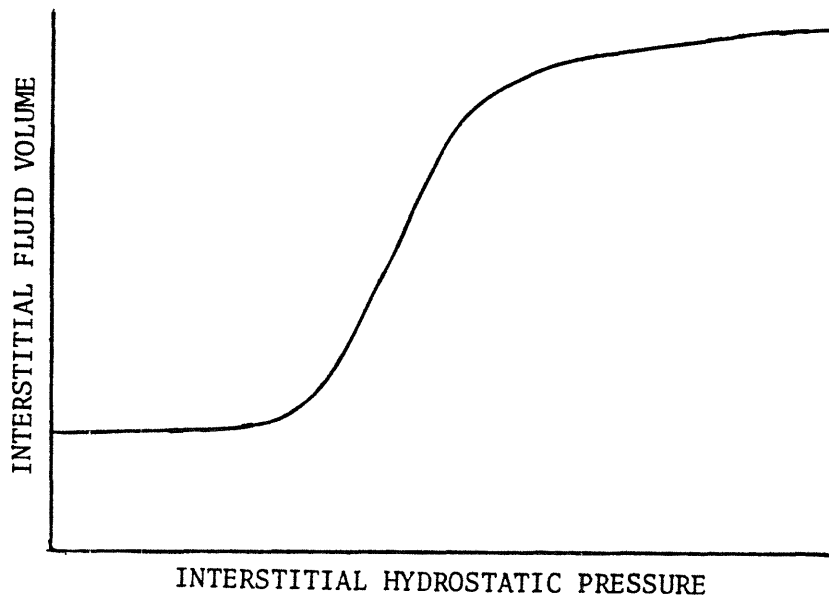
compartment. This approach has precedence in that no existing model treats the perialveolar and perivascular spaces separately. However, some models consider the interstitium as divided into cellular and extracellular compartments. We will neglect this possibility. Doing so does not modify the basic character of our results.

Besides water and cells, the interstitial compartment contains a meshwork consisting of collagen, elastin, and proteoglycans [72]. This meshwork serves as a space expander. Water tends to complex with this network creating an obligatory water volume. The mesh of the network may possibly be fine enough to partially exclude certain large molecules including protein. Thus, the effective volume for protein in the interstitium may be less than the effective volume for water. The network may also serve to impede water and protein flow, protein more than water. The exact magnitude of this effect is not known. In our models, we will assume no interstitial partitioning of protein and no interstitial resistance to water or protein flow. If significant interstitial resistance to flow does exist, its first order effect on our model can be taken into account by considering it in terms of an augmentation of capillary and lymphatic resistances.

3.3.2 Interstitial compliance

Many investigators consider the compliance of the interstitium to be highly non-linear with pressure. Figure 3-2 gives a sketch of a pressure versus volume relationship surmised to exist by Guyton et al. [31] which is based on measurements of interstitial fluid pressure made with implanted capsules. This non-linear compliance has provided a way of explaining the observed non-linear relationship between pulmonary edema

Figure 3-2: Guyton's Concept of Interstitial Compliance
redrawn from Guyton - 1975 [31]



and capillary pressure discussed in the previous chapter. Guyton explains the non-linear behavior as resulting from the presence of the interstitial meshwork [31]. Another very plausible mechanism is that there is a sequential filling of different volumes each with different compliances. Such volumes could be represented physically by the two interstitial compartments and the alveolar compartment.

We do not deny the possibility of the existence of non-linear compliance. Rather, we wish to determine how much of the non-linear system behavior can be attributed to factors other than non-linear compliance. Further, our concern is primarily with behavior in the normal and near normal conditions. Consequently, we choose to use a linear compliance relationship of the form:

$$V_i = V_{\emptyset} + K_i P_i$$

where K_i is the tissue compliance, V_{\emptyset} is the zero pressure volume, and P_i

is the interstitial pressure. This is a reasonable assumption. Should the interstitial compliance turn out to be in fact highly nonlinear, our model's basic structure would not be invalid. Its mathematical implementation would simply be more complex.

3.4 The Lymphatics

There is a long history to the study of the lymphatic [63, 24, 34, 33, 89, 64]. It is considered to play an important role in lung water dynamics. But its exact function is far from clear. Most of our functional understanding comes from inferences derived from structural studies.

3.4.1 Lymphatic structure

The first structural observation is that the lymphatics represent a complex conduit system. Thus a primary function is assumed to be transport. Another anatomical observation is the recognition of nodes distributed along the conductive path. These nodes are filled with lymphocyte cells leading to the conclusion that the lymphatics serve a lung defense function. Our interest is in the transport function.

Anatomically, the smallest lymphatics are seen to exist in the lungs in the perivascular interstitium. No positive evidence exists for any lymphatics in the perialveolar interstitium [63]. The smallest lymphatics have a size on the order of 2 to 5 times that of blood capillaries and are close ended but with "leaky" endothelial junctions with no basement membrane. The small lymphatic capillaries coalesce into larger vessels within the interstitium. One-way valves exist which prevent flow in the

direction of larger to smaller vessels. The large vessels have tight, relatively impermeable walls. As the vessels continue to coalesce, they pass through lymph nodes in which the contents of the lymphatic vessels come into intimate contact with blood. Eventually the lymphatics leave the lung through several routes and join with the systemic venous system.

3.4.2 Lymphatic function

If a lymph vessel leaving the lung is cut, a clear liquid known as lymph with composition similar to plasma (except with lower protein concentration) is exuded. The direction of flow is in accordance with the direction of valves. The conduit function of the lymphatics is thus that of a drainage system. Two issues of importance are:

1. Why does the lung need a second drainage system in addition to the venous system?
2. How does the lymph flow from a region of low hydrostatic pressure thought to exist in the tissue (based on implanted capsule measurements) to the higher pressure existing in the venous system?

The first issue will be considered later. The second issue necessitates the existence of a lymphatic pump [33]. No discrete pump has been anatomically identified. But the existence of valves means that the pumping function could be distributed along the lymphatics. All that is needed is a mechanism to alternately compress the vessels and relax. A strong contender for this function is the normal respiratory excursions of the lung which serve to change the tissue pressure to which the lymphatics are exposed. However, anatomical observations have identified the existence of muscle fibers surrounding certain lymphatics. Some or all of the pumping could be the result of active contraction of this muscle.

That some of the pumping action is active is also evidenced by the observation that anesthesia tends to decrease pumping independent of a decrease in respiratory activity [90].

An important but unanswered question is: what controls the pumping? What physical state does the pump attempt to maintain? Staub argues for the existence of a "skimming pump" [89], that is, a pump which attempts to maintain a constant interstitial pressure. Two control mechanisms could be postulated for such a pump. First one might postulate some neural or mechanical mechanism which is sensitive to interstitial pressure or volume which would directly control the pump. Secondly, a mechanism might be postulated whereby lymph flows through a passive resistance into an actively pumping lymphatic which would pump in proportion to the fluid entering it. In either of these cases, lymph flow is related to interstitial pressure. It should be noted that lymphatic flow increases when edema exists and usually increases with changes that are known to lead to edema.

3.4.3 Lymphatic model

We have assumed that the flow of lymph is linearly related to interstitial pressure and can be modeled by a two part structure. The lymphatic is considered to consist of a passive resistance separating the interstitium from the lymphatic segment which pumping maintains at a constant low pressure. The relation between interstitial pressure and lymphatic flow is thus linear with a gain and an offset :

$$J_{v1} = (P_i - P_1)G_1 = P_i G_1 - J_{v10}$$

where G_1 , the lymphatic conductance, is a measure of lymphatic resistance

and J_{v10} is the lymphatic flux at zero interstitial pressure. The same equation would be obtained with the assumption of no resistance and a pump controlled by sensors of interstitial pressure. But our approach permits lumping of the resistances that are known to exist in the interstitium and lymphatic into a single resistance.

3.4.4 Lymphatic valves

In observations on the lung, there is always finite lymph flow indicating that, at steady-state, water always flows in the direction of interstitium to lymphatic. However, after a system perturbation, the system forces may reverse so as to force water back into the interstitium from the lymphatic. The lymphatic represents a comparatively very small volume. In addition, anatomical one-way valves are commonly observed along its length. Thus, when necessary (and it is only necessary in transient models) we model the lymphatic as having a one-way valve preventing flow reversal.

3.5 The Capillary

The capillaries in skeletal and cardiac muscle are long and thin. Axially distributed models are often applied to their behavior, particularly in terms of tracer dynamics. But, as described in the first chapter, the pulmonary capillaries are arranged in a lattice-like network which may serve to laterally and longitudinally mix their contents. The pulmonary capillaries may thus be better described with a lumped model. There are two issues central to our modeling efforts emanating from the lumped versus distributed controversy: the proper treatment of capillary

solute concentration and the proper treatment of capillary pressure.

Protein continually leaves the capillary across the membrane. If the relative membrane fluxes of water and protein are different, the capillary protein concentration will be different from the arterial supply protein concentration. However, the capillary flow of water and protein is several orders of magnitude greater than membrane flows. In terms of protein concentrations, the capillary can be treated as an infinite, well stirred volume. Such a treatment is not, however, appropriate for indicator-dilution applications of tracers. The issues involved for this case will be discussed in chapter 7.

The question of capillary pressure variations is very intriguing. The classical approach used in lung water behavior analysis has been to consider pressure as uniform throughout the capillary with a value at a fixed fraction of the distance between pulmonary arterial and venous pressures [21]. However, recent micropuncture measurements of capillary pressure by Bhattacharya et al. [4] suggested that a significant pressure drop may occur in pulmonary capillaries. But their measurements were performed on pleural surface capillaries which are much closer in structure to skeletal muscle capillaries. Since our model is highly sensitive to capillary pressure, the possibility of a varying capillary pressure was a major concern. Most of our work considers the capillary to be at a uniform pressure. However, chapter 5 considers in detail the possible effects on steady-state lung water behavior of a non-uniform capillary pressure.

3.6 Other Considerations

In addition to the elements of the pulmonary circulation, there is a system that can deliver systemic blood to parts of the lung, the bronchial circulation. Certain researchers have implicated this system as a source of lung water [70]. This possibility is currently a point of controversy. In our treatment, we will ignore its presence.

In the Kedem and Katchalsky equation for solute flow, the osmotic pressure of the solute is assumed to be a linear function of solute concentration, an assumption known as the van't Hoff relation: $\pi_s = RTC_s$. But measurements on blood show significant deviation from this relation for the blood proteins, albumin and globulin. Pappenheimer gave an empirical cubic relationship between protein concentration and osmotic pressure [59]. This cubic equation can be reasonably well approximated over small ranges of pressures by a quadratic equation [15]. All models reported on in this thesis use the linear protein relationship. This is in keeping with the spirit of the rest of the thesis in which the various components are described with linear models. Describing protein behavior with a quadratic or cubic equation greatly complicates the model without adding any significant new insights.

There are two principle osmotically active solutes in plasma: albumin and globulin. Albumin is a protein of molecular weight of approximately 60,000. Globulin is the label for a group of proteins which range in molecular weight from 90,000 to 1,300,000. According to Landis and Pappenheimer, albumin contributes 2/3 of the total plasma osmotic pressure and globulin contributes the other 1/3 [59]. Many lump albumin and globulin together into a "total plasma protein" parameter. However,

globulin traverses the membrane much more poorly than albumin. Parker et al. measured plasma-to-lymph protein ratios for albumin of 0.8 at baseline conditions as compared to globulin ratios of 0.4 [67]. Thus it is not appropriate to treat albumin and globulin as having the same permeability.

The situation will be handled in this thesis by generally considering albumin to be the only permeable protein. Globulin is assumed to be restricted to the capillary having a permeability of zero and a reflection coefficient of one. When exploring the general system behavior predicted by our model, the presence of globulin will be ignored. However, when our model's predictions are to be compared with experimental data, the existence of globulin can be accounted for by combining plasma globulin osmotic pressure with capillary hydrostatic pressure to create an "effective" capillary hydrostatic pressure:

$$P_{c,\text{effective}} = P_c - \pi_{\text{globulin}}$$

We will treat the possibility of a permeable globulin in Chapter 5.

3.7 Parameter Values

After deriving the quantitative expression of our model and mathematically characterizing it, we will of course be interested in relating it to the physical situation existing in the lung. For this purpose, we need a reasonable set of parameter values. A published set would be preferred. Unfortunately, no such set exists. There is no sound review that simultaneously considers the values of the various parameter characterizing the lung water system. Katz [50] prepared a table of parameter values which he used in testing a model he created of water dynamics. Unfortunately, the methods he used for arriving at these values

are not very well detailed [48, 49].

Many isolated experiments have been done to identify various system parameter values, particularly those having to do with the membrane. However, it is difficult to pool these results because of differences in the experiments, differences in the organs tested, differences in the tracers used, and differences in the way the data is normalized. Nevertheless, we have collected what we consider to be a reasonable set of parameter values which will be employed in the subsequent chapters.

3.7.1 Membrane parameters

3.7.1.1 Hydraulic permeability

The hydraulic permeability of the membrane, L_p , is the parameter for which the most information exists. Unfortunately, few measurements of L_p for lung capillary exist. Many direct and indirect measurements of L_p do exist, however, for mesentery, skeletal muscle, kidney, and of course, a whole host of artificial membranes.

One problem that exists in comparing the values are that there is at least three ways of normalizing the results: per gram of tissue, per kilogram of body weight, and per surface area of membrane. Certain assumptions have to be made to permit the conversions. We assumed that there are 100 cm^2 of capillary surface area to every gram of tissue [66, 13, 30, 27].

Pappenheimer et al. reviewed the work of a number of people and presented the "relative filtration constant" for frog mesentery, mammalian muscle, mammalian kidney, and a collodion membrane [66]. The mesentery,

muscle, and collodion membrane were analyzed using direct measurements. The kidney filtration constant was derived from estimates of the membrane forces. Taylor et al. derived a hydraulic permeability by measuring lymph output from both cat ilium and dog hindpaw and making certain estimates of membrane forces [98]. Erdmann et al. used similar techniques to measure L_p in the lungs of intact sheep [17]. Cobbold et al. measured L_p in cat paw muscle using isogravimetric techniques [12]. Finally, Smaje et al. measured L_p directly in exteriorized cremaster capillaries using a micro-occlusion technique [83].

Table 3-1 presents the various values for L_p converted to units of cm/sec (that is, normalized to cm^2 capillary surface area). The values range from 1.3×10^{-8} to 1.0×10^{-6} (cm^3)/(cm^2 sec torr), two orders of magnitude. The lung is considered to be much less permeable than other organs. We thus select as our normal value a value near the small end of the range: $L_p = 2.0 \times 10^{-8}$ (cm^3)/(cm^2 sec torr).

3.7.1.2 Protein permeability of the membrane

We selected albumin, a plasma protein responsible for most of the osmotic pressure gradient across the membrane, as the solute in our model. The two major ways of obtaining solute permeability values have been the indicator-dilution and the lymphatic cannulation procedures [98]. Other methods include the osmotic transient method, the single injection, residue detection method, the tissue clearance method, and the tissue uptake method [38].

Perl presents a compartmental analysis of the data of Lassen et al. [60] who followed whole body dynamics after the injection of ^{131}I -albumin [69]. The result is a whole body, non-liver tissue albumin

Table 3-I: Experimental Values for L_p

SOURCE	L_p $\frac{\text{cm}}{\text{sec-torr}}$
Pappenheimer [66]:	
Frog Mesentery	7.6×10^{-7}
Mammalian Muscle	2.5×10^{-8}
Mammalian Kidney	4.2×10^{-6} - 2.7×10^{-7}
Colloidion Membrane*	1.4×10^{-4}
Taylor [98]:	
Cat Ilium	6.8×10^{-7} - 1.4×10^{-7}
Dog Hindpaw	4.3×10^{-8} - 5.0×10^{-7}
Erdmann [17]:	
Sheep Lung	1.7×10^{-8} - 3.4×10^{-8}
Cobbold [12]:	
Cat Skeletal Muscle	1.7×10^{-8} - 2.5×10^{-8}
Smaje [83]:	
Rat Cremaster Muscle	1.4×10^{-8}

*This artificial membrane listed for comparison only

permeability value of 1.8×10^{-8} cm/sec. A similar analysis of data from dog paw muscle leads to a value of $\omega = 1.0 \times 10^{-8}$ cm/sec.

Taylor, Granger, and Brace [98] calculated the protein permeability of cat ilium, dog hindpaw, and dog lung using lymph collection experiments in which lymph was collected at two different vascular pressures. Parker et al. [67] obtained protein permeabilities in the dog lung by collecting and fractionating lung lymph and using analysis techniques described by Taylor [98] and Renkin [75].

The values for ω obtained by the various authors are presented in tabular form in Table 3-II. The values for protein fall within the range

Table 3-II: Experimental Membrane Permeability Values

SOURCE	ω $\frac{\text{cm}}{\text{sec}}$
Perl [69]	
Whole-Body Non-liver Albumin	1.8×10^{-8}
Dog Hindpaw muscle Albumin	1.0×10^{-8}
Taylor [98]	
Cat Ileum Protein	1.15×10^{-8} - 7.0×10^{-8}
Dog Hindpaw Protein	2.7×10^{-9} - 7.5×10^{-9}
Dog Lung Protein	6.96×10^{-9}
Parker [67]	
Dog Lung Total Protein	1.3×10^{-9} - 1.9×10^{-9}
Dog Lung Albumin	1.8×10^{-9} - 3.6×10^{-9}
Dog Lung Sixth Fraction	3.8×10^{-10} - 4.6×10^{-10}

of 3.8×10^{-10} to 1.1×10^{-7} , a range of 2 1/2 orders of magnitude. The values obtained for the lung all dwell at the smaller end of this range. Based on this information, we choose our "normal" value of permeability as being $\omega = 5.0 \times 10^{-9}$ cm/sec.

3.7.1.3 Reflection coefficient for protein

This parameter is physically limited to being in the range of 0 to 1. It is often assumed to be 1 because of the relative impermeability of the membrane to protein. Taylor et al. [98] derive a value of 0.73 based on their analysis technique and lung lymph data. Parker et al. [67] derive values ranging from 0.54 to 1 for the various protein fractions in dog lung lymph. Katz [50] uses values of 0.48, 0.66, and 0.81 in his model.

Staub in his review article, describes a value of 0.9 as being normal in the human lung [94]. We will assume a reasonable value to be $\sigma=0.85$.

3.7.2 Interstitial compliance

In trying to assess V_{ij} and K_i , an obvious approach would be to measure volume changes with changes in interstitial pressure. Unfortunately, the methods that exist for measuring interstitial pressure, the fibrous wick, the perforated microsphere, and the micropipette, each suffer from two problems: the measurement modifies the system being measured and it is not clear exactly what is being measured [32]. The problem is with the small size ($< 20\mu\text{m}$ wide) and inaccessibility of the true perialveolar interstitium. The technology is improving but for now we consider it more prudent to rely on indirect determinations of compliance in which interstitial volume is measured as a function of capillary or pulmonary artery pressure. The implications of this will be discussed in chapter 7.

The major problem with the indirect measurements of compliance has been developing an experimental system in which stable elevations of volume can be produced. Erdmann and associates appeared to have success in this endeavor as reported in their 1975 article [17]. They produced stable edema in sheep with chronically cannulated lung lymphatics using a left atrial balloon. The sheep were sacrificed in the edematous state and the lung water determined by gravimetric assay. A range of left atrial pressure elevations was produced and compared to a set of baseline pressure sheep. We utilized their data by selecting the data from four sheep which had pressures elevated to values in the range of 40-45 cmH_2O . We also used the data from four baseline sheep (average pressure=20). We

used the average animal figures given in their article of 72.2 gm dry lung weight and 505 gm wet weight to calculate the following values:

BASELINE:

$$V_i = 2.64 \times 10^{-4} \text{ cm}^3/\text{cm}^2 \quad \text{at} \quad P_c = 15 \text{ torr}$$

ELEVATED:

$$V_i = 3.03 \times 10^{-4} \text{ cm}^3/\text{cm}^2 \quad \text{at} \quad P_c = 30 \text{ torr}$$

Our model required the parameters, V_{θ} and K_i , which are defined in terms of the interstitial pressure. The conversion was performed by solving our model steady-state model of the next chapter for P_i at P_c values of 15 and 30 torr, and then using the corresponding Erdmann values of V_i to solve for V_{θ} and K_i . But notice that tissue compliance values derived using this procedure are only valid in solutions using the same model and parameter set under which they were derived.

3.7.3 Other model parameters

We used the van't Hoff equation to provide a simple linear relationship between solute concentration and solute osmotic pressure:

$$\pi = RT C$$

In our model, concentration is given in terms of solute mass. The molecular weight of the solute (albumin) is used to convert the molar based gas constant to a mass-based parameter. Using $R=62400$ (torr cm^3)/(gm mole $^{\circ}\text{K}$) [102] and assuming an albumin molecular weight of 60000 [16] and a temperature of 310°K gives an 'RT' value in terms of gram-mass of 322 (torr)/(gm/ cm^3).

The value used for normal plasma albumin concentration was 0.04

gm/cm³ and was obtained from Diem [16]. Globulin plasma osmotic pressure was calculated using the above values for RT and albumin concentration to calculate an plasma albumin osmotic pressure of 12.9 torr and then assuming a globulin osmotic pressure of one half of this [59] to give a value of 6.4 torr. The value used for normal capillary hydrostatic pressure was obtained by using the Gaar relation [21] in which:

$$P_c = P_{1a} + 0.4(P_{pa} - P_{1a}) \quad (3.7)$$

and using normal pulmonary artery and left atrial pressures of 15 torr and 9 torr [42] to derive an approximate value of 12 torr.

The parameters for which the least amount of information exists are P_1 and G_1 . The interstitium is usually thought to be either at or below atmospheric pressure [89]. In our passive model approach, the pressure in the lymphatic must be even below this. Since P_c and P_1 always appear as a pair in our model, we choose to assign a value of 0 torr to P_1 with the realization that the effect of different values can be studied by examining the effect of changing P_c . G_1 also usually occurs in combination with another parameter, L_p . But it is important to know its value in order to interpret our fluid flux results in terms of interstitial fluid volume. A high lymphatic conductance would mean an interstitium very sensitive to variations in interstitial pressure. A low lymphatic conductance would produce a system with high interstitial pressure, an occurrence which is not born out by experimental information. We decided to select as our lymphatic conductance a relatively high value which was arbitrarily selected to be 10 times the membrane hydraulic permeability. Thus $G_1 = 2.0 \times 10^{-7}$ (cm)/(sec torr).

3.7.4 Summary of Parameter Value Selection

The complete list of the set of normal parameter values selected for illustrating our model is contained in Table 3-III.

Table 3-III: Parameter Set Used For Model Testing

$L_p = 2.0 \times 10^{-8}$ (cm)/(sec torr)	$\omega = 5.0 \times 10^{-9}$ (cm)/(sec)
$\sigma = 0.85$	$G_1 = 2.0 \times 10^{-7}$ (cm)/(sec torr)
$RT = 322$ (torr)/(gm/cm ³)	$C_c = 0.04$ (gm/cm ³)
$P_c = 12$ torr	$P_1 = 0$ torr
$\pi_{c, \text{globulin}} = 6.4$ torr	
$V_i = 2.64 \times 10^{-4}$ (cm ³)/(cm ²) at $P_c = 15$ torr	
$= 3.03 \times 10^{-4}$ at $P_c = 30$	

NOTE: All extrinsic parameters are in terms of 1 cm²
capillary membrane surface area

3.8 Summary

In this chapter we have presented the details needed to formulate and test our model. We first presented two qualitative "thought models" which demonstrate the possible interaction of the model components and show the importance of protein permeability to water flux. We showed that the membrane behavior can be reasonably described using the Kedem and Katchalsky equations and discussed the assumptions involved in their use. The interstitium was shown to be reasonably modeled as a single compartment with a linear compliance. We explained our rationale for modeling the lymphatic and its pump with a linear, passive resistance separating the interstitium from a fixed-pressure lymphatic segment. Finally, the reasoning was given for treating the capillary as an infinite, fixed-pressure compartment. The many other assumptions inherent in our model were also listed.

We ended the chapter with a presentation and discussion of appropriate values for the physical parameters in our model. In the next chapter, we present the mathematical formulation of the steady-state form of our model and characterize its behavior.

Chapter 4

THE STEADY-STATE MODEL

In the previous chapter, we presented the details and assumptions needed to assemble our model. In this chapter, we complete the assembly for the steady-state case. The model is rigorously formulated and reduced to a set of equations. These equations are then analyzed mathematically and physiologically.

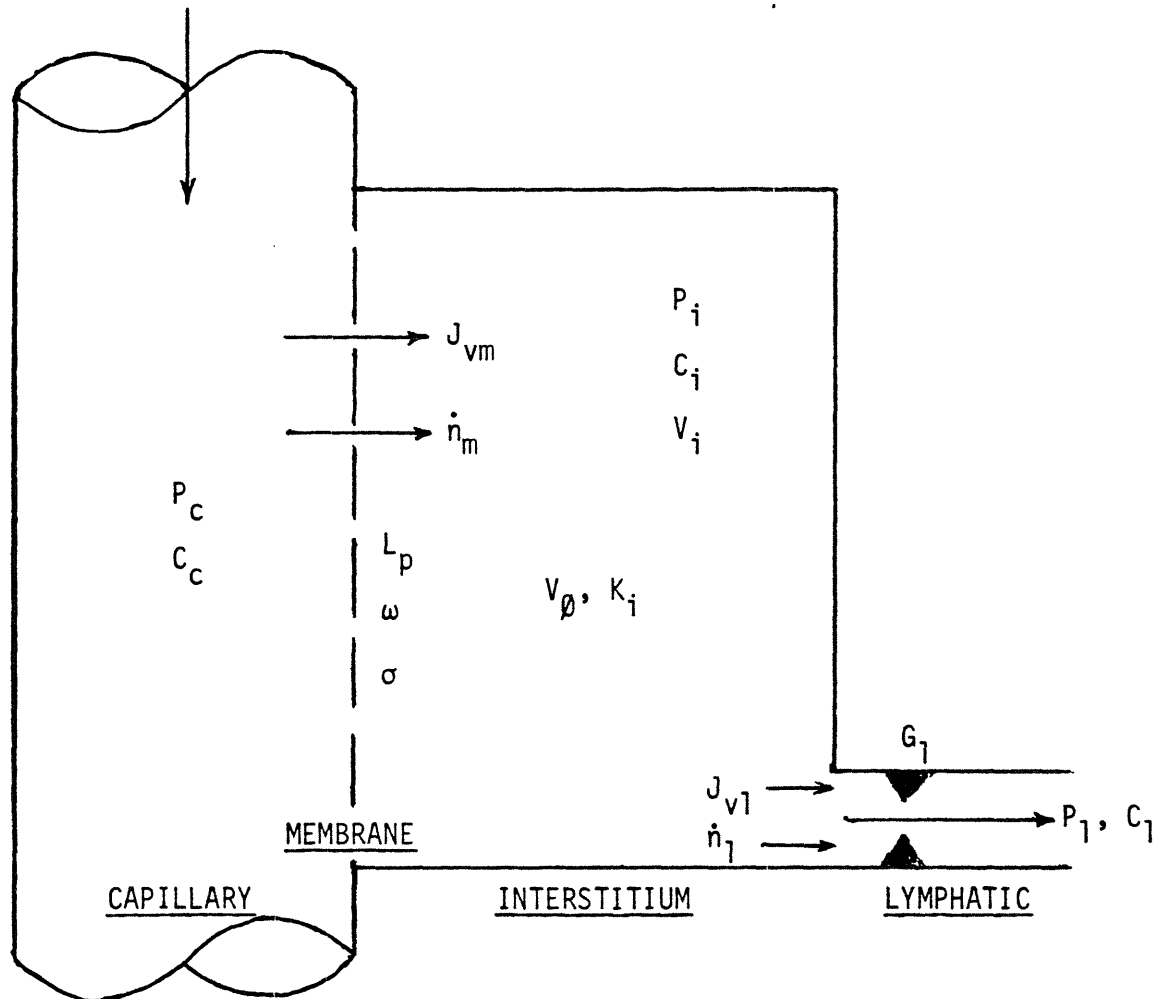
More specifically, in the first section, we present the quantitative model formulation and its simplification into various forms of solution, each represented by a single equation and each directed toward a different goal. We then analyze the equations mathematically looking for regions of behavior. In the third section, the equations are analyzed in physiological terms with plots presented of their predicted performance. This is followed first by a comparison of our models to published data and then by a discussion of the implications of our model.

4.1 Steady State Model Formulation and Mathematical Solution

4.1.1 Model formulation

The quantitative model is very similar to the thought model presented in the previous chapter. Figure 4-1 presents a detailed labeled diagram of the model. The interstitium, a finite, variable sized, well-stirred volume, is separated from the capillary by the capillary membrane and from the lymphatic by a non-sieving resistance. The capillary is treated as an infinite, well-stirred volume implying that hydrostatic pressure, P_c , and

Figure 4-1: Diagram of Lumped Single Solute Model



capillary solute concentration, C_c , are independent of the rest of the system. Likewise, the lymphatic hydrostatic pressure, P_1 , is considered to be independent of the system (a lymphatic pump is assumed to assure its constancy). The membrane is described in the Kedem and Katchalsky, non-equilibrium thermodynamics fashion. That is, three independent parameters are considered sufficient to completely describe the behavior of the membrane with respect to water and single-solute transport. The membrane parameters are L_p , the conductance for bulk fluid flow, ω , the conductance

for solute diffusion, and σ , the cross-coupling between fluid and solute movement. Flow of fluid into the lymphatic is considered to be limited by a linear conductance, G_1 . The lack of sieving at the lymphatic implies that lymphatic protein concentration equals interstitial protein concentration.

There are two fluxes (flow per membrane surface area) across the membrane: volumetric bulk fluid flux, J_{vm} (water plus solute), and solute mass flux, \dot{n}_m . Similarly, there are two fluxes into the lymphatic, J_{v1} and \dot{n}_1 . At steady-state, membrane and lymphatic fluxes of fluid and solute are equal: $J_{vm} = J_{v1} \triangleq J_v$, $\dot{n}_m = \dot{n}_1 \triangleq \dot{n}$. All fluxes and other parameters are normalized to capillary membrane surface area.

The state of the interstitium is described by four variables: P_i , the interstitial hydrostatic pressure, C_i , the interstitial solute concentration, N_i , the total moles of protein per unit membrane surface area, and V_i , the total interstitial volume per unit membrane surface area. By the definition of concentration: $C_i = N_i/V_i$. The interstitial volume is related to interstitial pressure by two parameters: V_0 , the volume at zero interstitial pressure, and K_i , the linear compliance of the interstitial volume.

In summary, the following are the key assumptions for this model:

1. Single solute
2. Kedem and Katchalsky equations describe the membrane.
3. Lymph flow rate is linearly related to the hydrostatic pressure difference between the interstitium and the lymphatic.
4. Capillary pressure and composition are constant.
5. Lymphatic pressure is constant.
6. Interstitium is well stirred.

7. Steady-state exists.

Table 4-I is a summary sheet of the equations, parameters, and variables of this model.

4.1.2 Method of characterizing the steady-state model

It is a relatively straightforward process to simplify these 6 equations into a single equation. The real issue is the choice of independent and dependent variables. There are two input variables to the system: capillary hydrostatic pressure and capillary protein concentration. They can be manipulated independently of the lung. They are the appropriate independent variables.

The response of the system to changes in the input can be expressed in terms of a single variable. The choice of this variable is somewhat arbitrary. Three of the possibilities are: interstitial volume, lymphatic fluid flux, and lymphatic protein concentration. All three have the potential for being measured. However, in the steady state, fluxes, pressures, and concentrations do not depend on interstitial volume. Rather, interstitial volume is a 'modified output variable'. That is, V_i does not need to be known to calculate J_v from C_c and P_c . But V_i can be calculated once J_v is known.

We choose to present the predictions of this model in terms of both J_v and C_1 (in the normalized form, θ , to be described later). Results in C_1 form are presented because this variable is commonly measured in lymphatic cannulation studies. Results are presented in the J_v form both because this variable itself can be crudely measured and because it is directly related to V_i . If the interstitium is governed by a linear compliance ($V_i = K_i P_i + V_{i0}$), then because $P_i = J_v / G_i + P_1$, it follows that

Table 4-I: Equations, Parameters, and Variables of Lumped Single Solute Model

EQUATIONS:

$$J_{vm} = L_p \left[(P_c - P_i) - \sigma (\pi(C_c) - \pi(C_i)) \right] \quad (1)$$

$$J_{vl} = G_l (P_i - P_l) \quad (2)$$

$$\dot{n}_m = J_{vm} (1-\sigma) \frac{C_c + C_i}{2} + \omega (C_c - C_i) \quad (3)$$

$$\dot{n}_l = J_{vl} C_i \quad (4)$$

$$J_{vm} = J_{vl} \quad (5)$$

$$\dot{n}_m = \dot{n}_l \quad (6)$$

$$\pi(C) = C RT \quad (7)$$

$$V_i = P_i K_i + V_\emptyset \quad (8)$$

OUTPUT VARIABLES AND STATE VARIABLES:

$$V_i, J_{vm}, J_{vl}, \dot{n}_m, \dot{n}_l, P_i, C_i, \pi_i$$

INTRINSIC PARAMETERS:

$$K_i, V_\emptyset, RT, L_p, G_l, \omega, \sigma, P_l$$

INPUT VARIABLES:

$$P_c, C_c, \pi_c$$

interstitial volume (water accumulation) behaves in the same fashion as J_v . If compliance is not linear, the basic behavior of V_i would still be evident in the observed behavior of J_v .

Although the analytical form of the model can be expressed with a single equation, we present two equations, one representing the model in terms of fluid flux and the other representing the model in terms of lymphatic protein concentration. These two equations are presented in Table 4-II.

Table 4-II: Single Equation Representations of Steady-State Model

Explicit Equations:

$$J_v = \frac{1}{2} \left[[\alpha\Delta P - \beta\gamma C_c - \gamma] + \sqrt{[\alpha\Delta P - \beta\gamma C_c - \gamma]^2 + 4\alpha\beta\Delta P} \right] \quad (4.1)$$

$$\Theta = \left[\frac{1}{2\varepsilon} \frac{\alpha\Delta P}{\beta\gamma C_c} + \frac{1}{\gamma C_c} + 1 - \sqrt{\left(\frac{\alpha\Delta P}{\beta\gamma C_c} + \frac{1}{\alpha C_c} + 1 \right)^2 - \frac{4\alpha\Delta P}{\beta\gamma C_c}} \right] \quad (4.2)$$

where:

$$\Theta = \frac{(C_c - C_1)}{C_c} \quad \Delta P = P_c - P_1$$

$$\alpha = \frac{1}{(1/G_1 + 1/L_p)} \quad \beta = \frac{2 \omega}{1 + \sigma}$$

$$\gamma = \frac{\sigma^2 RT}{\omega (1/G_1 + 1/L_p)} \quad \varepsilon = \frac{1 + \sigma}{2 \sigma}$$

Equations (4.1) and (4.2) are our "working equations". They are in a form in which the two output variables, J_v and Θ , are explicit functions of the input variables. They allow one to easily find J_v and Θ at any

particular ΔP and C_c if the system parameters, α , β , γ , and ϵ are known. This J_v expression represents our model-derived prediction of the lung water function ("Guyton") curve.

There are several points to be made concerning the above equations before exploring the system behavior which they predict.

1. Capillary pressure in these equations is given in terms of $P_c - P_1$, which represents the total hydrostatic pressure drop across the system. We do this because, for our model, these two pressures always appear as a pair.
2. In the concentration equation, we expressed lymphatic protein concentration in terms of a dimensionless concentration, θ , in which the difference between capillary and interstitial concentration is normalized to capillary concentration. This variable will equal one at zero lymphatic concentration and zero when lymphatic concentration equals capillary concentration. In the literature, it is known as the rejection coefficient [1].
3. There are a total of four parameters that appear in the pair of equations. In each equation, there are at most three. This is a significant reduction from the six relevant parameters that appear in the original formulation.
4. There are three other output variables of our system for which equations are not here presented: P_i , \dot{n} , and V_i . Each can be easily found from the solution for J_v by using the equations of table 4-I.
5. G_1 always appears in combination with L_p in a term which can be interpreted as representing the total system series resistance to convective flow. The existence of this combination reduces the importance of the specific value chosen for G_1 . The coupling means that the effect of changing G_1 can be studied by examining the effect of changing L_p .

Equation (4.1) (J_v versus ΔP) and equation (4.2) (θ versus ΔP) are plotted respectively in Figures 4-2 and 4-3 and give an indication of the basic behavior predicted by our model. These were prepared using the parameter values given in Table 3-III. The point to note is that both plots have a two-part nature involving a "knee". Again it must be stressed that, in the model, interstitial volume is linearly related to J_v .

Figure 4-2: Behavior of the Fluid Flux Equation

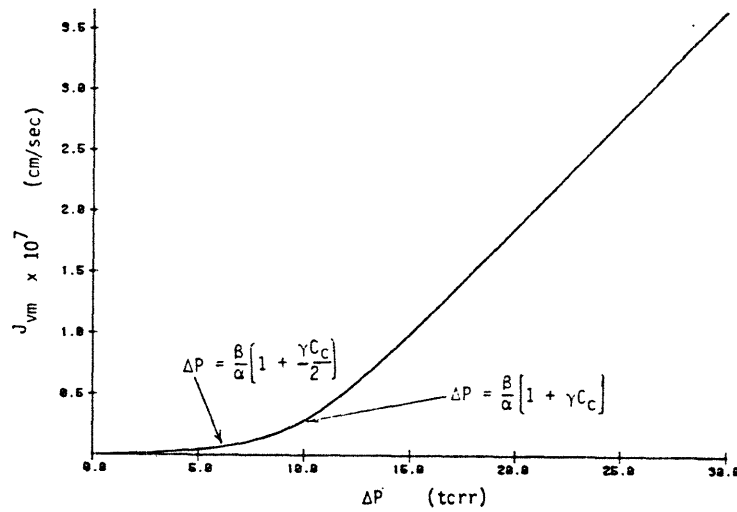
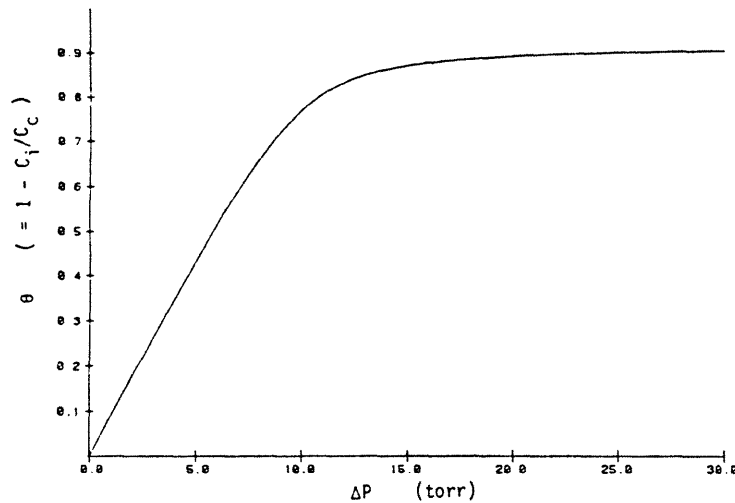


Figure 4-3: Behavior of the Lymphatic Concentration Equation



While the model behavior and these curves will be discussed in detail later, we must point out that both the knee of the "Guyton" curve and an attainment of steady state are described, thus satisfying part of our original goals. The clinical implications of the behavior displayed by these curves will be discussed later. In the next section, we will more thoroughly characterize the behavior predicted by the model.

4.2 Mathematical Analysis of Steady-State Model Equations

4.2.1 Alternate equation forms

Equations (4.1) and (4.2) are useful for calculating J_v and θ but they are not very useful forms for interpreting predicted model behavior. For this purpose, better model representations are given by equations ((4.3) and (4.3)) in Table 4-III. In these, fluid flux and lymphatic protein concentration respectively are given in implicit form. These two implicit equations will be utilized extensively in the next few sections.

It is extremely useful to condense the number of parameters that describe our system by appropriately scaling the system variables. The procedure for doing this is well developed and is known as dimensional analysis [104]. The idea is to search for combinations of the four variables (θ , J_v , ΔP , and C_c) and the four parameters (α , β , γ , and ϵ) of our model equations that would produce dimensionless variables. Several combinations are possible, but with the condition that no two of the original variables are to appear together in any of the new variables, only one combination is possible.

The definitions for the dimensionless variables and the resulting non-dimensional equations are presented in Table 4-III.

In each equation, the dependent variable is now a function of only two independent variables: a dimensionless pressure difference and a dimensionless capillary concentration. Or, looking at it another way, each equation can now be plotted on a single, two-dimensional plot with a single adjustable parameter. In these forms, we get a sense of the contribution of protein to our model, particularly from the form of

Table 4-III: Implicit and Non-Dimensional Forms of the Model

General Definitions:

$$\theta = \frac{(C_c - C_1)}{C_c} \qquad \Delta P = P_c - P_1$$

$$\alpha = \frac{1}{(1/G_1 + 1/L_p)} \qquad \beta = \frac{2 \omega}{1 + \sigma}$$

$$\gamma = \frac{\sigma^2 RT}{\omega (1/G_1 + 1/L_p)} \qquad \varepsilon = \frac{1 + \sigma}{2 \sigma}$$

Implicit Equations:

$$J_v = \alpha \Delta P - \beta \gamma C_c \frac{J_v}{J_v + \beta} \qquad (4.3)$$

$$\theta = \frac{1}{\varepsilon} \frac{\alpha/\beta \Delta P}{\alpha/\beta \Delta P + \gamma C_c (1 - \varepsilon \theta) + 1} \qquad (4.4)$$

Dimensionless Variable Definitions:

$$J_v^* = \frac{1}{\beta} J_v$$

$$\theta^* = \varepsilon \theta$$

$$C_c^* = \gamma C_c$$

$$\Delta P^* = \frac{\alpha}{\beta} \Delta P$$

Dimensionless Equations:

$$J_v^* = \Delta P^* - C_c^* \frac{J_v^*}{J_v^* + 1} \qquad (4.5)$$

$$\theta^* = \frac{\Delta P^*}{\Delta P^* + C_c^* (1 - \theta^*) + 1} \qquad (4.6)$$

equation (4.5). When the dimensionless concentration is zero, the equation becomes a straight line. However, as dimensionless concentration increases, the straight line is perturbed more and more with a tendency toward lower flows at a given pressure, a protective effect!

We can use the parameter values of Table 3-III to attach physical significance to these equations. Based on these, $C_c^* = 34$, $\Delta P^* = 41$, and $J_v^* = 10$, all of course without units. To show the behavior of the dimensionless equations, J_v^* and θ^* are plotted respectively in Figures 4-4 and 4-5 against ΔP^* with C_c^* as the single parameter. In essence, either one of these plots contains all the information of our model. We will discuss their significance later.

The dimensioned implicit equations and the non-dimensional equations find usefulness in different situations. The non-dimensional forms are the most compact representations of our model. They show at a glance its essence. They are also extremely useful in designing experiments because they cut down the number of different parameter combinations that have to be tested. The dimensioned forms find their main usefulness because they express the model's behavior in terms of variables with which lung physiologists have traditionally dealt. It is much easier to use them to interpret our model in terms of previous work.

4.2.2 Model limits and their characterization

The two-part behavior could have been predicted based on close examination of any of the model equations. In terms of the two explicit equations, (4.1) and (4.2), as ΔP increases, a change in the nature of the curves would be expected to occur at that pressure at which the term outside the radical changes sign. However, the implicit equations

Figure 4-4: Dimensionless Plot of J_v^* versus ΔP^* With C_c^* as a Parameter

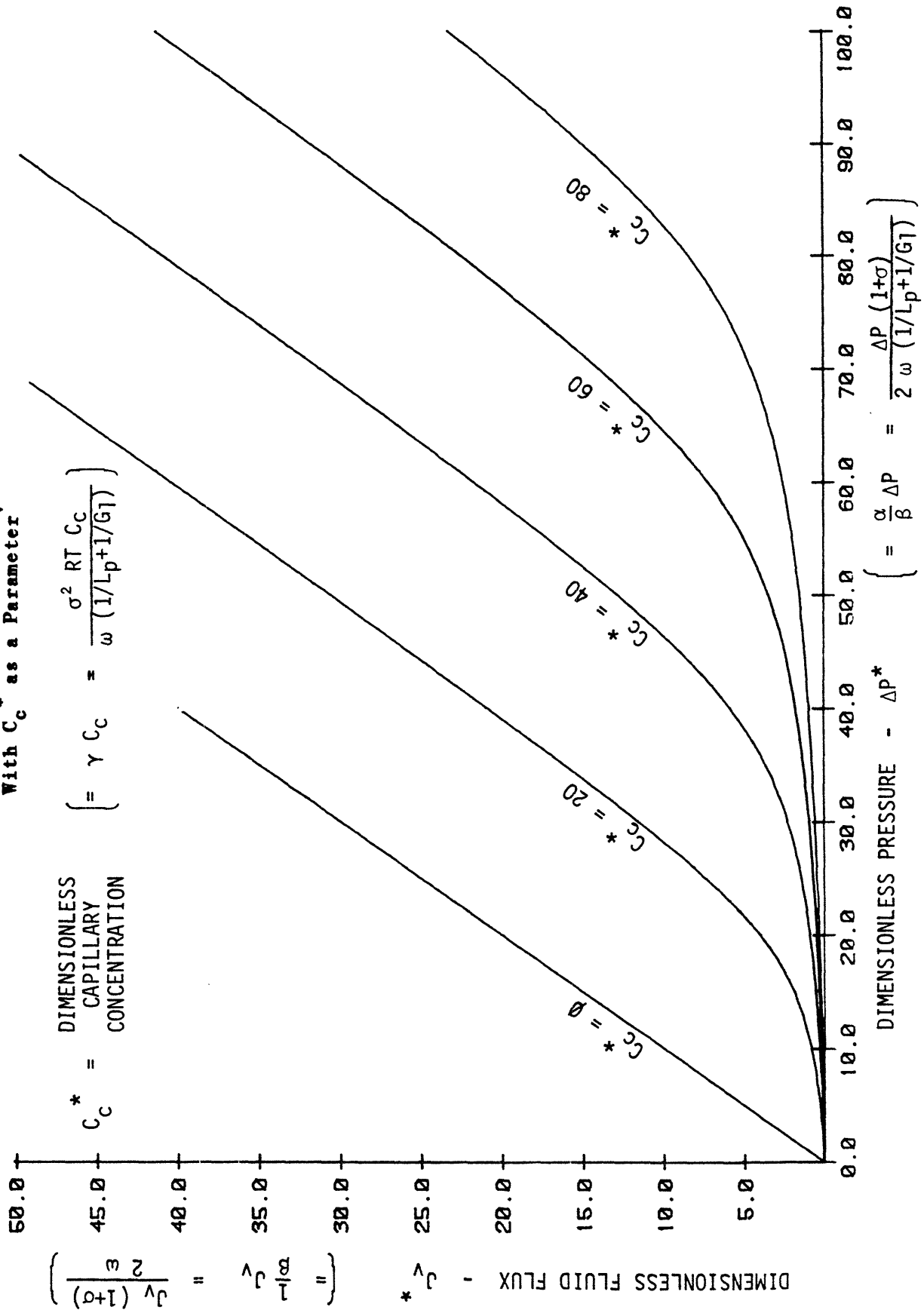
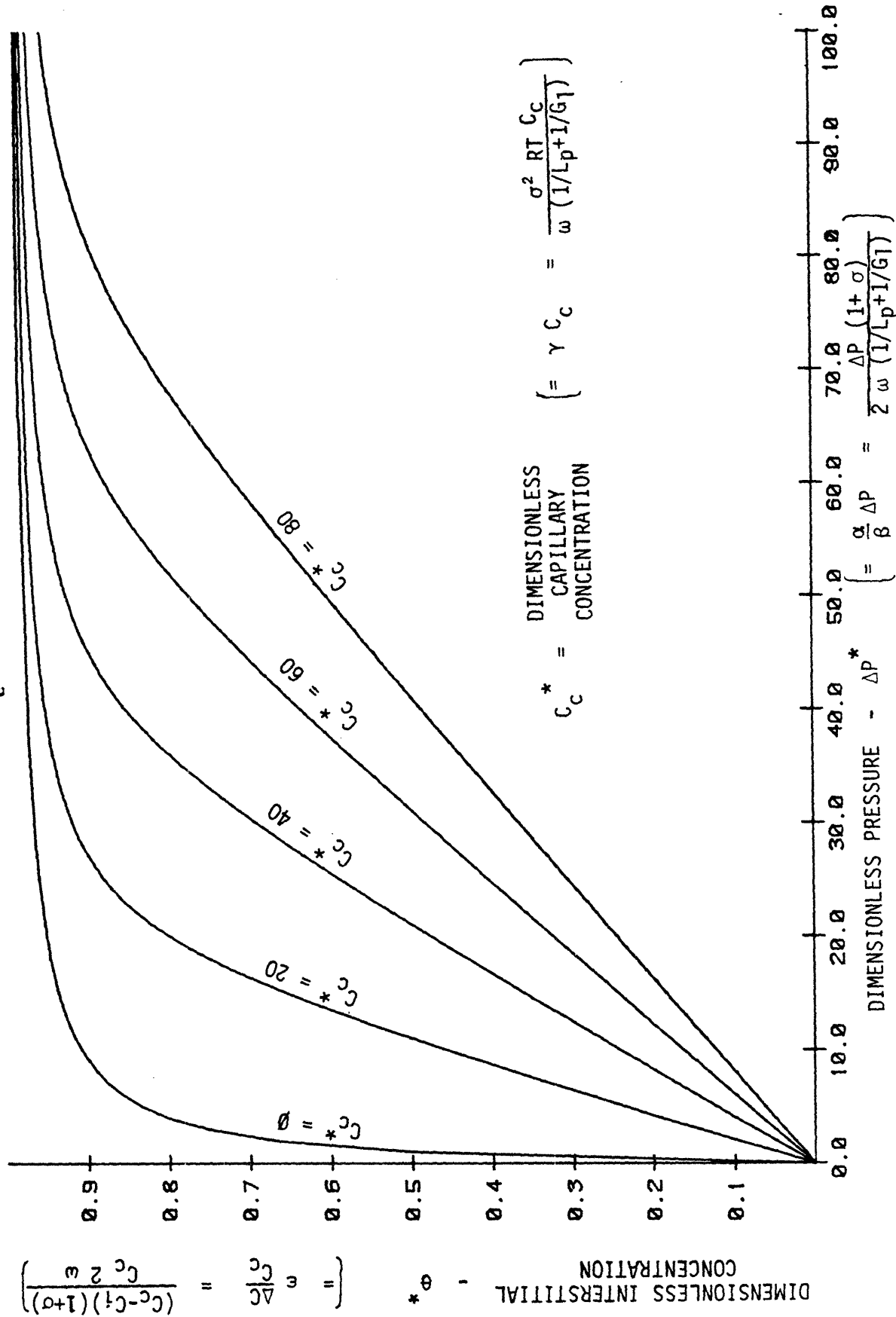


Figure 4-5: Dimensionless Plot of θ^* versus ΔP^* With C_c^* as a Parameter



((4.3) and (4.4)) are much better vehicles for exploring the details of this two-part behavior.

In studying these two-part functions, interest can be divided into three categories: 1.) the nature and boundaries of the zone of transition between the two regions, 2.) the nature and boundaries of the first (low pressure) region, and 3.) the nature and boundaries of the second (high pressure) region. We will discuss each in turn. Equations will be presented in both non-dimensional and dimensioned form.

4.2.2.1 The transition zone

First consider the fluid flux equations. Upon examination of either Equation (4.5) or Equation (4.3), it is apparent that the two-part behavior of the fluid flux curve occurs because of the interaction of two terms in a denominator. In terms of Equation (4.3), at low pressure (high flux), the β term predominates and at high pressure, the J_v term predominates.

At the point at which $J_v = \beta$ (or $J_v^* = 1$) the maximum interaction occurs. This can be defined as the mathematical "transition point". It is related to the curve knee, an issue we will discuss in more detail later (in section 4.2.2.5). In terms of pressure, the transition point occurs at:

$$P = \frac{\beta}{\alpha} \left[1 + \frac{\gamma C_c}{2} \right] \quad (4.7)$$

or:

$$\Delta P^* = \left[1 + \frac{C_c^*}{2} \right] \quad (4.8)$$

Note that the location of the transition point depends on the size of

$\gamma C_c/2$ (or $C_c^*/2$). If $\gamma C_c/2 \ll 1$, the transition point occurs at $\Delta P = \beta/\alpha$ (or $\Delta P^* = 1$) and if $\gamma C_c/2 \gg 1$, the transition point occurs at $\Delta P = \beta\gamma C_c/2\alpha$ (or $P^* = C_c^*/2$).

The transition zone is a region of complex behavior between the high and low pressure zones which are regions of relatively simpler behavior. In this zone, J_v and β are of the same magnitude. The two boundaries of this region are defined respectively by the pressure at which J_v is much smaller than β and by the pressure at which J_v is much larger than β . In order to quantitate the relative sizes of J_v compared to β and thus define the limits of the transition zone, we define the new parameter, ξ . Using this, the transition region is defined as the range of pressures in which $\beta/J_v > \xi$ and $J_v/\beta < \xi$. The larger the ξ value, the more certain it is that any pressure outside the transition zone can be adequately described by the high and low pressure limiting behavior equations to be presented below. In terms of pressure, we have:

TRANSITION REGION:

$$\frac{\beta}{\alpha} \left(\frac{1}{\xi} + \frac{\gamma C_c / \xi}{1 + 1/\xi} \right) < \Delta P < \frac{\beta}{\alpha} \left(\xi + \frac{\xi \gamma C_c}{1 + \xi} \right) \quad (4.9)$$

or:

$$\left(\frac{1}{\xi} + \frac{C_c^* / \xi}{1 + 1/\xi} \right) < \Delta P^* < \left(\xi + \frac{\xi C_c^*}{1 + \xi} \right) \quad (4.10)$$

Note that this definition is asymmetric in terms of pressure. The term involving C_c has more importance at low pressures and less at high.

The concentration equations, (4.4) and (4.6), also describes a two-part behavior which is determined by the relative sizes of terms in a denominator. It is more difficult to identify a "transition point" from these equations. In Equations (4.4), the transition point is determined

by size of the $\alpha\Delta P/\beta$ term compared to the rest of the denominator. However, the second part of the denominator contains the $\gamma C_c(1-\varepsilon\theta)$ term which changes with ΔP . $(1-\varepsilon\theta)$ has limits (as will be seen) of 1 for zero pressure and θ for large pressure. But the concentration equations and the flux equations describe the same model. The transition point should be the same for all such equations. This means that the transition point occurs at the same pressure as given above and thus at the transition point, $(1-\varepsilon\theta) = 1/2$. It is reasonable also to use the same definition for the transition region as that given above in equations (4.9) and (4.10).

4.2.2.2 The high pressure region

The definition of the boundaries of the transition region serves also to define region 1 (below the low pressure limit) and region 2 (above the high pressure limit). For region 2, one can assume that the β term in the denominator of Equation (4.3) is zero. This gives the equation that defines the high pressure limiting behavior:

$$\text{HIGH PRESSURE REGION} \quad \left[\Delta P > \frac{\beta}{\alpha} \left(\xi + \frac{\xi \gamma C_c}{1 + \xi} \right) \right]:$$

$$J_v = \alpha \Delta P - \beta \gamma C_c \quad (4.11)$$

or, in terms of dimensionless variables:

$$J_v^* = \Delta P^* - C_c^* \quad (4.12)$$

The first equation represents a straight line of slope α $[=1/(1/L_p + G_1)]$ and offset $\beta \gamma C_c$. This slope represents the series flow conductance of the system.

The limiting behavior of the lymphatic concentration curve is provided by the following two equations:

$$\text{HIGH PRESSURE REGION} \quad \left[\Delta P > \frac{\beta}{\alpha} \left(\xi + \frac{\xi \gamma C_c}{1 + \xi} \right) \right]:$$

$$\theta = 1/\varepsilon = \frac{2\sigma}{1+\sigma} \quad (4.13)$$

or, in terms of dimensionless variables:

$$\theta^* = 1 \quad (4.14)$$

That is to say, at high enough pressure, $\varepsilon\theta = 1$.

4.2.2.3 The low pressure region

When pressure is sufficiently low in equation (4.3), it can be assumed that J_v in the denominator equals zero. In this case the dimensional and non-dimensional equations that describe the behavior of the system are:

$$\text{LOW PRESSURE REGION} \quad \left[\Delta P < \frac{\beta}{\alpha} \left(\frac{1}{\xi} + \frac{\gamma C_c / \xi}{1 + 1/\xi} \right) \right]:$$

$$J_v = \frac{\alpha}{1 + \gamma C_c} \Delta P \quad (4.15)$$

or, in dimensionless form:

$$J_v^* = \frac{\Delta P^*}{1 + C_c} \quad (4.16)$$

In terms of the first equation, the result is once again a straight line but this time with a zero intercept. The expression for the slope is interesting in that it indicates that two different cases exist. If $\gamma C_c \ll 1$ (where $\gamma C_c = (\sigma^2 C_c RT) / (\omega(1/G_1 + 1/L_p))$), the slope of region 1 is α and is the same as that of region 2. The entire function is in this case a single straight line. If $\gamma C_c \gg 1$, the slope of region 1 is $\alpha/\gamma C_c$ [$=\omega/\sigma^2 C_c RT$].

In the case of the lymphatic concentration equations, both θ and ΔP in the denominator of Equation (4.4) can be neglected for low pressures.

The low pressure limiting behavior is thus given by:

$$\text{LOW PRESSURE REGION} \quad \left[\Delta P < \frac{\beta}{\alpha} \left(\frac{1}{\xi} + \frac{\gamma C_c / \xi}{1 + 1/\xi} \right) \right]:$$

$$\theta = \frac{1}{\varepsilon} \frac{\Delta P}{1 + \gamma C_c} \quad (4.17)$$

or, in dimensionless variables:

$$\theta^* = \frac{\Delta P^*}{1 + C_c^*} \quad (4.18)$$

For small γC_c , the slope is $\alpha/\beta\varepsilon$ [= $\sigma/(\omega(1/G_1+1/L_p))$]. For large γC_c , the slope is $\alpha/(\beta\gamma C_c)$ [= $1/(\sigma RTC_c)$]. The intercept in both cases is zero.

4.2.2.4 Physical relevance of limiting behavior

To see how our model applies to the physical situation, we can make use of the parameter set of Table 3-III. Using these values gives: $\alpha=1.8 \times 10^{-8}$, $\beta=5.4 \times 10^{-9}$, and $\gamma=850$. In order to define region boundaries, we also assign a value of 10.0 to ξ . Applying these values to the expressions given above indicates that the transition region is defined by $[0.9 \text{ torr} < \Delta P < 12.1 \text{ torr}]$ and the transition point occurs at $\Delta P=5.3 \text{ torr}$ and $J_v=5.4 \times 10^{-9} \text{ cm/sec}$. In this range of values, the transition zone is sensitive to changes in C_c [$\gamma C_c \rightarrow 850 \times 0.04 \gg 1$]. Region 1 is governed by the limiting equation:

$$J_v = \frac{\alpha}{1 + \gamma C_c} \Delta P \quad \Rightarrow \quad J_v = \frac{1.8 \times 10^{-8}}{(1+34)} \Delta P$$

The concentration term is dominant and thus the region has a slope that depends on C_c and is different from that of region 2. Region 2 is described by:

$$J_v = \alpha \Delta P - \beta \gamma C_c \quad \Rightarrow \quad J_v = 1.8 \times 10^{-8} \Delta P - 1.8 \times 10^{-7}$$

and is dependent on C_c only in offset.

For the lymphatic concentration curves, the transition region is defined as for J_v . The limiting equation for region 2 is:

$$\theta = \varepsilon \quad \Rightarrow \quad \theta = 0.92$$

The limiting equation for region 1 is:

$$\theta = \frac{\alpha}{\beta\varepsilon} \frac{1}{1 + \gamma C_c} \Delta P \quad \Rightarrow \quad \theta = 3.6 \frac{1}{1 + 34} \Delta P$$

Note here the importance of the capillary concentration term in the denominator.

4.2.2.5 Transition point: alternative definitions

The transition point definition given above gives a pressure value that does not agree with pressure at which the visual "knee" appears in the plots (see Figures 4-2 and 4-3). It gives a pressure almost half that which one would visually define as the knee. An alternative way of defining the knee is to define it as the pressure at which the slope of the J_v curve is changing most rapidly. This corresponds mathematically to finding the pressure at which the third derivative of Equation (4.1) equals zero. The result is:

$$\Delta P = \frac{\beta}{\alpha} \left[1 + \gamma C_c \right] \quad (4.19)$$

This has the same form as the previous definition except for the absence of the 1/2 in front of the γC_c term. With the same numerical values used above, it gives a pressure which is almost twice the pressure of the transition point definition which but corresponds very closely to visual estimates of the "knee".

This difference is intriguing. To explore this further, a third way of defining the knee is as the point at which the low and high pressure

limiting line equations intercept. The point of interception is given by:

$$\Delta P = \frac{\beta}{\alpha} [1 + \gamma C_c] \quad (4.20)$$

and:

$$J_v = \beta \quad (4.21)$$

In this definition, the value given for pressure agrees with the third derivative derived knee pressure but its J_v values agrees with the J_v of the transition point definition.

A way of reconciling these differences is to note that there are two different quantities of interest. One is a quantity that can be used to define when limiting behavior can be safely assumed. This is the function of the mathematical transition point value defined in section 4.2.2.1. It also defines the width of the transition region. The other is a quantity for defining the visual knee. This quantity has clinical importance because it describes a limit to effective "protection" against capillary pressure changes. The third derivative derived value seems more appropriate for this application. But the fact that the two differ means the visual knee actually occurs in the region in which the high pressure behavior is already starting to dominate.

4.3 Physiological Analysis of Steady-state Model Equations

The parameters physiologists usually deal with when discussing the lung are the parameters used to characterize the components of the lung water system such as the capillary membrane. Primary among these parameters are L_p , ω , and σ , the three membrane parameters. It is difficult to determine the effect of changes in these parameters directly

from the model equations given because any one may be buried in several of our four system parameters and produce simultaneous changes in these parameters.

4.3.1 Graphical presentation of behavior

To clarify the effects of variations in the component parameters, we present two figures in which J_v and θ are plotted respectively versus ΔP in Figures 4-6 and 4-7. In each figure, there are four plots which each represent the effect of varying one parameter out of a group that includes C_c , L_p , ω , and σ while holding the others constant. In each case, the point representing normal parameter values is marked with a square. P_1 or G_1 are not plotted because both always appear grouped with another variable or parameter. Their effect on the system can be studied by studying the influence of their respective complementary parameter.

Each of these plots displays the familiar two-part behavior. However, from these plots, it is clear that each parameter affects the lung water function curve in a different way. Looking at the plots in Figure 4-6, C_c and σ both influence the curve in the same general way except that the C_c effect is linear and the σ is not. L_p has its effect at high pressures but little if any at low. Changes in ω tend to change the "sharpness" of the knee. In terms of the θ curves, all curves approach a limiting horizontal line at high pressures. Changes in σ change the level of this line. L_p and ω affect the curve in exactly the same way which is different from that of C_c .

Figure 4-6: Effects of Various Parameters on Steady-State Plots of J_v versus ΔP

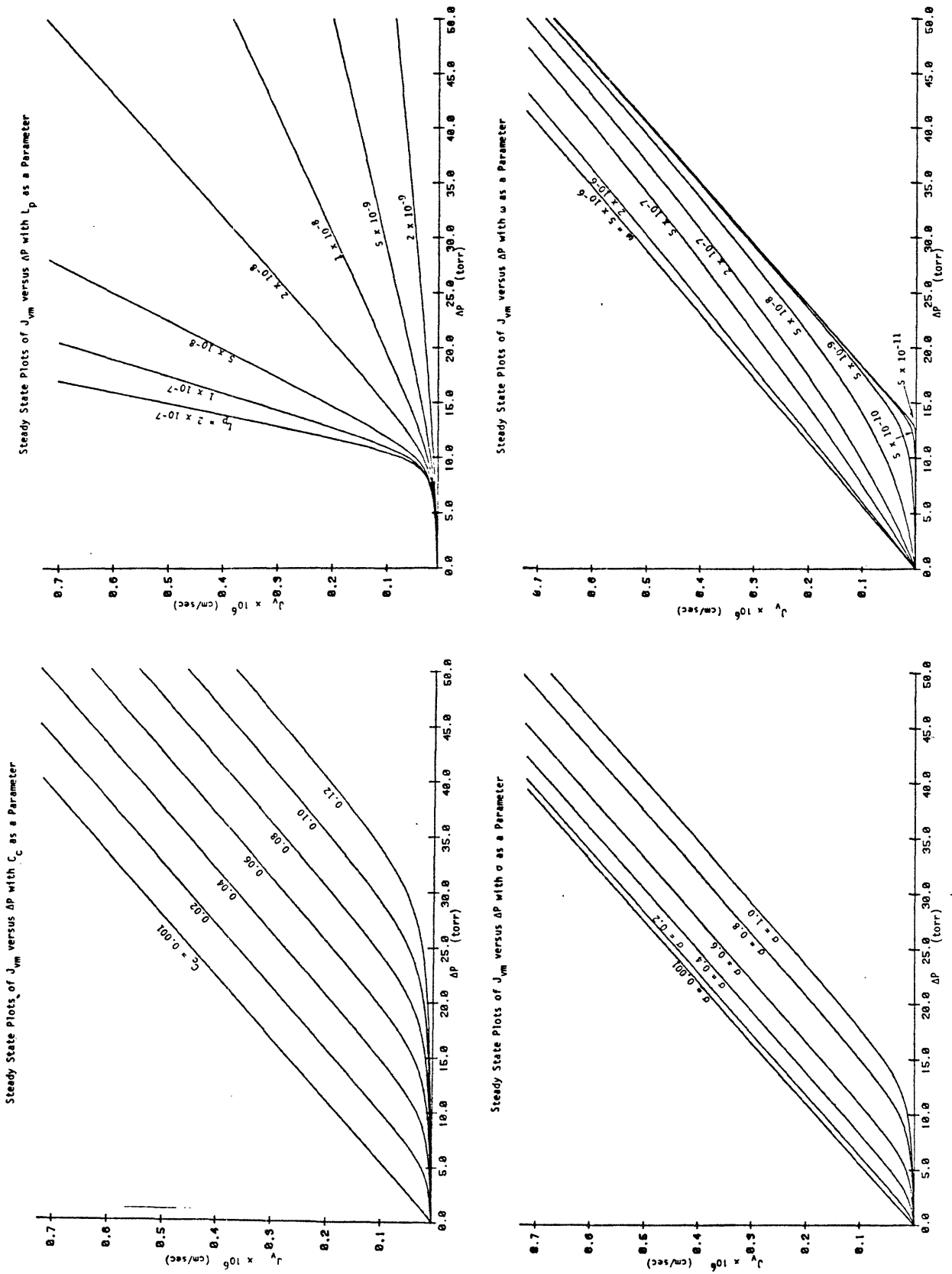
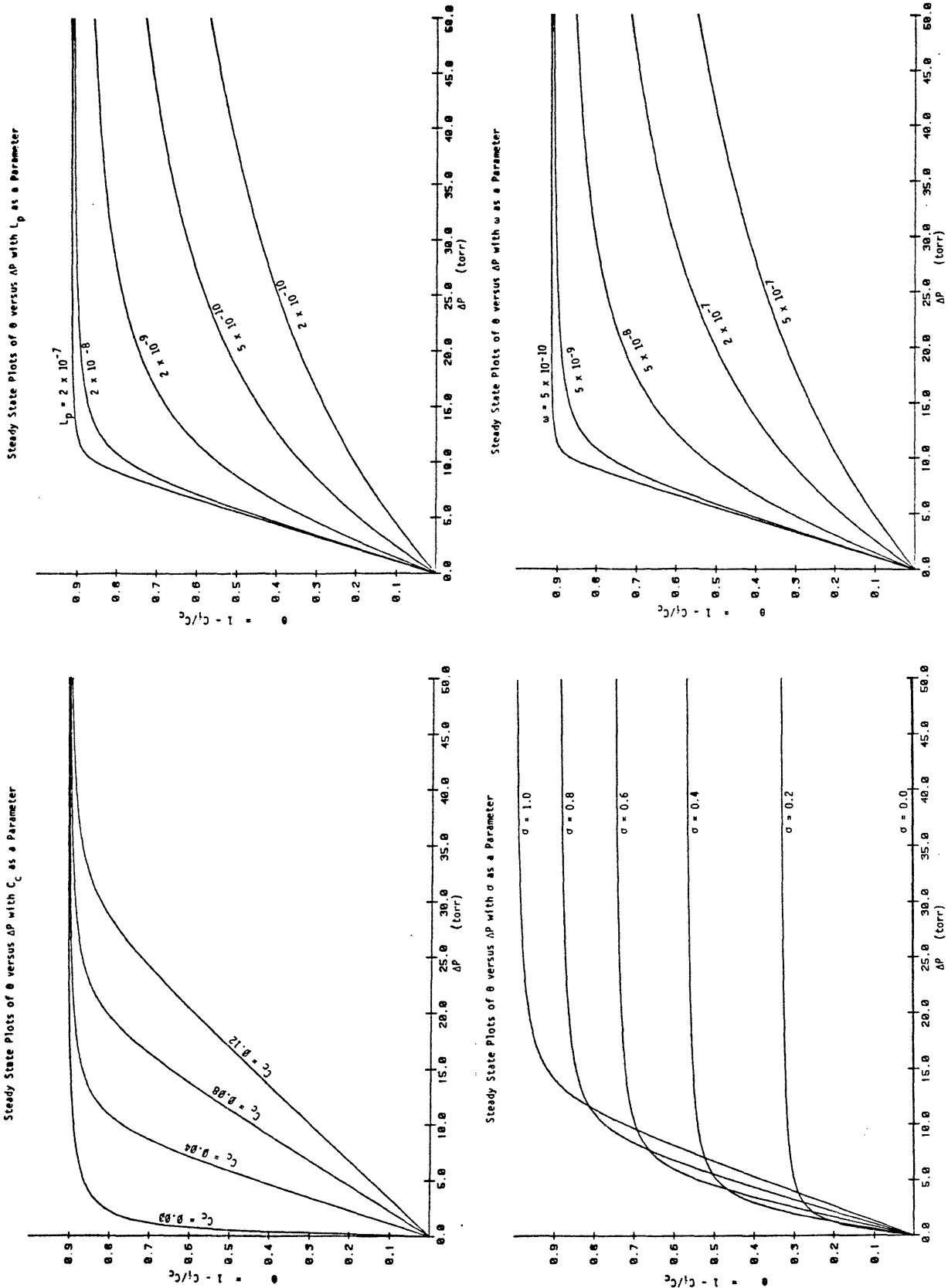


Figure 4-7: Effects of Various Parameters on Steady-State Plots of θ versus ΔP



4.3.2 Limiting behavior

It is possible to use the analysis of the previous section to study the behavior of the system at limiting values of the component parameters. From these equations, it is immediately apparent that the limiting flux equation for $C_c \rightarrow 0$, or $\sigma \rightarrow 0$, or $\omega \rightarrow \infty$ is:

$$J_v = \alpha \Delta P$$

That is, a single straight line with zero intercept. For $\omega \rightarrow 0$, the limiting fluid flux function is:

$$J_v = \begin{cases} 0 & : \Delta P < \beta\gamma C_c / \alpha \\ \alpha\Delta P - \beta\gamma C_c & : \Delta P > \beta\gamma C_c / \alpha \end{cases}$$

This says that, as ω approaches zero, the function approaches two straight lines with a slope discontinuity at their juncture.

The concentration function behaves somewhat differently. First, ω and $(1/L_p + 1/G_1)$ always appear together as a product. Thus, the limiting function for large ω is the same as that for small L_p . Actually, the limit for $\omega \rightarrow \infty$, $L_p \rightarrow 0$ and $\sigma \rightarrow 0$ is:

$$\theta = 0$$

The limiting function for $\omega \rightarrow 0$ and $(1/L_p + 1/G_1) \rightarrow 0$ is:

$$\theta = \begin{cases} \Delta P / (\sigma RT C_c) & : \Delta P < \beta\gamma C_c / \alpha \\ 1/\varepsilon & : \Delta P > \beta\gamma C_c / \alpha \end{cases}$$

The behavior at limiting values of the component parameters given above must be approached with extreme care. The assumption was made here that the membrane parameters are completely independent. This follows the Kedem and Katchalsky approach. But, as discussed in the previous chapter, there is good reason to believe in the physical situation that these

parameters are coupled. Thus, for example, the limit for ω or $(1/L_p + 1/G_1)$ going to zero given in our last expression above may not have as much meaning if ω goes to zero while $(1/L_p + 1/G_1)$ goes to infinity (which occurs with the membrane pore theory).

4.4 Comparison of Model Predictions to Published Data

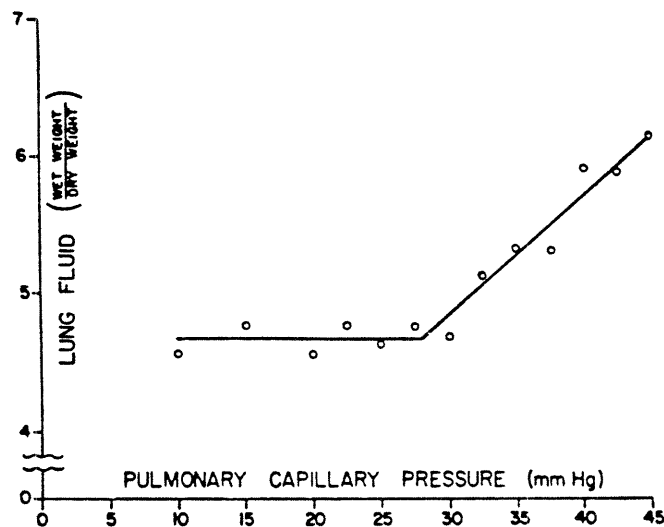
Before comparing our model to experimental data, several points must be made. First, as noted in the previous chapter, we have derived this model by assuming that globulin is impermeable and that its contribution to total plasma osmotic pressure can be accounted for by lumping it with capillary hydrostatic pressure. Our ΔP independent variable is in fact an "effective" driving force which includes the presence of globulin. To compare our results to experimental results, which are in terms of true pressure, we must add the plasma osmotic pressure of globulin, 6.4 torr, to ΔP .

The "Guyton" plot presented in Chapter 2 uses left atrial pressure as the independent parameter. In our model calculations, we use P_c , the capillary pressure, as the independent variable. Although pulmonary vascular changes can alter capillary pressure independently of left atrial pressure, capillary pressure is normally considered to be linearly related to left atrial pressure as expressed in equation (3.7) [21]. Thus, the J_v versus ΔP plots given above can be reasonably compared to the V_i versus P_{1a} plot of Guyton and Lindsey.

4.4.1 Fluid flux and accumulation

The general behavior of our model agrees very closely with the experimental results obtained by others. We have already presented the "Guyton" plot (Figure 2-2) in chapter 2. A similar plot was produced by Gaar et al. [21] and is presented in Figure 4-8.

Figure 4-8: Lung Water Function Curve of Gaar [21]



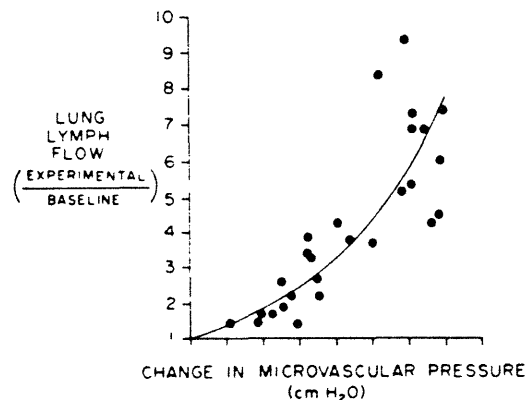
This plot was produced using an isolated lung preparation. Each point represents a separate lung in which vascular pressure was elevated and, after 1 hour, a wet-to-dry gravimetric analysis performed. Arterial and venous pressures were maintained very close to each other so that the results could be given directly in terms of capillary pressure.

Others have produced similar plots [17, 106]. By inspection, the knee in the Guyton plot occurs at $P_{1a} = 24$ torr and the knee in the Gaar plot occurs at $P_c = 28$ torr. Our model gives a value for the knee of $10.5 + 6.4 = 16.9$ torr using the "visual knee" definition of section

4.2.2.5 (the 10.5) and including the adjustment for globulin (the 6.4). The Guyton and Gaar values are higher than our value. Although both authors fit double straight lines to their results, the data given can also be easily fit with the type curves produced by our model.

Parker et al. [67] present a plot of lung lymph flow versus capillary pressure which they obtained in chronic lymphatic cannulated sheep whose pulmonary vascular pressure they elevated with an atrial balloon. This plot is presented in Figure 4-9.

Figure 4-9: Lymphatic Flux versus Capillary Pressure
Plot of Parker et al. [67]



It is useful because, unlike the previous experimental results, no assumption needs to be made about the relationship between water flux and interstitial water volume to compare it with our model results. Although there is quite a bit of scatter in the data, the general nature of the curve looks very similar to our model results, and the knee, which appears to be at about 15 torr, is very close to that of our model.

No experimental attempts are reported in the literature to determine how the lung water function curve may vary with abnormal conditions. This

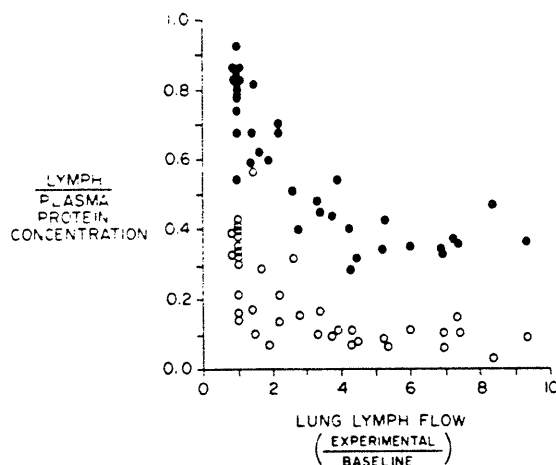
is unfortunate because the ability to predict the nature of such changes is a major feature of our model.

4.4.2 Experimental lymphatic concentration

We were not able to find in the literature any presentations of lymphatic concentration as a function of vascular pressure. Parker et al. produced a plot of lymphatic protein concentration versus lymph flow rate using the cannulated-lymphatic sheep preparation in which lymph flow rate was varied by inflating a balloon implanted in the left atrium [67]. This plot is contained in Figure 4-10 in which their lymphatic concentration corresponds to our $(1-\theta)$.

Figure 4-10: Example of Lymphatic Cannulation Experimental Results

from Parker - 1981 [67]



The closed circles represent a fraction consisting of small protein molecules (~ 67,000 molecular weight) and the open circles represent a fraction consisting of large protein molecules (~ 1,300,000 molecular

weight). This plot gives an indication of the scatter experienced. From this it can be seen that if one were trying to make measurements that assume a limiting low concentration, quite a few points would have to be collected before one could be reasonably certain about this assumption.

It is a relatively straightforward matter to combine our equations to derive a form in which lymphatic concentration is a function of fluid flux. The result is:

$$1 - \theta = \frac{C_i}{C_c} = \frac{\omega RT + J_v [(1-\sigma)/2]}{\omega RT + J_v [(1+\sigma)/2]}$$

This is an equation which has, in fact, a long history in describing the behavior of isolated membranes [36]. The equation predicts that, at zero J_v , $(1-\theta)$ will equal 1 and that $(1-\theta)$ asymptotically approaches $(1-\sigma)/(1+\sigma)$ at high J_v . This behavior agrees with the limiting behavior of our model described on page 107 and with the experimental behavior of Figure 4-10. However, in our deriving this equation, all the interstitial and lymphatic related features of our model dropped out. The relevance of our model in this circumstance is that it relates pressure to lymphatic protein concentration and allows one to better predict when limiting conditions may exist. By examining the plots of Figure 4-6 it can be seen that circumstances may exist in which the transition region is greatly widened making it impossible to obtain a limiting low interstitial concentration at any physiologically possible pressure.

4.5 Discussion

4.5.1 General behavior: the knee

The appearance of the knee is an intriguing feature given that no non-linear component descriptions are included in the underlying model. The basic logic for its appearance was given in the description of our thought experiment, the essentials of which are repeated here. Steady state exists only when the fluxes across the membrane equal the fluxes into the lymphatic. Increases in P_c are counteracted by decreases in C_i until a minimum in C_i is reached. If no protein can cross the membrane, that is, if $\sigma=1$ and $\omega=\emptyset$, this minimum is β . If σ is not equal to one, the minimum is that concentration given by the ratio of protein carried by convection to total flow. That is, any water that flows carries with it a fixed ratio of protein and thus the interstitial protein is limited in how low it can go. If ω is non-zero, protein can enter independently of bulk flow. This will tend to equalize protein concentrations on either side of the membrane. However, with higher bulk flows, the effect of diffusion is completely overwhelmed by solute convection.

The existence of the knee is clinically useful because it provides a safety factor against water accumulation. If the membrane were considered to be impermeable to protein, a sharp end to the safety zone would occur when the oncotic pressure of the capillary equaled the hydrostatic pressure gradient across the system. Based on this premise, most authors try to fit a double-line to lung water function curves: a horizontal line in the safety zone and a line of positive slope beyond. Up until this time, it has not been clear what effect a non-zero protein permeability might have on the water function curve. Our model attempts to provide

this information and shows that once ω is different from zero, multiple system parameters become important in controlling the system.

4.5.2 Clinical implications

4.5.2.1 The lung water function curve

We have spoken of the "Guyton" curve as the lung water function curve. The reasoning behind this application deserves discussion. A clinical goal is to differentiate edema caused by changes within the lung from edema caused by changes external to the lung.

The Guyton curve serves as a useful vehicle for this process. The premise behind its use is that the exact shape and position of the curve is the result of factors intrinsic to the lung. The position on the curve at which the system is operating is determined by the extrinsic factors. An extrinsic change would, after a period of time sufficient for a new steady state, cause a shift in the operating point along the curve. We are interested in possible changes in the position and shape of the curve.²

There are two forms which changes in this curve can take. A vertical shift in the curve would result in the existence of more lung water with no change in external pressure. A curve rotation, on the other hand, may mean more water existing at normal pressure but, as importantly, results in total water being much more sensitive to changes in external

²This is a somewhat simplified view. For example, changes in capillary pressure can be caused by a change in vascular impedance which is intrinsic to the lung. But this approach does serve as a framework for organizing thought.

conditions.

These two represent potentially different clinical situations. In one type of lung pathology, a patient may have increased water at normal pressure and yet be normally sensitive to increased pressure. In another type of lung pathology, a person may have normal water at normal pressure yet be more susceptible than normal to changes in pressure. Both situations represent lung pathology but produce quite different lung water effects.

4.5.2.2 The propensity for lung water accumulation

When the state of a system is described by a plot, an attempt is often made to try to derive an index that extracts the essence of the plot into a single number. An appropriate label for an index describing the intrinsic water state of the lung would be "the propensity for lung water accumulation." However, as pointed out above, we really need at least two indices to describe the lung water function curve, one propensity for lung water accumulation representing curve position and a second propensity for lung water accumulation representing curve slope. Further, if the lung water function curve is non-linear, the values assumed by these indices would depend on the vascular pressure at which defined.

With this discussion in mind, we are in a better position to explore the clinical implications of the various parameters that exist in our model. We will discuss each parameter's impact on the lung water function curve. By "lung water function curve", we mean the behavior predicted by our J_v versus ΔP curves. It must be reemphasized that, while our results are presented in terms of J_v , we assume a simple linear relationship between J_v and V_i and thus treat all of the J_v plots and equations as if

they applied to V_i (which is the dependent variable of the "true" lung water function curve).

4.5.2.3 Component characterization parameters

Protein is the material that provides the protective effect. Therefore, the observed influence of capillary protein concentration on our model is reasonable. At low pressure, increasing protein decreases the lung water susceptibility, that is, decreases the slope of the lung water function curve. At high pressures, changes in protein have no effect on the susceptibility to water but do decrease the amount of water present. This occurs by a right shift in the curve caused by a shift in the transition point.

The hydraulic permeability, L_p , has little effect on the system at low pressures if capillary protein concentration is sufficiently high. That is, if the pressure is low enough, changing the water permeability will not change the amount of water present or the water susceptibility! Above the transition zone, the susceptibility to water is very dependent on L_p . However, the transition zone is not modified significantly by changes in L_p .

Protein permeability, ω , provides a "leak" to the protective effect. Thus, with zero permeability, there is a sharp break between the high and low pressure regions. However, as ω increases, the transition zone becomes more and more spread out. The system become more susceptible to water changes at low pressures. With reasonable ω values, the transition zone may easily spread to encompass the highest physiologically possible pressure. In such a case, at high pressures, the susceptibility to water is decreased while the total water present is increased.

The reflection coefficient, σ , produces its effect on the system in two ways. It acts as an attenuation on protein concentration and thus has an effect similar to changes in C_c . It also acts as a convective "leak" of protein and thus has an added effect similar to ω . The net effect is that, increasing σ decreases the low pressure water susceptibility, increases the high pressure total water, and shifts the transition region right. It does not have an effect on high pressure water susceptibility.

The other component parameters influence the curve shape of the lung water function curve in the same ways as the parameters already presented. Changes in P_1 have no effect on the curve (because of its incorporation into ΔP). Changes in V_0 will shift the whole curve up and down. Changes in K_i will rotate the entire curve. Changes in G_1 will have a dual effect. If $1/G_1$ is significant compared to $1/L_p$, a change in G_1 will produce the same effect as a change in L_p . In addition, G_1 acts as the gain between J_1 and V_i regardless of its magnitude. Thus, changing G_1 will rotate the entire curve.

The model can be interpreted in terms of dominating behavior in the two regions. In the low pressure region, the dominant process is the diffusion of protein into the interstitium. In the high pressure region, the dominant process is the hydrostatic pressure driven flow of water into the interstitium.

4.5.2.4 "System" parameters

Although various possibilities existed, there is a reason for the particular groupings of component parameters chosen to form the three system variables, α , β , and γ and for expressing our model function in terms of these variables. This particular combination of variables is

best for characterizing key features of the behavior of the system.

As stated before, α represents the total system series conductance. At high fluxes, when the effect of protein is unimportant, it specifies how easily fluid flows from the capillary into the lymphatic. β has units of flux and can be labeled the "critical fluid flux". It, in effect, represents the ratio between protein entering the interstitium by diffusion to convective protein "wash-out". γ has units of inverse concentration and represents the ratio of total system hydrodynamic conductance to total system protein conductance. At low pressures it specifies the importance of capillary protein resistance in limiting water flow.

The system parameter, α , expresses the slope of the function curve at high pressure limiting conditions. It is important only at high pressures. Its makeup indicates that G_1 and L_p compete in importance in determining this slope.

The parameter, β , expresses the flux at which the transition point will occur. Its composition indicates that ω and σ are equally likely to influence this point, but in opposite ways.

γ give information about the slope of the function curve at lower pressures. It is only of importance if near or greater in magnitude to one. If much greater, it acts as a scale to α , the slope at high pressure. Its composition indicates that changes in σ are more important than changes in ω .

Combinations of these variables characterize other features of the system. $\beta\gamma C_c/\alpha$ gives the x-intercept (zero flux) of the high pressure line. The parameters $\beta\gamma C_c/\alpha$ and $\beta\gamma$ give information about the boundaries

of the transition zone (and therefore its width). The choice between these depends on the size of $\beta\gamma$ and on which boundary. On the left boundary, $\beta\gamma C_c/\alpha$ is the relevant combination if $\gamma C_c \gg 1$, otherwise it is β/α . On the right boundary, $\beta\gamma C_c/\alpha$ is used if $\gamma C_c \gg \xi$ and β/α is used otherwise.

4.5.2.5 Implications of lymphatic concentration prediction

Our model contains no new information for the interpretation of high flow conditions in lymphatic cannulation experiments. Under such conditions, traditional models that consider only the membrane provide the same relationship between interstitial protein concentration and reflection coefficient as ours. But our model does provide new insights involving the lower pressure and transition pressure region. We have shown that a transition region exists and is probably important in measurement on normal lung. In abnormal lung, the transition region may extend to the highest possible pressures. In such a case, any attempt to derive a reflection coefficient from lymphatic data would give erroneous results.

4.5.3 Assumptions and considerations

This is the appropriate place to discuss the validity of some of the assumptions employed in our model. In all of the above calculations, we have considered the membrane parameters to be completely independent of one another. While this is the proper approach dictated by the Kedem and Katchalsky membrane representation, it is probably physically unreasonable. The homogeneously sized pore model, for example, shows a high degree of interdependence between the membrane parameters. It is

probably unreasonable to expect to be able to increase L_p without increasing ω or σ . But a physical situation could be hypothesized in which this would be possible. Such a situation would exist if there were two pore sizes, one large enough for both albumin and water and one large enough for only water. Changes in the small pore size would change L_p but not ω . Since it has not yet been possible to select the correct physical model describing the membrane, we have elected to keep the membrane parameters independent to explore limiting behavior.

We have modeled the behavior of the interstitium and lymphatic with linear models. This differs from the practice of many others. The results of our model do not by any means preclude the existence of non-linear behavior of the interstitium or lymphatic. But, neither do they require it to explain the observed behavior of the lung. Incorporating a non-linear component model into our system would merely change the curvature of our curve. It might be that the mechanisms of our approach predominate at lower pressures whereas saturation of the lymphatic or non-linear compliance becomes important at higher pressures.

Since G_1 always appears as a pair with L_p in our fluid flux equation, the behavior of the presented plots would not change at all if $1/G_1$ were set equal to zero. This indicates that the basic behavior of our curves can be explained using only the membrane parameters. But G_1 is necessary to connect our plots to lung water function plots (plots of V_i). Further, if $1/G_1$ is on the same order in size as $1/L_p$ or much larger, it would have an influence on curve shape in the same fashion as reported for L_p . This possibility, which might be caused physically by a large interstitial fluid flow resistance or a poorly responsive lymphatic pump, has not been considered by others. This means that interpretations of membrane state

based on, for example, lymphatic measurements, may be in serious error.

To interpret our results in terms of lung water accumulation, one has to include the presence of the interstitium and describe its behavior. Thus, while a curve with a shape like that of the experimentally measured lung water function curve may be produced with a model considering only the membrane, the actual lung water function curve can only be produced by considering interstitial compliance and may be incorrect unless one also considers the contribution of lymphatic conductance. A multi-component system model is needed to properly study lung water dynamics.

4.5.4 The Prichard model

The only model we found in the literature which takes an integrated approach to lung water modeling similar to ours is one created by Prichard, Rajagopalan, and Lee [71]. Their formulation is as follows (expressed in terms of our variable set). They start by using the Kedem and Katchalsky equations to describe the membrane:

$$J_{vm} = L_p ((P_c - P_i) - \sigma RT (C_c - C_i))$$

$$\dot{n}_m = J_{vm} \bar{C} (1-\sigma) + \omega (C_c - C_i)$$

Note that the first equation assumes a linear relationship between solute concentration and osmotic pressure. They next assume that $\sigma = 1$, effectively decoupling protein and water flow and producing the following two equations:

$$J_{vm} = L_p ((P_c - P_i) - RT (C_c - C_i)) \quad (4.22)$$

$$\dot{n}_m = \omega (C_c - C_i) \quad (4.23)$$

The lymphatic fluid and solute fluxes are described by the two equations:

$$J_{v1} = f_2(V_i) \quad (4.24)$$

$$\dot{n}_1 = J_{vm} C_i \quad (4.25)$$

where $f_2(V_i)$ is a function that describes the dependence of lymphatic fluid flux on interstitial volume. They relate the interstitial hydrostatic pressure to interstitial volume using the function:

$$P_i = f_1(V_i) \quad (4.26)$$

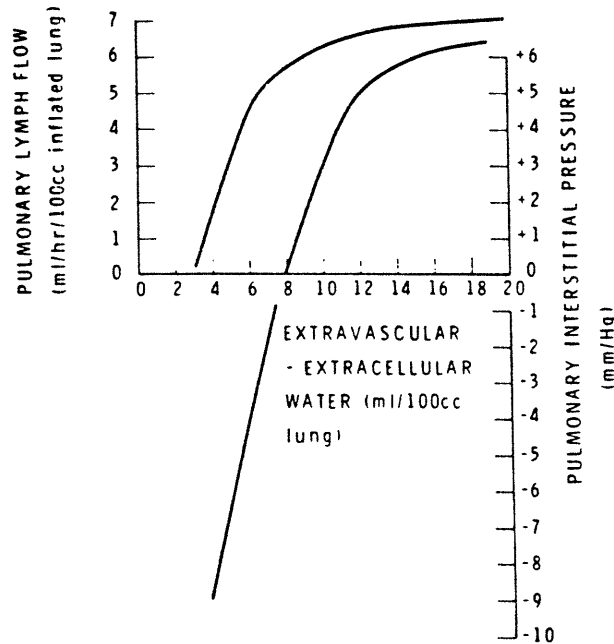
Equations (4.22), (4.23), (4.24), (4.25), and (4.26) are combined by noting the $J_{vm}=J_{v1}$ and $\dot{n}_m=\dot{n}_1$ at steady-state to produce the following equation which embodies their entire model:

$$f_2(V_i) = L_p \left((P_c - f_1(V_i)) - RT C_c \frac{f_2(V_i)}{f_2(V_i) + \omega} \right) \quad (4.27)$$

The derivation up to this point differs from our model only in the assumption that σ equals one. The two diverge when assigning the functions, $f_1(V_i)$ and $f_2(V_i)$. We chose linear relationships for both. Prichard et al. used the functions diagrammed in Figure 4-10. In their words: "These curves were constructed from the discussion in a recent comprehensive view (sic) by Staub [89] and in addition rely particularly on the data of Pearce and Wong [68] and Hughes et al. [40, 41]". A review by us of these four articles showed that none of them explicitly presents either of these two functions. Apparently, Prichard et al. created the functions by assuming a certain functional shape based on the discussions of Staub and then defined the positions of the curves by using data gathered by Pearce and Wong and Hughes et al.

Prichard et al. present the results of their model in the form of plots of extravascular water versus capillary pressure with either π_c (capillary osmotic pressure), L_p , or ω as a variable parameter. Below are two of their plots. These are to be compared with our plots of Figure

Figure 4-11: Prichard's Functions for Interstitial Compliance and Lymphatic Conductance

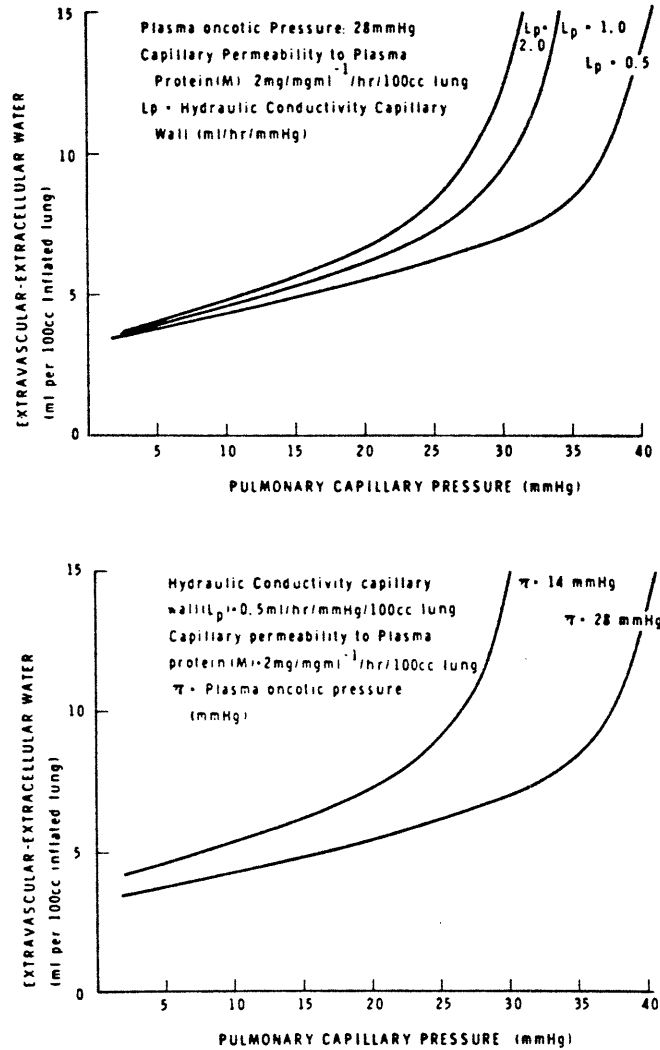


4-5. In the first, non-cellular extravascular water is plotted as a function of capillary pressure with capillary osmotic pressure ($\pi=C_cRT$) as the variable parameter. In the second, the same variables are plotted with L_p as the parameter.

The plots are of the same general form as ours. However, they do not give the same parameter dependencies. For example, in the first figure, doubling the protein concentration does not produce a doubling of the protective effect as our model predicts it would. Similarly, in second figure, changing L_p causes a shift in the curve without a change in slope, precisely the opposite effect predicted by our model.

The discrepancy results from the functions chosen by Prichard to describe compliance and lymphatic flux. Although their choices were based on the discussion of Staub, Staub was suggesting these choices to explain

Figure 4-12: Lung Water Behavior Predicted by Prichard Model
in Prichard et al. - 1977 [71]



the non-linear function curve without considering the possible contribution of the protein dilution effect described in this thesis. Prichard et al.'s work is thus not a fair examination of the acceptability of using the protein protective effect as the sole means for explaining the shape of the lung water function curve. But it is still of extreme importance to our work.

The Prichard et al. model is the only model found that quantitatively predicts the shape of the lung water function curve. Yet it produces results quite different from ours. The differences can be tested by experimentally determining the dependence of the shape of the lung water function curve on L_p , ω , and C_c . Such experiments would go a long way in determining whether it is acceptable to assume linear compliance and/or lymphatic conductance.

4.5.5 Measurements and Dimensional analysis

We started with 6 variables and 6 parameters and, through our model, reduced these to three variables and three parameters. Then through dimensional analysis, these were reduced to three variables with no parameters. This sequence deserves discussion.

When a physiologist studies the lung, he or she describes the system in terms of the properties of the components of the system such as L_p and σ . The physical meaning of these are well understood. Measurements on the system attempt to attach values to these parameters. When a model is made for a system, a new set of parameters comes into being. Their meaning depends on the definition of the model. But they are real parameters nonetheless.

In dimensional analysis, new variables are derived which have the system parameters incorporated into them. Their meaning, however, still depends on the definition of the model. Lung physiologists try to attach values to the component parameters. But there is no inherent reason why values obtained for component parameters should be any more useful than values obtained for α , β , and γ . Similarly, there is no inherent reason why measurements could not be geared directly towards measuring the

dimensionless parameters. Taking the approach of dealing with "high level" parameters and variables can greatly simplify the clinical analysis of the lung if the underlying model is reasonable. And dealing with non-dimensional forms of the model also makes it much easier to validate the reasonableness of the model.

4.6 Summary

In this chapter, we formulated, solved, and analyzed the steady-state form of our model. The results were presented in terms of equations of both membrane fluid flux and of lymphatic protein concentration as functions of capillary protein concentration and capillary hydrostatic pressure.

Both the flux equation and the concentration equation had two-part behaviors. The flux equation demonstrates a significant "safety region" at low pressures in which pressure changes produce little changes in membrane flux and total lung water. Three parameters are found sufficient to characterize the behavior of either equation with two of these shared by both equations.

Dimensional analysis showed that the model function could be expressed in terms of three dimensionless variables with no parameters. With reasonable physical parameters values used in the equation, the model predicted behavior similar to that observed experimentally. In the next chapter we will extend our work by exploring the behavior of a multi-solute system and the implications of assuming a distributed system as compared to the current lumped-system approach.

Chapter 5

MODIFICATIONS TO THE STEADY-STATE MODEL

In the previous chapter, we presented and characterized the single-solute, steady-state model. In this chapter, we develop two models which explore the effects of two important variations in the assumed structure of the basic lung water system. The first model considers the effects on the system of more than one permeable solute. The second model is a two-segment serial model which is presented as an approximation to a serially distributed system.

The chapter is organized as follows. In the first section, we develop, characterize, and discuss the multiple solute model. In the second section we present the two-segment serial model. First we present the reasoning behind its creation. Then the model is formulated and the methods used to characterize it presented. Next we explore the system behavior predicted by this model concentrating on differences between it and the basic steady-state model. Finally, we discuss the implications of the behavior exhibited by the serial model. In the third section the two-solute and two-segment serial models are summarized.

5.1 Multiple Solutes

The model just presented considered a single solute. How would the existence of multiple solutes modify the behavior of the model? A two solute model should serve to manifest the essential behavior changes caused by the presence of multiple solutes. A specific application of

this effort is to examine the behavior of a system in which both albumin and globulin have non-zero permeability. In the model of previous chapter, only albumin could cross the membrane. In that model, globulin was handled by treating its capillary osmotic pressure contribution as a correction to the capillary hydrostatic pressure. But how might the system behave if globulin was treated as having a finite permeability? Table 5-I summarizes this model. The important additional assumption is that the solutes do not interact. Thus the membrane behavior of each solute is governed by two parameters, σ and ω . The major modification embodied in this model is the addition of new membrane and lymphatic flux equations for the new solute.

Again we choose C_c and ΔP as the independent variables and J_v as the dependent variable. The solution has J_v implicit in the equation:

$$J_v = \alpha \Delta P - \left(\beta_1 \gamma_1 C_{c1} \frac{J_v}{J_v + \beta_1} \right) - \left(\beta_2 \gamma_2 C_{c2} \frac{J_v}{J_v + \beta_2} \right) \quad (5.1)$$

where:

$$\Delta P = P_c - P_1$$

$$\alpha = \frac{1}{(1/G_1 + 1/L_p)}$$

$$\beta_1 = \frac{2 \omega_1}{1 + \sigma_1}$$

$$\beta_2 = \frac{2 \omega_2}{1 + \sigma_2}$$

$$\gamma_1 = \frac{\sigma_1^2 RT}{\omega_1 (1/G_1 + 1/L_p)}$$

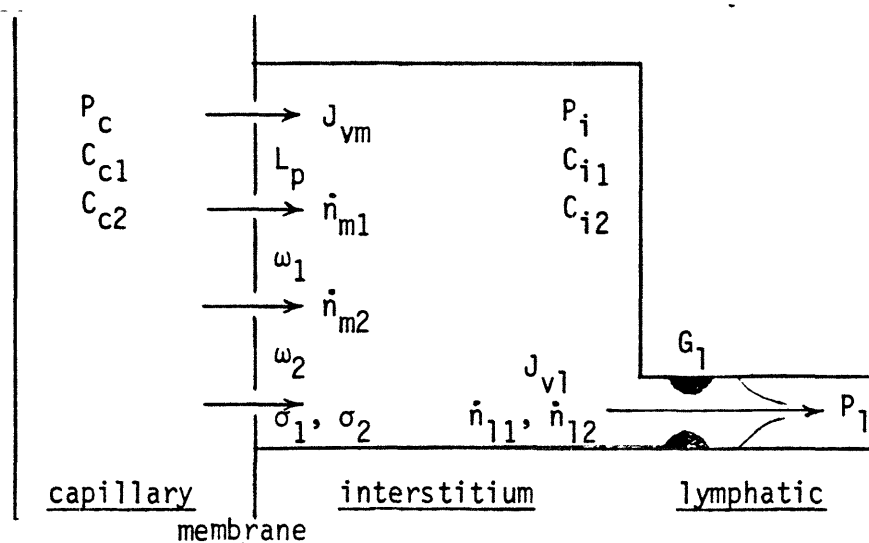
$$\gamma_2 = \frac{\sigma_2^2 RT}{\omega_2 (1/G_1 + 1/L_p)}$$

This can be given in non-dimensional form as:

$$J_v^* = \Delta P^* - C_{c1}^* \frac{J_v^*}{J_v^* + 1} - \rho_2 C_{c2}^* \frac{J_v^*}{J_v^* + \rho_2} \quad (5.2)$$

where:

Table 5-I: Essentials of the Two Solute Steady-State Model

Equations

$$J_{vm} = L_p \left[(P_c - P_i) - \sigma_1 RT (C_{c1} - C_{i1}) - \sigma_2 RT (C_{c2} - C_{i2}) \right]$$

$$J_{vl} = (P_i - P_l) G_l$$

$$\dot{n}_{m1} = J_{vm} \left[\frac{C_{c1} + C_{i1}}{2} \right] (1 - \sigma_1) + \omega_1 (C_{c1} - C_{i1})$$

$$\dot{n}_{m2} = J_{vm} \left[\frac{C_{c2} + C_{i2}}{2} \right] (1 - \sigma_2) + \omega_2 (C_{c2} - C_{i2})$$

$$\dot{n}_{l1} = J_{vl} C_{i1}$$

$$\dot{n}_{l2} = J_{vl} C_{i2}$$

$$\frac{dV_i}{dt} = J_{vm} - J_{vl} = \emptyset$$

$$\frac{dN_{i1}}{dt} = \dot{n}_{m1} - \dot{n}_{l1} = \emptyset$$

$$\frac{dN_{i2}}{dt} = \dot{n}_{m2} - \dot{n}_{l2} = \emptyset$$

Variables: C_{i1} , C_{i2} , P_i , J_{vm} , J_{vl} , \dot{n}_{m1} , \dot{n}_{m2} , \dot{n}_{l1} , \dot{n}_{l2}

Parameters: L_p , RT , σ_1 , σ_2 , ω_1 , ω_2 , G_l

$$\Delta P^* = \frac{\alpha}{\beta_1} \Delta P \qquad J_v^* = \frac{1}{\beta_1} J_v$$

$$C_{c1}^* = \gamma_1 C_{c1} \qquad C_{c2}^* = \gamma_2 C_{c2} \qquad \rho_2 = \beta_2 / \beta_1$$

The complete contribution of each solute is contained in separate terms. Additional solutes would add new terms of the same form as the solute terms already present.

Looking at limiting behavior:

limit for small J_v :

$$J_v = \frac{\alpha \Delta P}{1 + \gamma_1 C_{c1} + \gamma_2 C_{c2}} \qquad (5.3)$$

limit for large J_v :

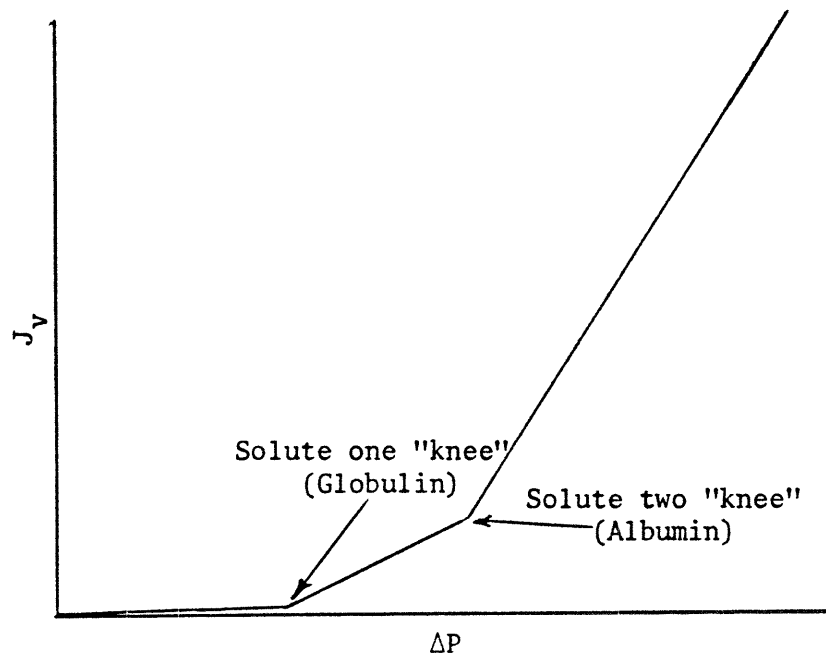
$$J_v = \alpha \Delta P - \beta_1 \gamma_1 C_{c1} - \beta_2 \gamma_2 C_{c2} \qquad (5.4)$$

At low values of J_v , the effect of each solute is to change the slope. Each solute acts as an additional effective resistance in series with the membrane and lymphatic fluid flow resistances. At higher values of J_v , the effect of each solute is to shift the lung water function curve but leave the slope unchanged. The region of transition from one behavior to the other depends on the relative size of the two terms in the denominator of each solute expression and is different for each solute. The effect, diagrammed in Figure 5-1 is that each solute will produce a separate knee.

This is not a completely unexpected result. The presence of multiple solutes has the effect of broadening the transition zone, modifying the slope at low pressure, and modifying the offset at high pressure.

These results can be interpreted in terms of albumin and globulin by considering the two solutes of this model to represent these two proteins. Each protein will have a transition point which will depend on the value

Figure 5-1: Diagram of Effect of Presence of Multiple Solutes



of its respective $\beta = 2\omega/(1+\sigma)$ parameter. Since globulin has a larger σ and a smaller ω than albumin, it will have its knee at a lower pressure. At low pressures, the presence of globulin will decrease the slope of the lung water function curve. At high pressures, it will cause a rightward shift in terms of pressure equal to:

$$C_{cg} \left(\frac{\beta_g}{\alpha} \right) \gamma_g = C_{cg} \frac{2 \sigma_g^2}{1 + \sigma_g} RT$$

where the subscript "g" represents globulin. This shows that the shift caused by globulin depends only on σ_g and C_{cg} . If σ_g is near one, the shift is given by $C_{cg}RT$ which is π_{cg} , the capillary osmotic pressure of globulin.

In summary, at high pressures, it makes little difference whether globulin is incorporated directly into the model as with the above treatment or indirectly in the form of a correction to capillary

hydrostatic pressure as in the treatment of the previous chapter. However, incorporating globulin both modifies the slope in the low pressure region and complicates the behavior of the transition region. But even in these two regions, albumin is responsible for most of the behavioral features of the system. Thus the treatment of the previous chapter is a reasonable simplification which can be easily modified if circumstances warrant.

5.2 Multiple Serial Segments

5.2.1 Background to the serial-segment model

The steady state model presented in the last chapter considers the behavior of a single compartment, lumped system. As discussed in Chapter 3, the pulmonary capillary might be better modeled as an axially distributed system. Because the membrane fluxes are small compared to capillary flow, it is reasonable to assume that capillary concentration is axially constant even in a distributed system. But the capillary pressure may not be constant.

How might a distributed system behave differently from our lumped system? A distributed model containing all of the components of our lumped model would be extremely complicated to formulate and solve. As a compromise, we elect to use a two-segment model as a first-order approximation to the behavior of an infinite-segment (distributed) model. In this model, blood flows serially through two capillary segments, each surrounded by a corresponding interstitial segment. The two segments are interdependent.

The possible complications that arise if the actual system is better

described by the two-segment model become clear if one examines the behavior of one of the J_{vm} versus $P_c - P_1$ (ΔP) plots of Figure 4-5. It is possible that the capillary pressure in one segment places it on the left of the knee while the pressure in the other segment places it on the right of the knee. In this case, the average behavior of the system is not the equivalent of a lumped system with the same average pressure. In terms of total system J_{vm} , for example, the higher pressure segment will completely dominate the behavior of the system.

There are two major objectives underlying the creation of the two-segment model. The first is to determine general behavioral differences that might exist between a lumped and a distributed system. The second is to determine the sensitivity of our conclusions of the previous chapter to the assumption of a lumped system.

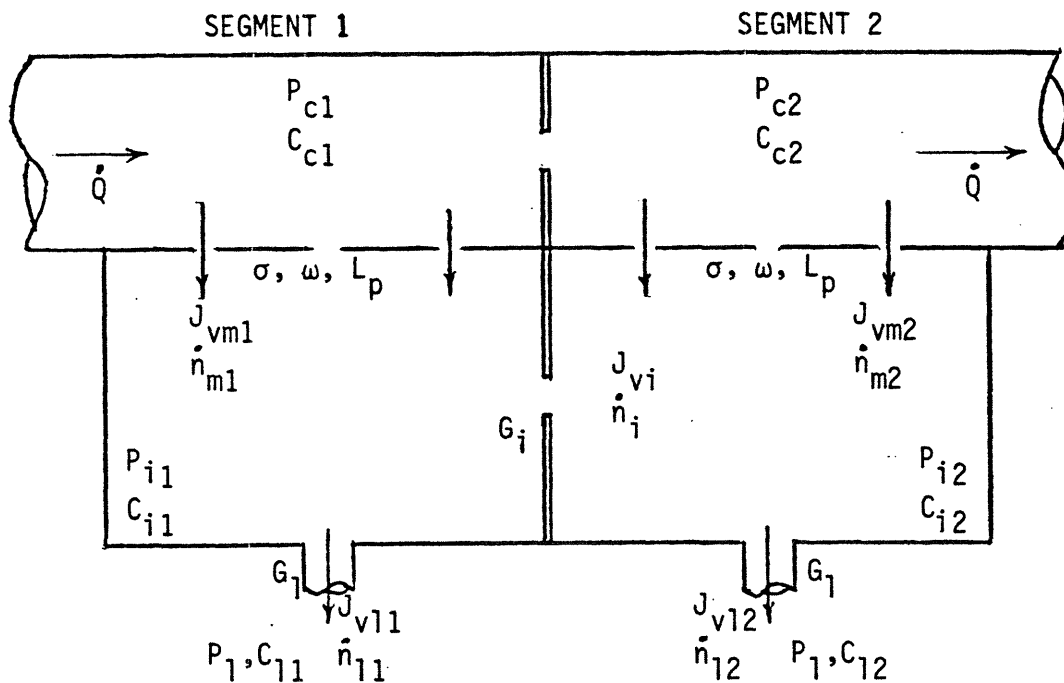
5.2.2 Formulation of the two-segment model and its solution

The model developed to meet these objectives consists of two functionally identical lumped systems in series. The capillaries of the two segments are connected through a passive resistance allowing the pressures in the capillaries of the two segments to be different. Similarly, the interstitiums of the two segments are connected through a passive, non-sieving resistance having a conductance, G_i . For simplicity, we assume no diffusion across the interstitial connection. The implications of this assumption will be discussed later. Pressure driven flow, J_{vi} , can occur between the two segments. The same parameter set is used for both segments. In particular, both segments have identical membrane parameters, capillary concentrations, lymphatic conductances, and lymphatic pressures. The only additional parameter (besides a second

capillary pressure) is the interstitial bulk fluid conductance, G_i . A major issue in characterizing this model is examining the importance of the value assigned to G_i .

Figure 5-2 presents a diagram of the model and Table 5-II presents the mathematical formulation of the model and a list of the model parameters and variables.

Figure 5-2: Diagram of Serial Two-Segment Model



The mathematical formulation is similar to that of the single-segment case except that each membrane and each lymphatic outlet has a separate set of equations to define the fluxes of water and solute. In addition, there are two sets of mass balance equations for water and solute in each interstitium plus a final equation describing the behavior of the interstitial barrier for a total of 11 primary equations.

Table 5-II: Mathematical Formulation of Serial Two-Segment Model

ASSUMPTIONS:

1. Pressure drop in capillary is concentrated at a single point
2. Q is large compared to J_{vm} : Q is effectively constant
3. $Q C_c$ is large compared to \dot{n}_m : $C_{c1} = C_{c2}$
4. Lymphatic conductance is constant
5. Pressure drop in interstitium is concentrated at a single point
6. Membrane parameters are constant and homogeneous

EQUATIONS:

$$J_{vm1} = L_p [(P_{c1} - P_{i1}) - \sigma(C_{c1} - C_{i1})RT]$$

$$J_{vm2} = L_p [(P_{c2} - P_{i2}) - \sigma(C_{c2} - C_{i2})RT]$$

$$J_{v11} = (P_{i1} - P_1) G_1$$

$$J_{v12} = (P_{i2} - P_1) G_1$$

$$\dot{n}_{m1} = J_{vm1} \bar{C}_1 (1-\sigma) + \omega(C_{c1} - C_{i1})$$

$$\dot{n}_{m2} = J_{vm2} \bar{C}_2 (1-\sigma) + \omega(C_{c2} - C_{i2})$$

$$\dot{n}_{11} = J_{v11} C_{i1}$$

$$\dot{n}_{12} = J_{v12} C_{i2}$$

$$J_{vi} = (P_{i1} - P_{i2}) G_i$$

$$\frac{dV_{i1}}{dt} = \emptyset = J_{vm1} - J_{vi} - J_{v11}$$

$$\frac{dV_{i2}}{dt} = \emptyset = J_{vm2} + J_{vi} - J_{v12}$$

$$\frac{dN_{i1}}{dt} = \emptyset = \dot{n}_{m1} - \dot{n}_{11} - C_{i1} J_{vi}$$

$$\frac{dN_{i2}}{dt} = \emptyset = \dot{n}_{m2} - \dot{n}_{12} + C_{i1} J_{vi}$$

VARIABLES: J_{vm1} , J_{vm2} , J_{v11} , J_{v12} , \dot{n}_{m1} , \dot{n}_{m2} , \dot{n}_{11} , \dot{n}_{12} , J_{vi} , C_{i1} , C_{i2} ,
 P_{i1} , P_{i2}

PARAMETERS: P_{c1} , P_{c2} , C_c , L_p , σ , ω , G_1 , G_i , P_1

These 11 equations can be collapsed down to three which are not amenable to further analytical solution. The behavior of this model was explored using a numerical solution implemented on a digital computer using the COSNAF subroutine, a routine designed for solving coupled sets of equations, which is part of the Numerical Algorithms Group (NAG) scientific subroutine package. All computations were performed on a Honeywell 680 computer running under the Multics operating system. The parameter values employed are the same as those used for the single-segment model which were presented in Table 3-III. Note again that all extrinsic parameters are normalized to capillary surface area.

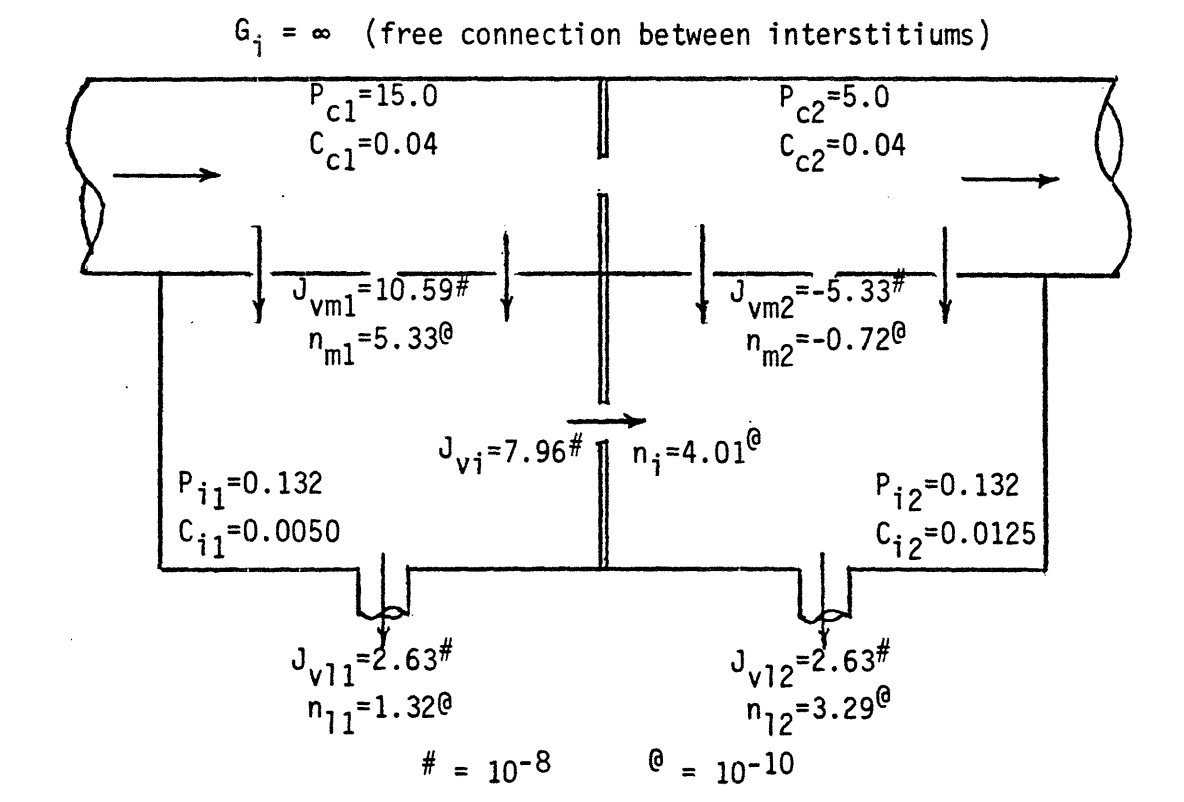
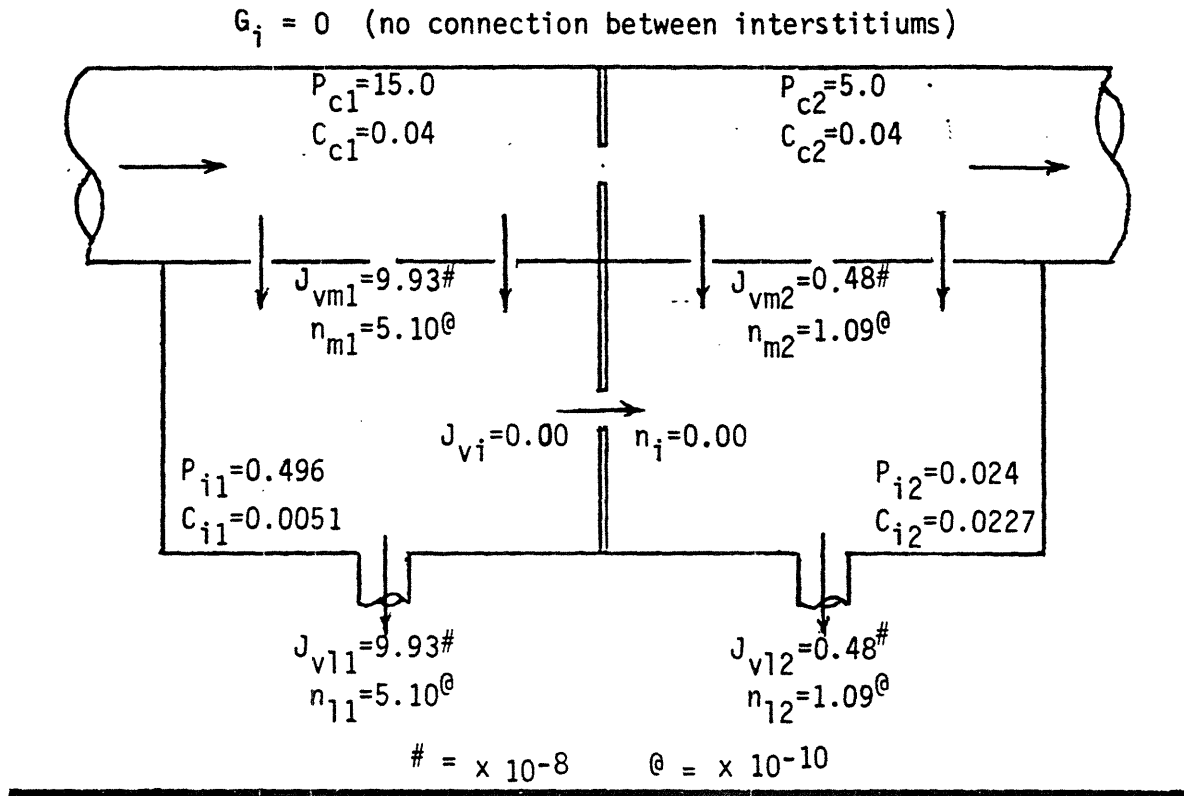
5.2.3 Characterizing the two-segment Model

5.2.3.1 General behavior of the model

Figure 5-3 presents, in the form of labeled diagrams, the results of the solution of the model for two different values of G_i . In both cases, the ΔP value in the first segment is 15 torr and in the second segment is 5 torr. In the first diagram, $G_i=0$. That is, the two segments are completely independent. For this case, the values for J_{vm1} , J_{v11} , \dot{n}_{sm1} , \dot{n}_{s11} , P_i , and C_i are all identical to the values obtained by solving the two segments separately using the analytical solution for the single-segment model, equation (4.1). Note that, although the capillary pressure is one third as high in segment 2 as in segment 1, J_{vm} and P_i are only 5% as high and C_i is over 400% as high. This is the first hint of the possibility that "aberrant" behavior may occur when the two segments can interact.

Figure 5-3b illustrates the same situation except with G_i set equal to 1×10^4 (effectively infinite). An infinite conductance would be

Figure 5-3: Diagrammatic Presentation of Behavior of Serial Two Segment Steady-State Model



expected to make the interstitial pressures in the two segments equal leading to the equality of lymphatic fluid fluxes. This is born out in the diagram. But note that the capillary membrane fluid fluxes are not equal to each other nor are they equal to their corresponding lymphatic fluxes. The difference is accounted for by the flow existing from the interstitium of segment 1 into the interstitium of segment two. The volume of this cross-interstitial flow is very significant. In fact, it is greater than either individual segment's lymphatic flow. It carries with it a very dilute concentration of solute and thus serves to greatly dilute the solute within the segment 2 interstitium.

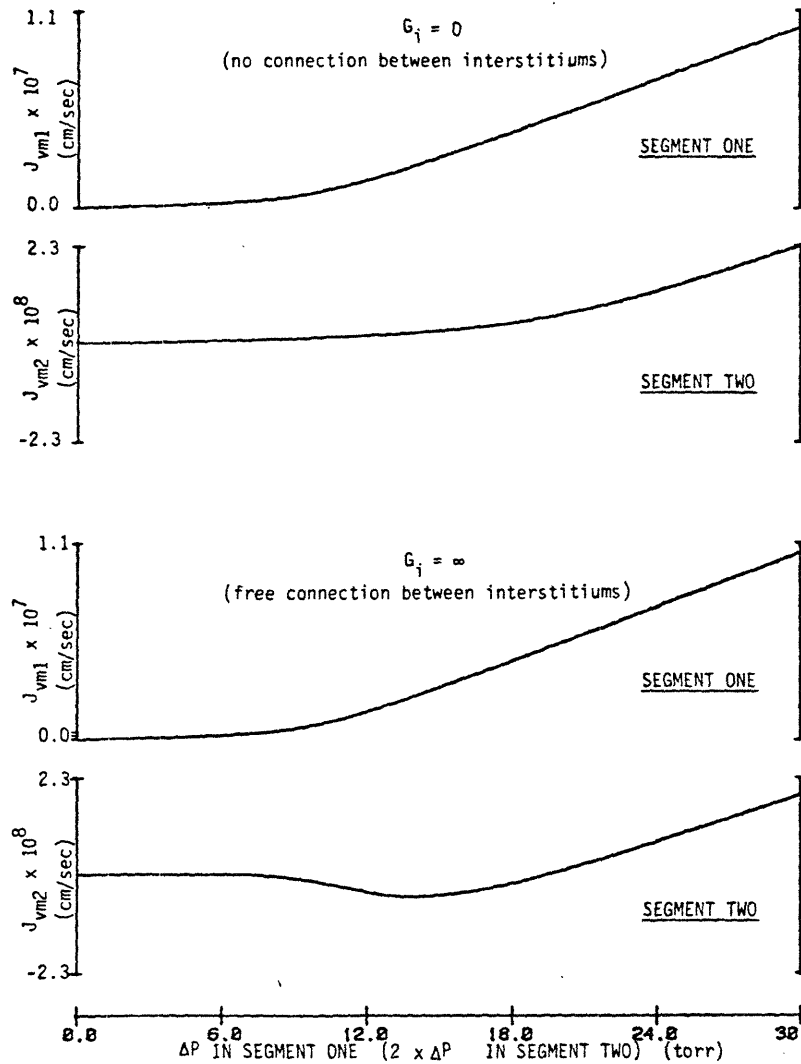
An extremely interesting behavior occurs in segment 2: its membrane fluid flux is actually negative! That is, fluid is entering the capillary from the interstitium. Since the only entrance of fluid into the entire system is across the segment 1 capillary membrane, a fluid circuit exists in which fluid enters through the segment 1 capillary membrane, crosses through the interstitium into the interstitium of segment 2 and crosses the segment 2 capillary membrane back into the capillary.

5.2.3.2 "Aberrant" behavior of the two-segment model

Exactly how much effect a connected interstitium has on the system can be observed in Figure 5-4 which contains plots of J_{vm} versus ΔP for both segments. These were produced by solving the model equations at a range of ΔP pairs but always maintaining a fixed ratio between ΔP_1 and ΔP_2 of 2:1. In effect, this assumes a "linear" pressure drop in the capillary. Included are curves for both small G_i and large G_i .

The curves for small G_i are, as expected, identical to the corresponding curves produced by the single-segment model for both segment

Figure 5-4: Plots of J_{vm} versus ΔP for the Serial Two-Segment Model



1 and segment 2 (see Figure 4-5). The segment 1 curve for the large G_i case is not much different from the corresponding small G_i segment 1 curve. The main effect observed is that J_{vm1} is raised slightly because there are now two ways for fluid to escape the interstitium of segment 1 once it has entered. In contrast, for the case of large G_i , the character of the segment 2 curve is changed completely. It rises very slightly with

increasing pressure at low pressure, then starts dropping, actually going negative, and then start rising again. This "aberrant" behavior occurs when segment 1 is operating on the opposite side of the "knee" from segment 2. Note, however, the magnitude of J_{vm2} . It is far smaller than J_{vm1} . The total J_{vm} flux thus shows only the slightest hint of "aberrant" behavior.

Figure 5-5 shows the corresponding plots for interstitial protein concentration. For the large G_i case, note once again the small effect on segment 1 behavior caused by the cross-interstitial flow but the significant dilution of segment 2 interstitial protein.

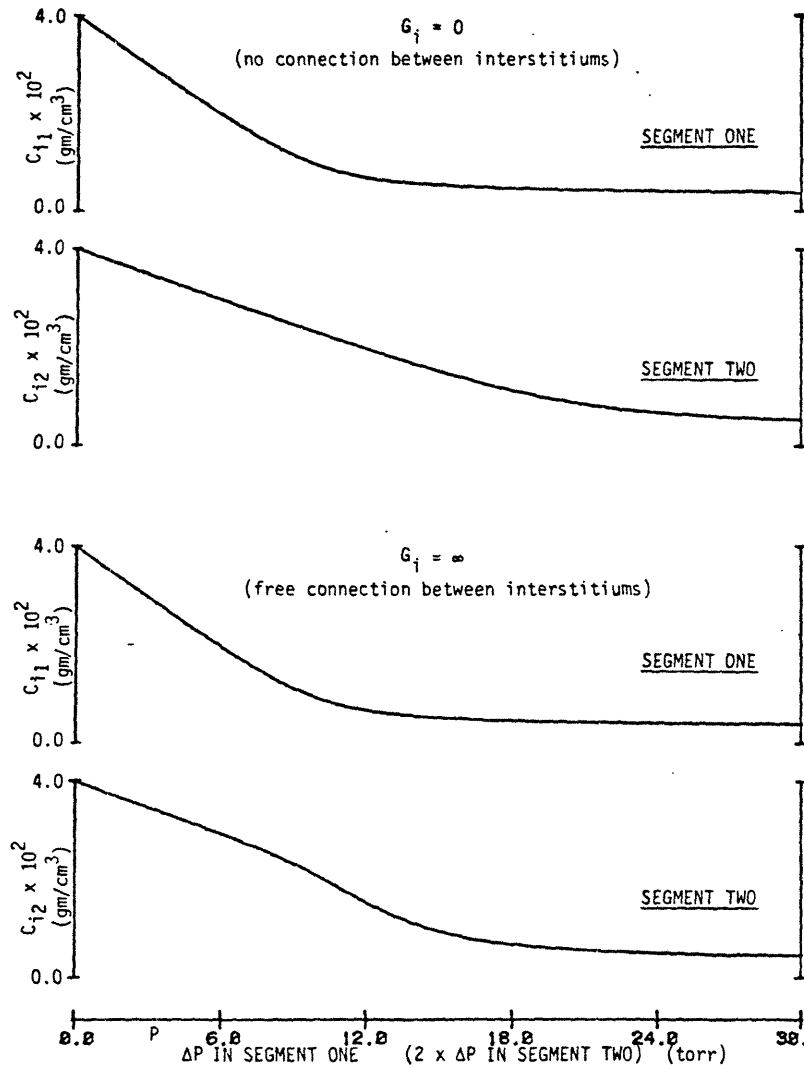
5.2.3.3 Comparison of water behavior of one and two segment models

It is of interest to examine how the overall behavior of a two-segment model is different from the equivalent one-segment model in terms of lung water dynamics. For this, we compared the behavior of a two-segment system with segment capillary pressures at 15 and 5 torr to a single-segment model with the same average capillary pressure, 10 torr. In this case, the interest was not in the individual segments but in the behavior of the overall system. Table 5-III presents a comparison of the single-segment model to the two-segment model at three different values of G_i :

$$\begin{aligned} G_i &= 0.001 G_1 \\ G_i &= 0.5 G_1 \\ G_i &= 1000 G_1 \end{aligned}$$

Our interest is in the system variables representing the total lymphatic fluid flow, the total lymphatic albumin flow, the interstitial pressure, and the lymphatic albumin concentration. Since the extrinsic system variables, J_v and \hat{n} are normalized to membrane surface area, the

Figure 5-5: Plots of C_i versus ΔP for the Serial Two-Segment Model



appropriate way of comparing the two-segment model to the one-segment model is by using the average value of these two variables, $J_{v,average}$ and $\bar{n}_{average}$. P_i is not an extrinsic variable, but we are interested in it because of its relationship to V_i . Assuming a linear relationship between P_i and V_i , the appropriate method of presenting P_i in terms of the whole systems behavior is $P_{i,average}$. Our concern with C_i is its use as a way

Table 5-III: Total System Behavior of Serial Two Segment Model

	TWO SEGMENT MODEL			SINGLE SEGMENT MODEL
	$G_i=0.001G_1$	$G_i=0.5G_1$	$G_i=1000G_1$	
$J_{v,average}$	5.20×10^{-8}	4.04×10^{-8}	2.63×10^{-8}	2.83×10^{-8}
$\dot{n}_{average}$	3.10×10^{-10}	2.68×10^{-10}	2.30×10^{-10}	2.58×10^{-10}
$P_{i,average}$	0.260	0.202	0.132	0.141
$C_{1,average}^*$	0.0059	0.0066	0.0087	0.0091

$$J_{v,average} = (\text{cm/sec})$$

$$\dot{n}_{average} = (\text{gm/cm}^2)$$

$$P_{i,average} = (\text{torr})$$

$$C_{1,average} = (\text{gm/cm}^3)$$

* $C_{1,average}$ is the flow weighted average of lymphatic concentrations

of relating the behavior of our model to the results of lymphatic cannulation experiments. For this reason, the appropriate system behavior in terms of albumin concentration is given by a flow-weighted average of lymph albumin concentration, $C_{1,average}$. Thus, presented in the table are values for $J_{v,average}$, $\dot{n}_{average}$, $P_{i,average}$, and $C_{1,average}$.

The first thing to note from Table 5-III is the general progression of the numbers in going from the low interstitial conductance to the high interstitial conductance case. The average lymphatic fluid flux is almost halved as is the average interstitial pressure. However, the lymphatic albumin flux decreases by only 26%. The flow-weighted average lymphatic albumin concentration increases by 47%.

The results for all three two-segment cases are within the same range as the values for the single-segment case. Specifically, the $J_{v,average}$, $\dot{n}_{average}$, and $P_{i,average}$ values for the single-segment case all fall between those of the high and medium interstitial conductance cases, lying a little closer to those of the high conductance case. The value for $C_{1,average}$ for the single-segment model fall outside of the range of values of any of the two-segment model cases. However, it is closest to that of the high conductance case.

5.2.4 Serial-segment model discussion and implications

5.2.4.1 Specific issues

It is evident from Figure 5-3 that a gradient of solute exists between the two segments' interstitiums. It would be expected that this gradient might produce diffusion of solute between segments, a possibility ignored in this model. The result of having allowed inter-compartment diffusion would have been to slightly concentrate the segment 1 interstitium and thus increase J_{vm1} . But the existence of diffusion would still not be expected to alter significantly the general behavior observed here.

An important result of modeling the system with a two-segment model is that, unlike the single-segment model, the lymphatic conductance, G_1 , has an importance independent of L_p . Thus the argument of Chapter 4 can no longer be used that the effect of changes in G_1 on the system can be studied by looking at the effect of changes in L_p . For the two-segment model, it is much more critical that a reasonable value of G_1 be known.

In the results given above, we showed that under certain conditions,

an axially distributed system may have a flow circuit of fluid from one end of the capillary to the other through the interstitium. The existence of such a fluid circuit is interesting for a number of reasons. First, its existence indicates that there is a path for significant axial interstitial movement of solute and fluid. This is of possible importance when considering the behavior of tracers in which it is normally assumed that no axial movement occurs. It is also of physiological significance as a possible means for augmenting transport of metabolic substances to and from the interstitial cells.

The existence of an interstitial flow circuit was postulated by Guyton [30]. He used the pressure gradient between the arterial and venous ends of systemic capillaries measured using micropuncture techniques to create an argument for such a circuit [30]. However, he describes the situation in only semi-quantitative terms. Ours is a quantitative presentation in which a value for the magnitude of this circuit can be calculated and its sensitivity to system parameters studied. The key feature of note is the non-linear relationship between the axial capillary pressure drop and the cross-interstitial flux. It is interesting to note that, even though Guyton postulated a fluid circuit simply because of the existence of a capillary pressure gradient, the results of this model indicate that this pressure gradient could still exist without such a circuit if the axial conductance were sufficiently low.

All of the three methods we used to characterize the two-segment model have the interstitial fluid conductance, G_i as a parameter. In each case, the results vary significantly depending on the value of G_i . In work not presented, the effect of changes in G_i was found to have an upper

limit and a lower limit. Maximum sensitivity occurred at $G_i = 0.5 G_1$. As we stated above, there is no optimal basis for the selection of any particular G_i value except that it is probably not infinite because of the interstitial fibrin network that is known to exist.

Table 5-III is useful to determine how the two-segment model compares to the single-segment model in terms of interstitial fluid volume. For this application, we assume that $P_{i,average}$ is a good indicator of total interstitial fluid volume (this assumes a linear compliance). Except for very high conductances, the two-segment model has more fluid at equivalent capillary pressures: up to twice as much. At the highest interstitial conductance, the volume for the two-segment model is slightly lower than that of the one-segment model (about 7%). It is difficult to know the significance of this observation in the actual system without having an accurate value for G_i .

The lymphatic cannulation experiments discussed in the Chapter 2 assume a lumped system for their calculations of σ . Here again the results presented in Table 5-III prove interesting. The equation used for this calculation is usually $\sigma = 1 - (C_1/C_c)$ [67]. Table 5-III shows that, regardless of the value of G_i , the two-segment model always produces smaller lymphatic concentrations than the lumped model. In the extreme case with small G_i , the two-segment value is only 65% of the single-segment model. If an axially distributed model is a better representation of the actual system than a lumped model, values of σ currently being obtained by lymphatic cannulation experiments might significantly overestimate the true value.

5.2.4.2 General issues and conclusions

Capillary pressure must vary along its length for the two-segment model to predict results different from the one-segment model. As reported before, such a variation has been observed in the lung. If such a variation exists, it is likely to be continuous rather than occurring at a discrete point as in our model. However, this model is meant only as a first-order approximation of the behavior that might be expected in a true axially distributed system. For this application, the model serves its purpose. It shows the general areas in which an axially distributed model might be expected to behave differently from an axially lumped model.

To address the questions which directed the creation of this model, the following are the general conclusions resulting from this model. Firstly, the two-segment model, and by implication the distributed model, have some extremely interesting behavior which is quite different from that of a lumped model. This behavior might have particular bearing on tracer studies. But secondly, the magnitude of the difference in behavior does not seem great enough to warrant abandoning the use of a lumped model as a reasonable, simple approach useful for understanding steady-state lung water behavior.

5.3 Summary

In this chapter, we presented two extensions to the basic lumped, single-solute, steady-state model. In the first we modeled the effect of the presence of multiple solute and showed that additional solutes each add a new "knee" and tend to broaden the zone of transition, decrease the slope at low pressures, and shift the lung water function curve right with

no change in slope at high pressures. Multiple solutes (such as the combination of albumin and globulin) can thus be easily incorporated into our model without changing its basic character.

In the second model extension, we approximated the behavior of a axially distributed model through the use of a model in which the system is treated as having two serial segments. The model was formulated using the same principles and parameters as in the lumped model except that a finite pressure drop was allowed to exist between the capillaries compartments and between the interstitiums of the two segments.

Several interesting types of behavior were noted. For example, under certain conditions, there can be a 'negative' water flux across the capillary membrane in one of the segments in steady-state. There were differences between the lung water function curves produced by this model and by the lumped model. But the differences are not great enough to justify using a multi-segment model instead of a simpler lump model when modeling lung water dynamics in the lung.

Chapter 6

TRANSIENT BEHAVIOR OF THE LUNG WATER SYSTEM

In the previous two chapters, we explored how the steady-state condition of the lung water system might depend on the parameters and variables of the system. In this chapter we explore the nature of the transient response of the system to changes in these parameters and variables. This is done both to augment the steady-state related discussion and conclusions of the previous chapters and to provide general information on the time course of lung water events.

The chapter is organized into six sections. In the first section, we discuss in detail the rationale for studying transient behavior in the lung. Next, the formulation and method of characterization of the model is presented along with its predictions of system behavior. In the third section, we derive and test model simplifications that can be applied under limiting conditions. Next we present a qualitative discussion of the sequence of events that occur after various system variable changes. In the fifth section, we present relevant experimental data from the literature. Finally, the implications of this model and its results are discussed in detail.

6.1 Background and Rationale for Transient Model

There is both a clinical and a measurement related interest in understanding the transient behavior of the lung water system. One clinical interest is in understanding the pathological progression of

pulmonary edema. The clinician would like to understand both the sequence of events and the timing of each event leading up to edema in order to plan optimum treatment. There is also a clinical interest in understanding the time course of events following various treatments. Such knowledge would allow better assessment of the effectiveness of treatment.

In terms of measurements, the steady-state models in the previous two chapters assume "sufficient time" for transients to die out. Yet in the real world, unlimited time does not exist for stabilization. An understanding of system transient behavior is important in order to know how much time is sufficient after a system change to allow the assumption of steady-state. It is also important to know what problems might result from assuming steady-state in making measurements when this condition does not exist. For example, some of the features of the steady-state model might not be significant in a transient or "short term" experiment.

Our interest in this chapter, then, is to study how the system responds over time to changes in external conditions and internal component parameters. To conduct this study, we employ an extension of our basic steady-state model.

6.2 Transient Model Formulation and Characterization

6.2.1 Model formulation

The transient model presented in this chapter is a single-solute, single-segment, lumped model. It has the same structure as the steady-state model presented in Chapter 4 except that provisions have been included for water and protein accumulation. It is described as follows.

A membrane separates an infinite, well stirred volume (the capillary) from a variable-volume interstitium. The membrane is described in a Kedem and Katchalsky phenomenological fashion with three independent parameters, L_p , σ , and ω , used to characterize its behavior. The state of the interstitium is characterized by the variables: C_i , P_i , N_i , and V_i where N_i is the total interstitial mass of protein and V_i is the total interstitial volume. It is described with a linear compliance:

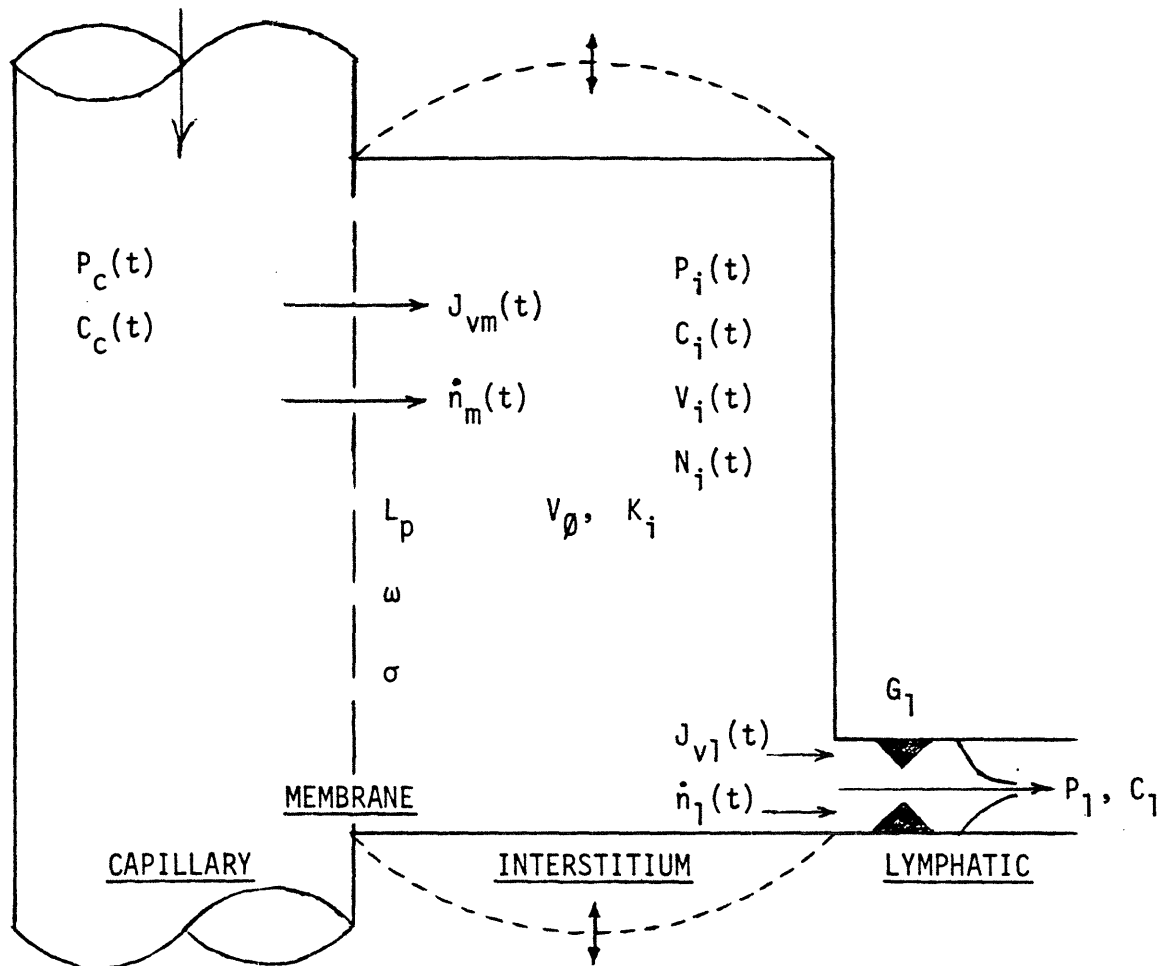
$$V_i = K_i P_i + V_\emptyset$$

where K_i and V_\emptyset determine the behavior of the interstitium. The interstitium is drained by a non-sieving lymphatic which is modeled as a linear resistance, with conductance G_1 , which separates the interstitium from a fixed pressure lymphatic "compartment" of pressure, P_1 . One-way valves are assumed to allow lymph flow in one direction only. This assumption is implemented in the model by setting G_1 equal to zero when $P_i < P_1$.

The transient system model is diagrammed in Figure 6-1. The nine equations which describe the behavior of the various components of the system are presented in Table 6-I. The membrane and lymphatic fluxes of the fluid and solute are not necessarily equal with the result that either accumulation or depletion of interstitial fluid and solute can occur. All nine variables in this formulation are considered to be functions of time. The nine equations can be condensed into two coupled differential equations in which the two remaining variables are V_i and N_i , the interstitial total volume and total solute. These two equations are presented in Table 6-II.

The terms in these two equations are labeled for reference. Term (A)

Figure 6-1: Diagram of Lung Water Transient Model



represents membrane flux of fluid caused by osmotic pressure forces and terms (B) and (C) represent fluid fluxes caused by hydrostatic pressure differences across the membrane and lymphatic respectively. Term (E) represents protein flux across the membrane caused by diffusion. Term (F) represents convection of protein across the membrane and term (G) represents protein convection into the lymphatic. Term (D) is a cross-coupling term between protein and fluid fluxes.

Table 6-I: Essentials of the Lung Water Transient ModelASSUMPTIONS:

1. Single solute
2. Interstitium is well stirred (lumped)
3. Kedem and Katchalsky equations describe the membrane
4. Lymph flow is governed by linear conductance, no sieving
5. Capillary pressure and composition are uniform
6. All system parameters are uniform

EQUATIONS:

$$J_{vm}(t) = L_p \left[(P_c - P_i) - \sigma (C_c - C_i) RT \right] \quad (1)$$

$$J_{vl}(t) = G_l (P_i - P_l) \quad (2)$$

$$\dot{n}_m(t) = J_{vm} (1-\sigma) \frac{C_c + C_i}{2} + \omega (C_c - C_i) \quad (3)$$

$$\dot{n}_l(t) = J_{vl} C_i \quad (4)$$

$$\frac{dV_i(t)}{dt} = J_{vm} - J_{vl} \quad (5)$$

$$\frac{dN_i(t)}{dt} = \dot{n}_m - \dot{n}_l \quad (6)$$

$$C_i(t) = N_i / V_i \quad (7)$$

$$V_i(t) = P_i K_i + V_\emptyset \quad (8)$$

OUTPUT VARIABLES AND STATE VARIABLES:

$$V_i, N_i, J_{vm}, J_{vl}, \dot{n}_m, \dot{n}_l, P_i, C_i, t$$

INTRINSIC PARAMETERS:

$$K_i, V_\emptyset, RT, L_p, G_l, \omega, \sigma, P_l$$

INPUT VARIABLES: P_c, C_c

Table 6-II: Differential Equations Representing Transient System Behavior

$$\frac{dV_i}{dt} = \underbrace{L_p \sigma RT \left(\frac{N_i}{V_i} - C_c \right)}_{(A)} + \underbrace{L_p \left(P_c - \frac{V_i - V_{\theta}}{K_i} \right)}_{(B)} - \underbrace{G_1 \left(\frac{V_i - V_{\theta}}{K_i} - P_1 \right)}_{(C)} \quad (6.1)$$

$$\frac{dN_i}{dt} = \underbrace{L_p \sigma RT \frac{(1-\sigma)}{2} \left(\left(\frac{N_i}{V_i} \right)^2 - C_c^2 \right)}_{(D)} + \underbrace{\omega \left(C_c - \frac{N_i}{V_i} \right)}_{(E)} \quad (6.2)$$

$$+ \underbrace{L_p \frac{(1-\sigma)}{2} \left(P_c - \frac{V_i - V_{\theta}}{K_i} \right) \left(C_c + \frac{N_i}{V_i} \right)}_{(F)} - \underbrace{G_1 \left(\frac{V_i - V_{\theta}}{K_i} - P_1 \right) \left(\frac{N_i}{V_i} \right)}_{(G)}$$

where $G_1 = \emptyset$ when $P_i < P_1$ and is positive otherwise

It should be noted that these two equations simplify, as expected, to a single steady-state equation of the same form as in Chapter 4 when the derivatives are set equal to zero.

V_i and N_i are used here as the two "output variables" of the system. The other system variables, particularly C_1 , J_{vm} , and J_{v1} can be found once V_i and N_i are obtained using the equations of Table 6-I. These represent "derived output variables".

There are three possible behaviors that can be exhibited by these two equations after a system change: the volume derivative may be larger than

the protein derivative, the volume derivative may be smaller than the protein derivative, or the two may be of comparable magnitude. With our model in this general form, it is not possible to state which of these three possibilities might be the case. To make such a statement, we need numerical information on the model's behavior.

6.2.2 Method for analyzing transient model equations

The two differential equations embodying our transient model are coupled and highly non-linear. An analytical solution was not found. In order to characterize the model, we solved the equations numerically at selected parameter values. The solutions were carried out on a Honeywell 680 digital computer operating under the Multics operating system. We made use of the D02BBF subroutine contained in the Numerical Algorithms Group (NAG) scientific subroutine package. This subroutine solves systems of ordinary differential equations using a variable order, variable step-size Runge-Kutta method. It adjusts the order and step size dynamically in order to obtain a specified precision with minimal number of steps.

The equations were used to predict system transient behavior in the following manner. Steady-state values of V_i and N_i were found using equation (4.1) of Chapter 4 and the normal physiological parameter set of Table 3-III. Then, starting the system with the derived steady-state values for V_i and N_i , one of the eight system parameters, P_c , C_c , L_p , ω , V_0 , K_i , or G_1 , was changed in a step fashion. In each case except for σ , the perturbed variable was changed from its normal value to a new value twice normal. σ is physically limited to a maximum of 1 but has a normal value of 0.85. It was perturbed by increasing its value to 1.1 times normal. The differential equations were then solved at 100 discrete

sequential time points spaced so as to span a total time period suitable for observing the time response of the system to this change. The results are values of V_i and N_i as functions of time. These were used, along with the equations in Table 6-1 to solve for the other system variables: C_i , J_{vm} , and J_{v1} .

6.2.3 System behavior predicted by the transient model

The results of these computations are presented in the form of figures in which each of the two model output variables, V_i and N_i , and the three derived output variables, C_i , J_{vm} , and J_{v1} , are plotted as functions of time. The plots are presented in a form scaled so as to fill the allocated space of the figure. A separate figure is used for each perturbed parameter. The four figures which represent the system's response to changes in either P_c , C_c , σ , or ω are presented as Figures 6-2 through 6-5. The figures which represent the system's response to changes in either L_p , G_1 , V_{θ} , or K_1 are presented as Figures 6-6 through 6-9.

Each of the first four figures illustrates slightly different system behavior. In the two figures representing the system's responses to step changes in P_c and σ , all of the fluid related variables, V_i , J_{vm} , and J_{v1} have a rapid initial change with a time constant on the order of minutes reaching a fairly constant final state. The protein related variables, N_i and C_i , have a much slower response on the order of hours. Note however that the changes in the fluid curves for P_c and σ are in the opposite direction whereas the changes in the protein related curves are in the same direction. In the ω step response curves, there is no initial rapid change in the fluid curves but all variables experience the slow change.

Figure 6-3: Transient System Response to a Step Increase in C_c

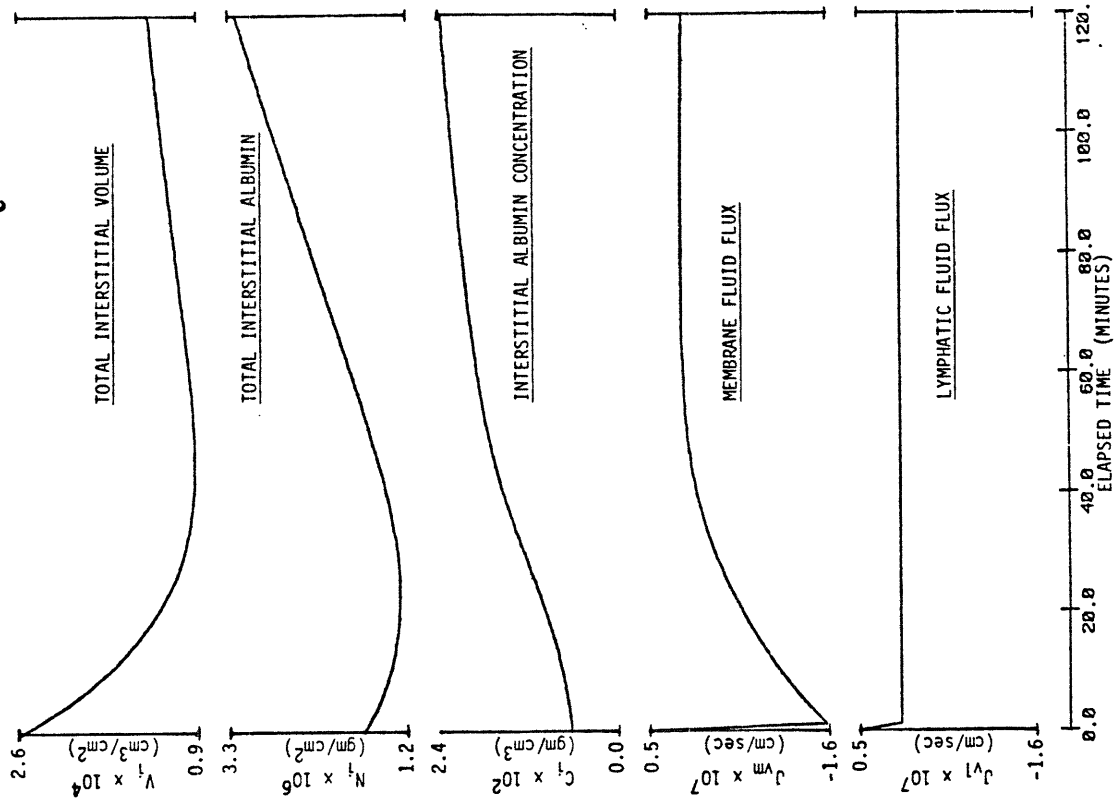


Figure 6-2: Transient System Response to a Step Increase in P_c

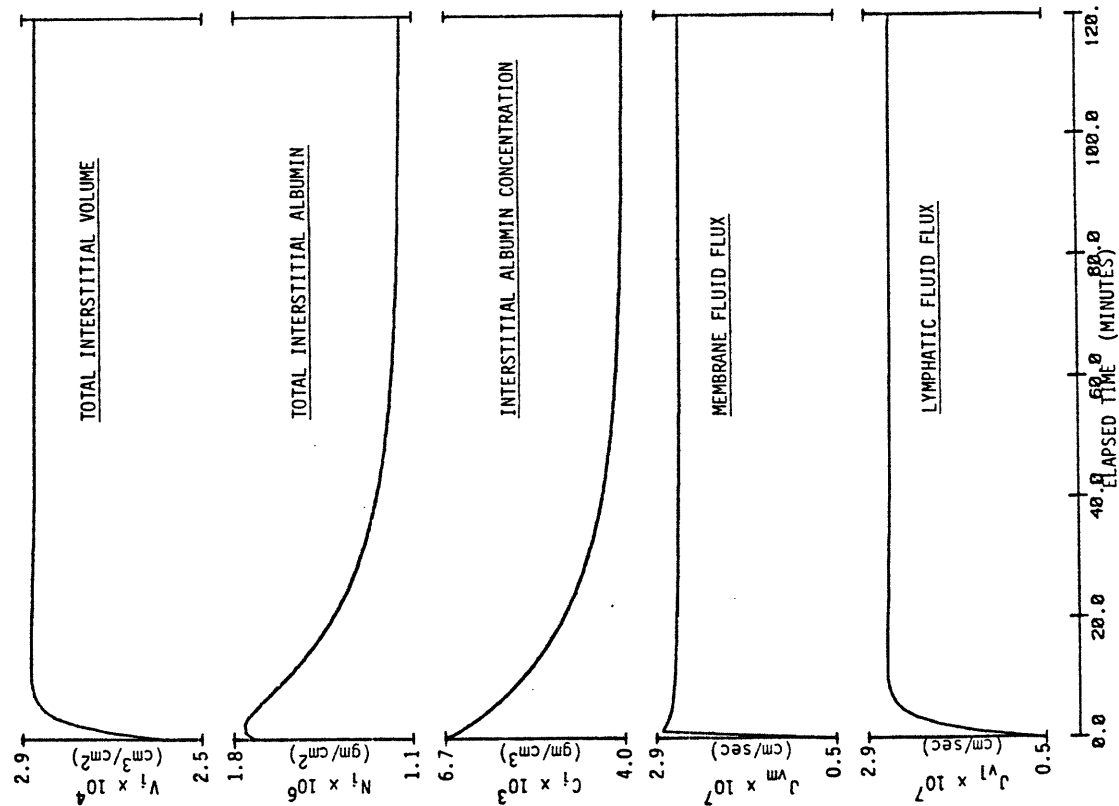


Figure 6-5: Transient System Response to a Step Increase in ω

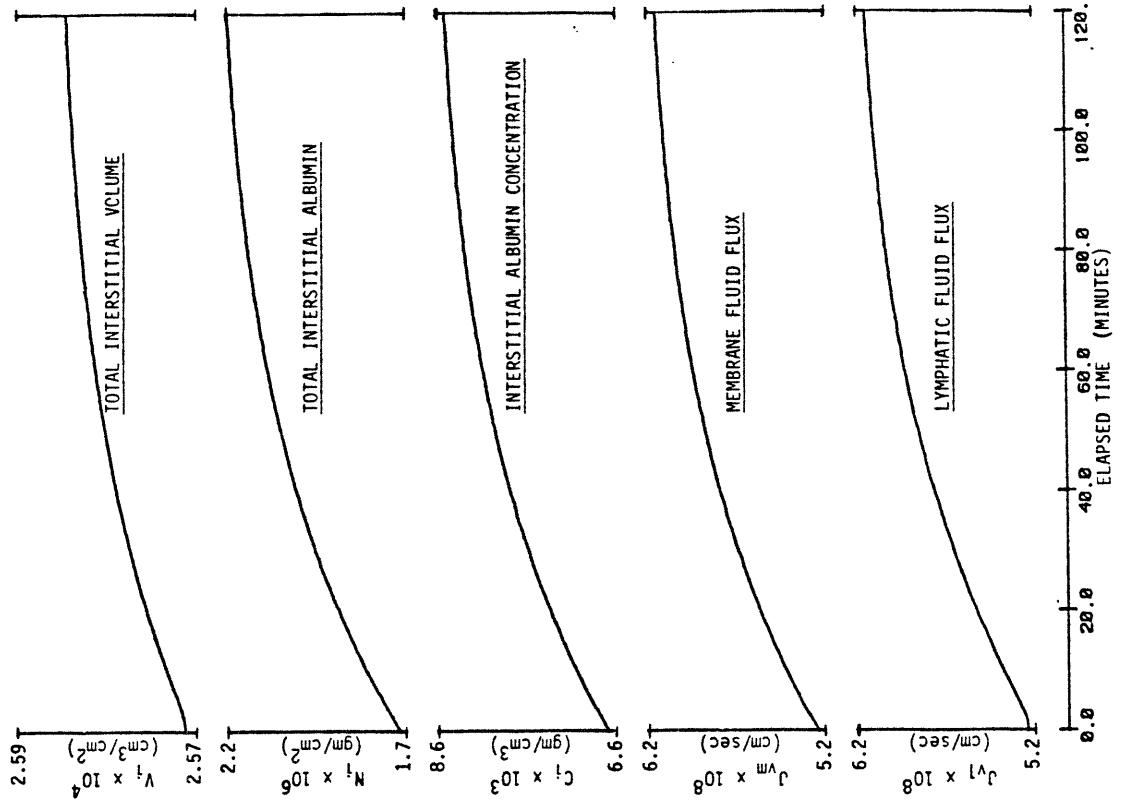


Figure 6-4: Transient System Response to a Step Increase in σ

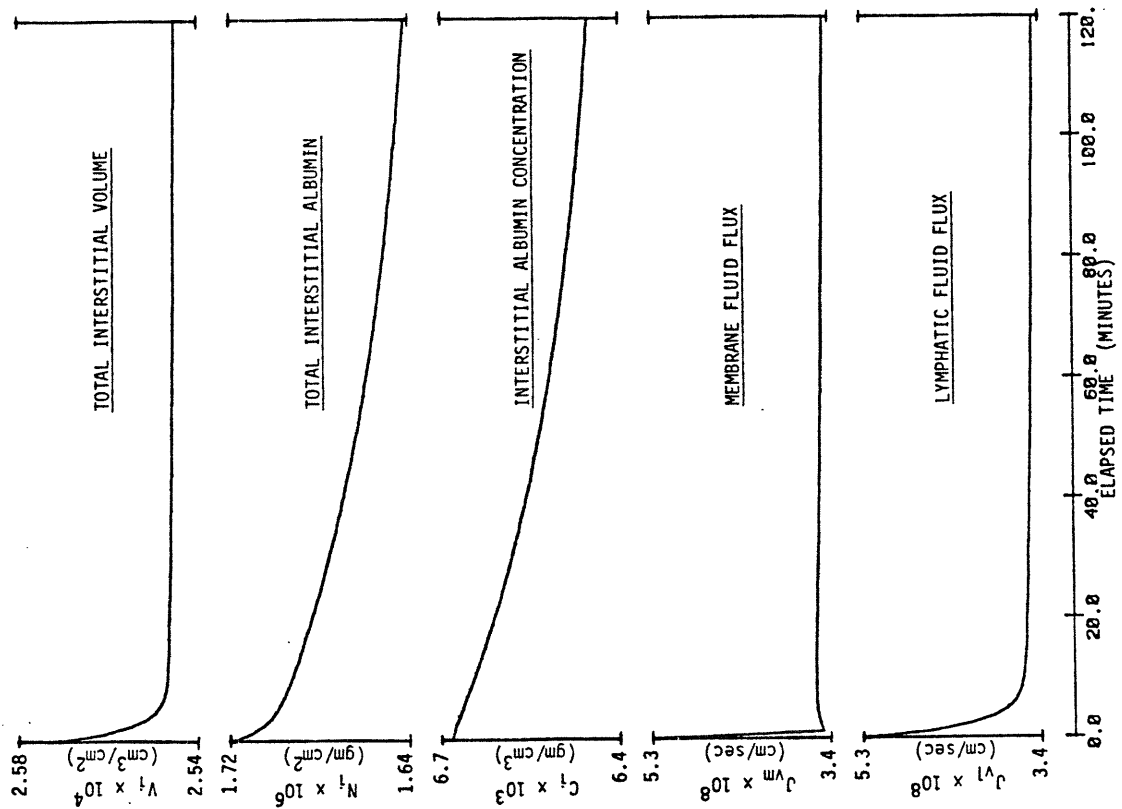


Figure 6-7: Transient System Response to a Step Increase in G_1

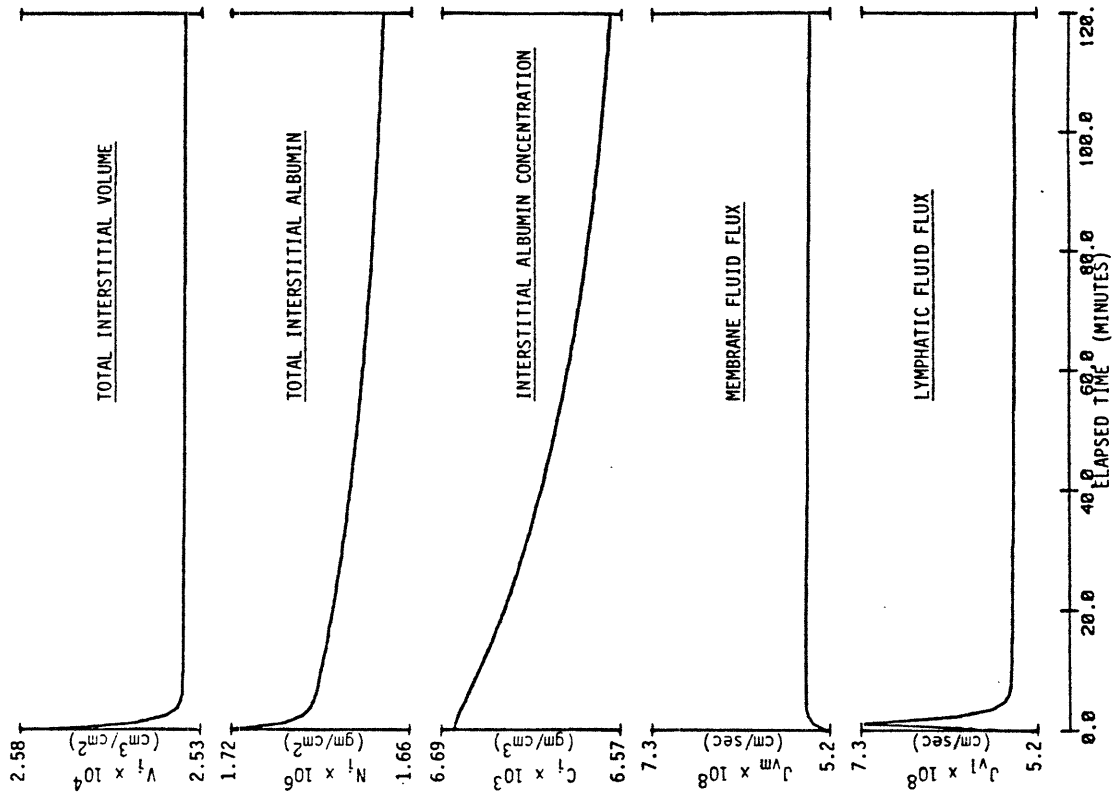


Figure 6-6: Transient System Response to a Step Increase in L_p

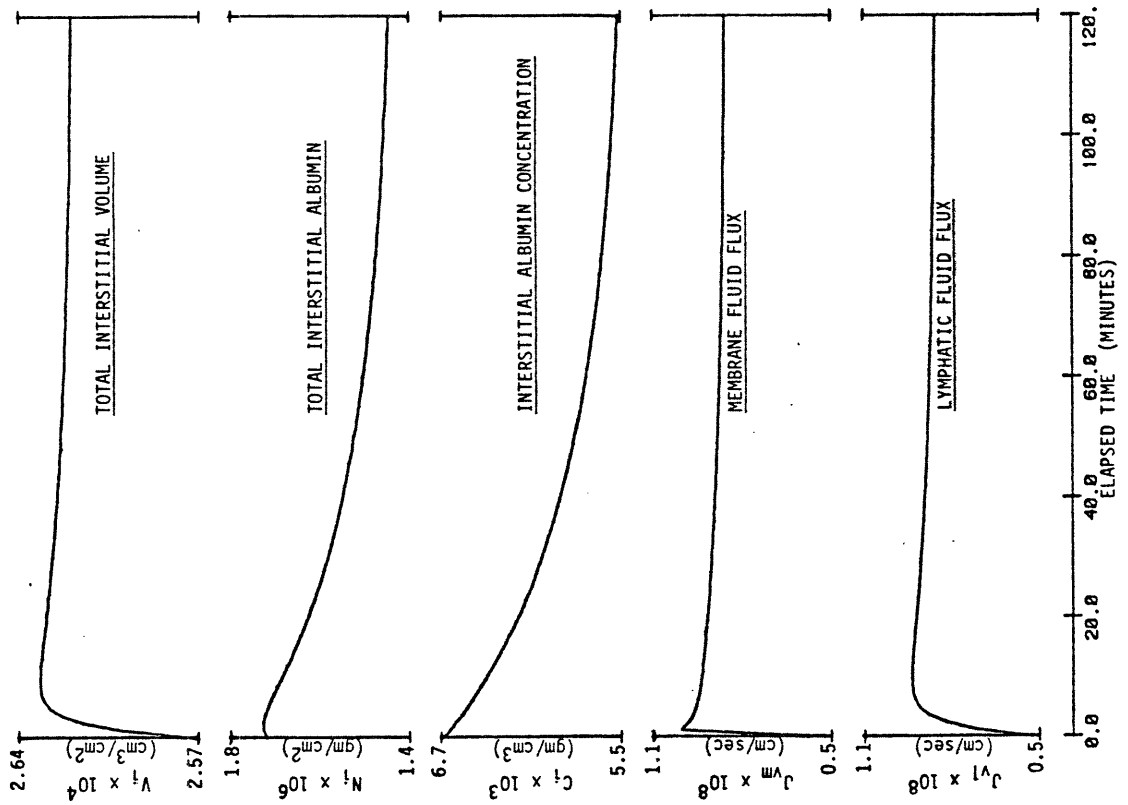


Figure 6-9: Transient System Response to a Step Increase in K_1

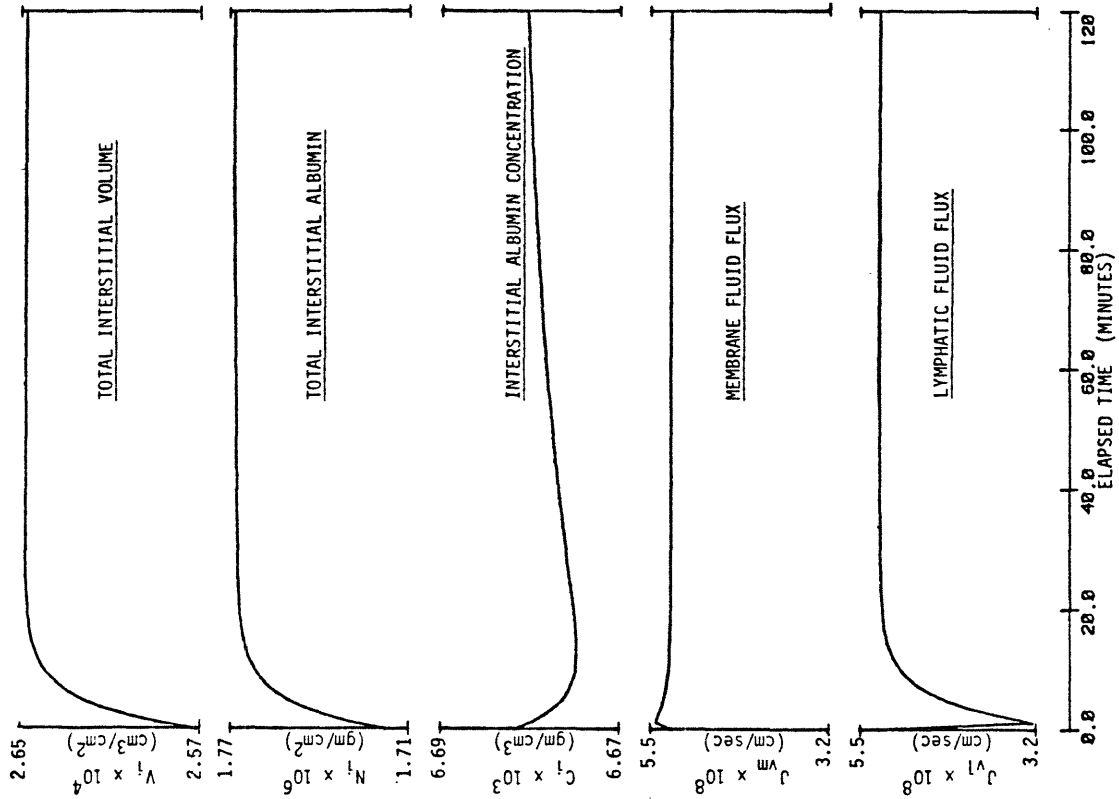
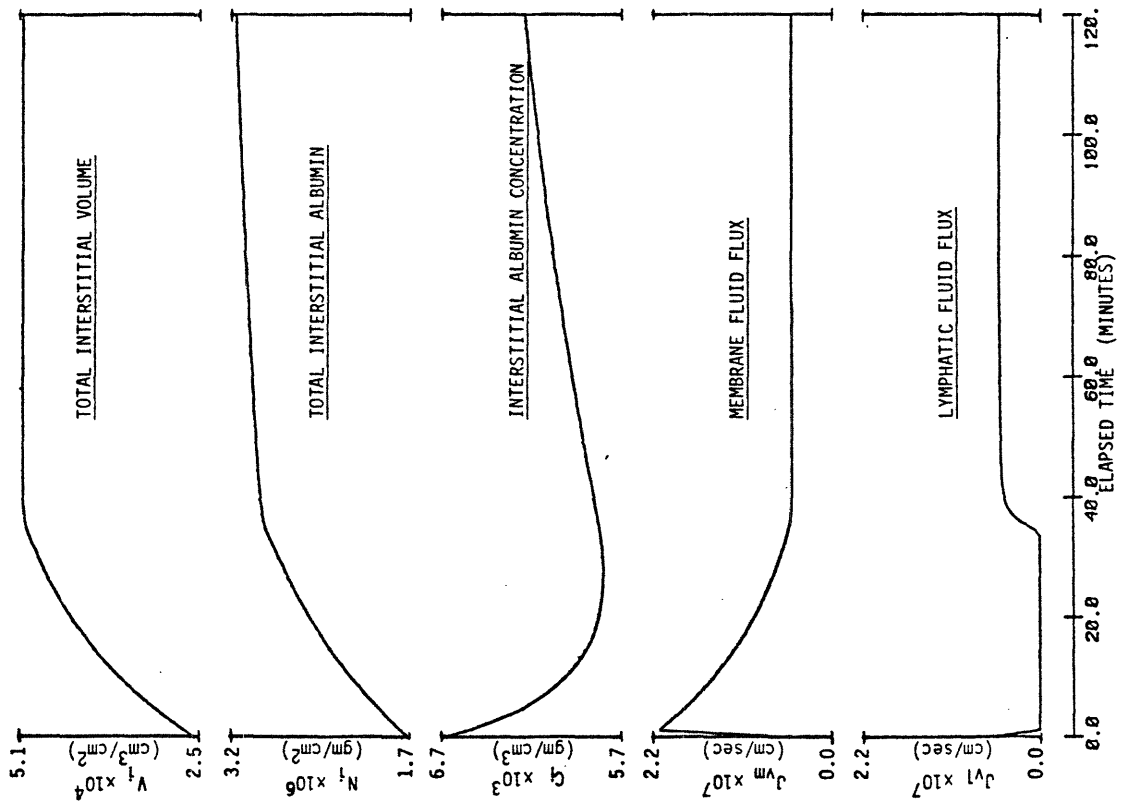


Figure 6-8: Transient System Response to a Step Increase in V_0



The behavior of the C_c step response curves are unlike any of the others. A key to explaining their behavior is noting that J_{v1} goes to and stays at zero for the entire time plotted. The other four curves change very slowly without the initial rapid changes in the fluid related curves.

Actually, although the magnitude of the initial change obscures it, there is a slow late-time change in the fluid related curves which parallels the protein curve changes. The plots for the other perturbed variables, V_{θ} , K_i , L_p , and G_1 , all show behaviors similar to those of the first four perturbed variables presented.

In summary, there appears to be three general types of behavior. When it occurs, the early time change in V_i , J_{vm} , and J_{v1} is very rapid. Almost universally there is a late-time slow change in all variables which is most obvious in the N_i and C_i curves. In the C_c curves, there is a greatly lengthened late time response to the change which is profoundly evident in all of the system variables. In the next section we present a detailed analysis of the three types of behavior just described. In the section following that, we present a qualitative description of the events that underlie the behavior exhibited in these figures.

6.3 Limiting Transient Behavior

We have just shown how three types of behavior are exhibited by our model of system transient behavior. Relating this to the differential equations, this behavior corresponds to the case of the volume derivative being much larger than the solute derivative. The two are fairly independent except in the intermediate time range. It might be expected that limiting case simplified models in which the two are assumed to be

independent might prove useful.

Our goal here is to create analytical expressions to describe the observed behavior. These expressions represent simplifications of the basic transient model using certain assumptions of limiting behavior. These models are useful in they make explicit the parameters of importance in determining the behavior occurring in various system operating regions.

6.3.1 Short-time limiting behavior

The first model describes the initial fast fluid response that occurs in many of the figures. The major assumption of this model is that, at small time, the transient contribution of protein can be ignored. The time for steady-state is simply the time it takes for V_i to reach a level at which J_{vm} equals J_{v1} . This assumption is the equivalent of setting the time derivative of N_i equal to zero. Only the time derivative of V_i is non-zero. This is given by equation (6.1), which is repeated here (with N_i/V_i replaced by C_i):

$$\frac{dV_i}{dt} = L_p \sigma RT (C_i - C_c) + L_p \left(P_c - \frac{V_i - V_0}{K_i} \right) - G_1 \left(\frac{V_i - V_0}{K_i} - P_1 \right) \quad (6.1)a$$

At sufficiently large time, additional changes in V_i are due to the changing protein process. For the simplified system in which protein is assumed constant, we define this large time as "steady state" such that $dV_i/dt = 0$. Solving this "steady state" equation for V_i , defining the result as $V_{i\infty}$, and substituting this into equation (6.1)a gives

$$\frac{dV_i}{dt} = - \frac{(L_p + G_1)}{K_i} [V_i - V_{i\infty}]$$

This is a simple linear differential equation whose solution is:

$$\frac{V_i - V_{i\infty}}{V_{i0} - V_{i\infty}} = \exp \left[- \frac{(L_p + G_1)}{K_i} t \right] \quad (6.3)$$

This model predicts a negative-exponential behavior for V_i after a perturbation which is governed by the time constant:

$$\tau = K_i / (L_p + G_1) \quad (6.4)$$

This time constant is the ratio between a capacitance (K_i) and an effective resistance ($L_p + G_1$) and determines how rapidly the interstitial volume can change. Note that anything that changes $V_{i\infty}$, i.e., changes in V_g , K_i , P_c , G_1 , L_p , or C_c , are predicted to produce this behavior.

This equation represents a convolution giving the systems response to a step change in the input variable, $V_{i\infty}$.

To test this model, we applied it to the P_c perturbation results given by Figure 6-1. A time constant was calculated for the initial part of the V_i curve using the values of V_i at $t=0$ and $t=72$ seconds and using the peak curve value to represent $V_{i\infty}$. The result was $\tau=129$ sec. This compares very well with the value of 133 sec predicted by our limiting model. The agreement was similarly close for the L_p , σ , G_1 , and K_i perturbation simulations.

6.3.2 Late-time limiting behavior

The second simplified model represents the late time behavior of the protein related curves in most of the figures. For this case, a reasonable limiting assumption is that V_i is constant. Interstitial protein content changes because of the difference in membrane and lymphatic albumin fluxes. This is described mathematically by:

$$\frac{dN_i}{dt} = n_m - n_l$$

Using the expressions in Table 6- and following the same general details as the above case gives a formula for the limiting late-time behavior of:

$$\frac{N_i - N_{i\infty}}{N_{i0} - N_{i\infty}} = \exp \left[- \frac{1}{V_i} \left(\frac{J_v(1 + \sigma)}{2} + \omega \right) t \right] \quad (6.5)$$

This model predicts a negative-exponential type transient behavior for N_i when $N_{i\infty}$ is changed. Such a change can be caused by changes in C_c , ω , σ , J_{vm} , or V_i . But, as already noted, V_i is influenced by changes in V_0 , K_i , P_c , G_1 , and L_p . Thus a perturbation in any system parameter will change $N_{i\infty}$ and potentially come under the domain of this model.

The time constant given by this model is:

$$\tau = \left\{ \frac{V_i}{J_{vm} \frac{(1 + \sigma)}{2} + \omega} \right\}$$

This expression is the ratio between the total capacity for protein (V_i) and the effective net flux of protein leaving the interstitium and represents the 'washout time' for protein from the interstitium. For the parameters used in our calculations, the ω term contributes less than 2% to the time constant. With this in mind, a reasonable approximation for the time constant is:

$$\tau = \frac{2 V_i}{J_{vm} (1 + \sigma)} \quad (6.6)$$

Calculating the time constant for the late portion of the N_i curve from the P_c perturbation curve set using data points at $t = 4320$ and $t = 5040$ sec gives a value for the time constant of $\tau = 1164$ sec. This is very close to the limiting model derived value of $\tau = 1206$ sec. Calculations of the late time constant for the ω , σ , G_1 , V_0 , and K_i cases are not quite as close giving differences of up to 30%. The problem is in

the existing complex interplay of water and protein dynamics. But, in spite of the lack of complete accuracy, this model still is useful in giving order of magnitude estimates of the rate of change of N_i (and C_i).

6.3.3 Late behavior after a change in C_c

As we stated above, the curves representing the system behavior after an increase in C_c behave differently from those of the other parameter perturbations. This difference is caused by the fact that the system is operating in the non-linear behavior region of G_1 . That is, over the entire range of the curves, J_{V1} is clamped to zero because flow is not allowed from the lymphatic into the interstitium. In the model representing this case, bulk flows are assumed to be so low that most of the protein is carried in by diffusion. The descriptive equation is:

$$\frac{dN_i}{dt} = \dot{n}_m = \omega (C_c - N_i/V_i)$$

The large time limiting value of N is given by:

$$N_{i\infty} = V_i C_c$$

Using this gives:

$$\frac{dN_i}{dt} = -\frac{\omega}{V_i} (N_i - N_{i\infty})$$

The solution to this is the equation we seek:

$$\frac{N_i - N_{i\infty}}{N_{i0} - N_{i\infty}} = \exp[-\omega/V_i t] \quad (6.7)$$

In this case, water follows protein into the interstitium. Thus the time behavior of water is the same as that of protein.

The time constant of this system is:

$$\tau = V_i/\omega. \quad (6.8)$$

This is the ratio between the total capacity for protein and the rate of protein entering the interstitium and represents the interstitial 'wash-in' time. Using data at $t=5040$ and $t=5760$ sec from the C_c perturbation curve gives a time constant value of $\tau = 18411$ sec. The limiting model predicts a value of $\tau=23460$ sec (using V_i defined at $t=5400$ sec). The error is not insignificant. The problem is that V_i is not by any means constant.

The agreement can be improved somewhat if V_i is made into a function of N_i . Two arbitrary possibilities for this dependence which were tested are $V_i=A+BN_i^2$ and $V_i=N_i/(A+BN_i)$. Coupling of V_i and N_i produces behavior that is not described well by a negative-exponential type time behavior. It is closer to being a linear function of time. However, if the objective is an expression to obtain an order of magnitude estimate of the response time and determine what parameters influence it, the original simple model should suffice.

6.4 Qualitative Description of Transient Events

6.4.1 Qualitative system response to P_c change

The figures of transient system behavior predicted by the model presented here can be used as a guide in understanding the physiological sequence of events that occur within the lung after a parameter change. Figure 6-2 represent a graphical description of the following sequence of events. Doubling P_c changes the Starling forces across the membrane and causes an instantaneous surge of fluid across the membrane (increased J_{vm}). This extra membrane flux causes a rise in interstitial volume, V_i , and the corresponding rise in P_i . The increase in P_i has the dual effects

of increasing the flux out of the interstitium into the lymphatic and decreasing the fluid flux in across the membrane. Both these actions have the effect of decreasing the rate of increase of V_i . Eventually, a new higher V_i is reached in which the higher J_{vm} is exactly offset by the higher J_{v1} . This total sequence of events happens in a period of minutes.

Initially, the increased membrane flow brings in large quantities of protein by convection. However, as lymphatic flow increases, a "washout" effect occurs in which the effective concentration of protein in the fluid entering the interstitium is less than the concentration of protein in the fluid leaving the interstitium. The interstitial protein concentration thus declines. The entering concentration is lower because the higher fluid flow causes increased convective transport of protein making the contribution of diffusive transport, which concentrates the interstitium, less important. The washout effect causes total interstitial protein and interstitial protein concentration to decline even in the face of an expanding volume. The washout effect occurs over a period of minutes to hours. The decline in C_i also upsets the membrane forces so that J_{vm} decreases slightly causing V_i to decrease. There is therefore an overshoot in the behavior of V_i in which there is the rapid initial rise directly related to the initial capillary pressure change followed by a slow decline brought on by the protein washout.

6.4.2 Qualitative system response to C_c change

Figure 6-3 represents the results of the step change in C_c and shows an entirely different behavior. The initial sudden change in C_i causes a change in the forces across the membrane leading to an instantaneous surge of fluid out of the interstitium into the capillary. This flux decreases

interstitial volume and thus P_i . It also causes the concentration of interstitial solute to increase because of membrane sieving. When the dropping P_i equals P_1 , the lymphatic flow stops (it is constrained from reversing direction). Eventually the combined effects of decreasing P_i and increasing interstitial osmotic pressure reduces the net force across the membrane to zero and membrane fluid flux stops.

The initial outwardly directed convective protein flux more than offsets the increased inwardly directed diffusive flux caused by the increased concentration gradient. The result is an initial net flux of protein out of the interstitium into the capillary. The convective protein transport stops when the fluid flow stops.

When membrane fluid flux stops, the only non-zero driving force in the system is the protein concentration gradient. Protein diffuses into the system. This upsets slightly the fluid forces so that water follows protein. But this water dilutes the interstitial protein maintaining much of the concentration gradient. Protein continues to enter the interstitium and water continues to follow until P_i again rises above P_1 permitting outwardly directed lymphatic flow to start. But note that, up until this point, it is the diffusion of protein that controls the rate of change of the whole system. This is a slow process meaning that the recovery from the initial C_c change is greatly prolonged. For the conditions of our simulations, the recovery is less than 25% complete at the end of 2 hours. The tight coupling of protein and water flows also means that the recovery is closer to being a linear function of time rather than the normal negative exponential function of time.

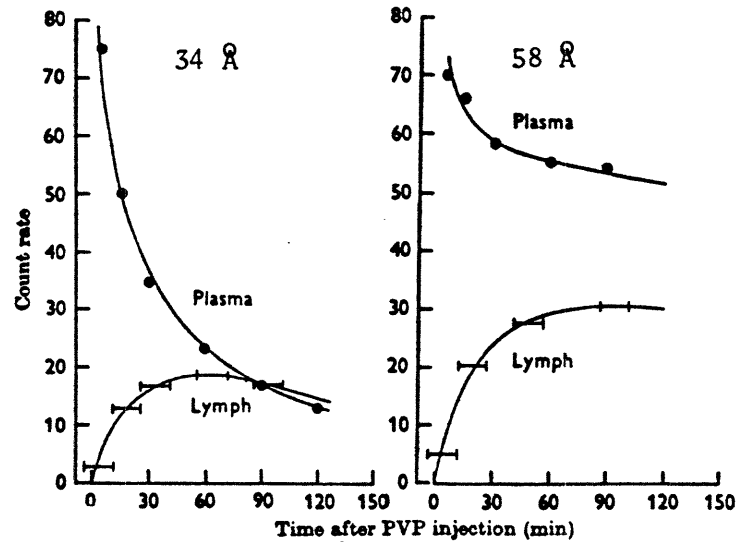
6.5 Relevant Experimental Data in the Literature

With our model, it is interesting that a system which has dimensions on the order of micrometers can have time constants ranging from minutes to hours. It must be emphasized that this behavior did not result from any sort of curve fitting. Unfortunately, although processes that occur over a period of hours might be experimentally observable, processes that occur over a period of minutes are too fast for any of the current means which make measurements on the lungs to detect.

A experiment relevant to the time behavior of protein was performed by Boyd et al. in 1969 [8]. They injected a mixture of various molecular sizes of the polymer, ^{125}I -labeled polyvinylpyrrolidone, intravenously into fetal sheep and followed the radiation counts of separated fractions from both plasma and lung lymph over time. Figure 6-10 contains the results obtained for particles of two different molecular radii, 34\AA and 58\AA (as determined by gel filtration). These results can be roughly compared to our results by noting that albumin has a molecular size on the order of 37\AA [3]. From Figure 6-10, it can be seen that Boyd obtained a time constant for the appearance of tracer in the lymph on the order of 20-40 minutes. This compares very well with the value we derived for the time constant of our protein curve of 20 minutes (1164 sec).

Experimental results relevant to the time course of fluid flow changes were presented by Staub in 1979 [93] and are repeated in Figure 6-11. This figure represents the results of a lymphatic cannulation experiment in which left atrial pressure was suddenly raised using a left atrial balloon. Lymph fraction were collected every 15 minutes. The lymph flow rate is seen to undergo a step change in just one collection

Figure 6-10: Experimental Time Behavior of Protein-Like Tracers
from Boyd 69 [8]



interval. This would be consistent with the time constant for fluid flow changes reported by us above of 129 seconds. The fact that no lymph flow rate change was seen in the first collection interval could be attributable to the delay that might occur between the time when lymph first enters the lymphatic system and the time when it reaches the collection catheter. Our model does not consider this delay. But the lymph flow rate is effectively at its steady-state value by the end of the second collection interval indicating that the water time constant must be significantly smaller than 15 minutes. Note also that the decrease in albumin shown in this figure occurs over a period of 30-60 minutes, once again comparable to our results.

These results are not necessarily representative of all lymphatic cannulation data. In many, particularly if the system perturbation is a

Figure 6-11: Experimental Transient Behavior of Fluid Flow
from Staub - 1979 [93]

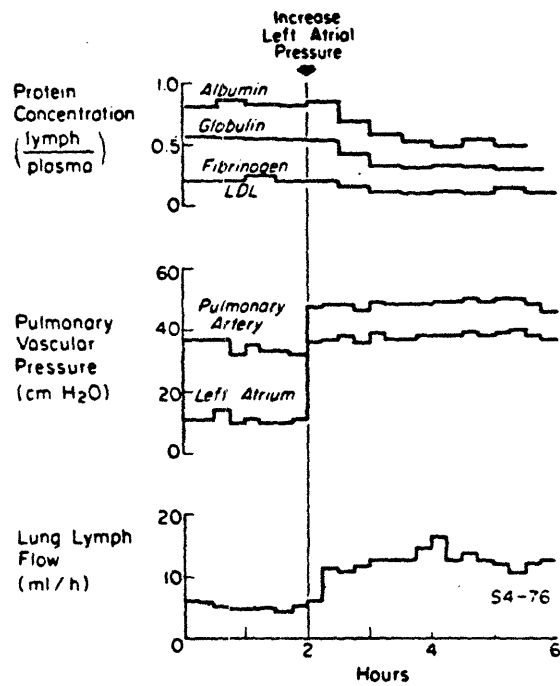


FIG. 4. Time course of lung lymph flow and L/P concentration ratios for 4 different plasma proteins in response to steady-state elevation of left atrial pressure in a conscious sheep. At all times, the L/P ratios for fibrinogen and low-density lipoprotein (LDL) were identical.

chemical insult such as histamine infusion, the flow change occurs over the period of minutes to hours. This increased length of the delay might be caused by the time it takes for the insult to change system parameters. However, it also should be noted that our model treats the lymphatic as a microscopic structure immediately adjacent to the interstitium whereas experimental results are obtained from the cannulation of a large lymphatic. Many potential delays can occur in the travel of fluid from the interstitium to the cannulation site.

6.6 Discussion: Implications of the Transient Model

6.6.1 Suitability of lumped system assumption

An important assumption made in creating our basic water dynamics model was that the system could be treated in a lumped fashion. We considered the implications of an axially distributed pressure in Chapter 5. We have not considered the validity of assuming a radially well-mixed interstitium. The major concern here is how the time for radial diffusion of albumin compares to the general transient behavior of the system.

An approximation for a time constant of diffusion is given by L^2/D where L is a characteristic distance and D is the solute diffusivity. The thickness of the interstitium is on the order of $10\mu\text{m}$ [103] and free albumin diffusivity has been given by Blake [5] as $9.3 \times 10^{-7} \text{ cm/sec}^2$. Using these values gives $L^2/D = 1.1 \text{ sec}$. Even admitting a smaller interstitial diffusivity because of the meshwork within the interstitium, the fact that the smallest time constant of our system is on the order of minutes means that radial equilibrium can be safely assumed.

6.6.2 Implications for the steady-state knee

The results presented in Chapter 4 show how in steady-state, the knee in the lung water function curve might relate to the various system parameters. Is the nature of this curve changed if the measurements are made before steady-state exists?

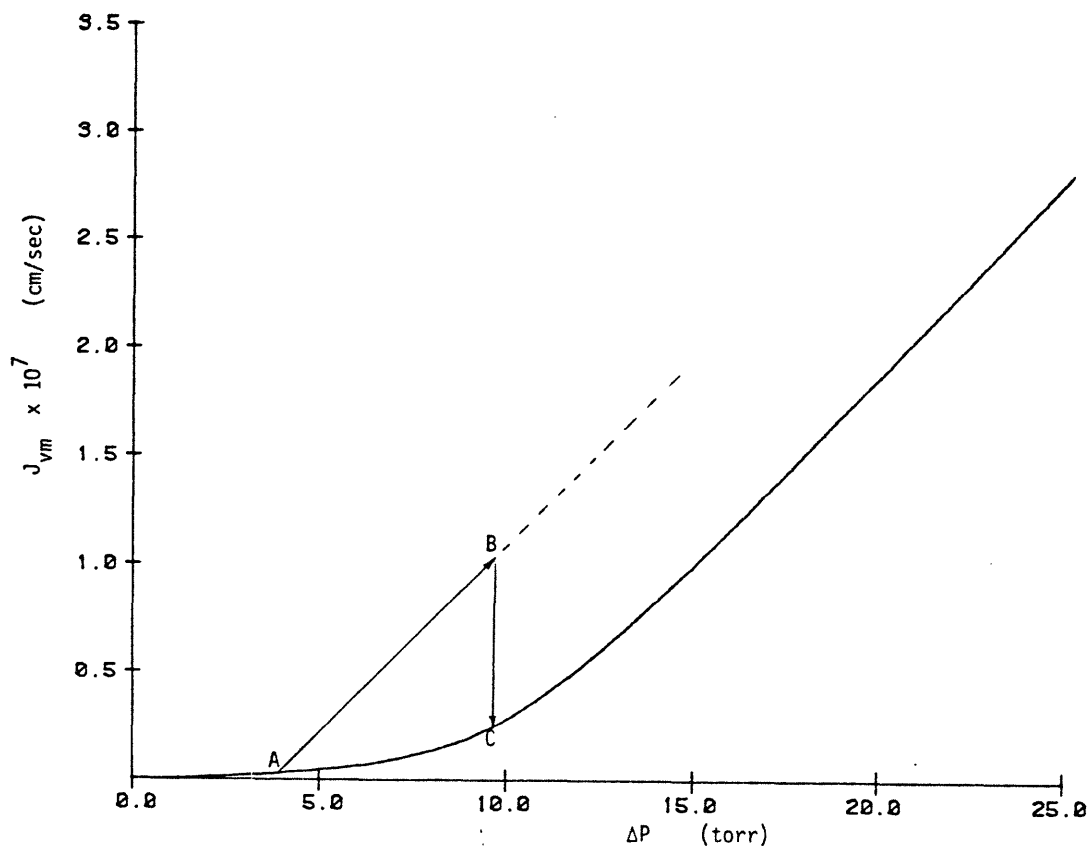
The material given in this chapter allows the connection to be made between this transient measurement and steady-state measurements. The steady-state protective effect is caused by any increase in capillary pressure being countered by a decrease in interstitial protein

concentration which prevents interstitial volume from rising as high as it otherwise might. Our model has shown that water changes tend to occur quickly and protein changes occur slowly.

Actually, the sudden inrush of fluid after a pressure increase brings with it fluid at a concentration very near the final steady-state interstitial concentration. But it takes time for the protein previously in the interstitium to wash out into the lymphatic. If the initial interstitial volume is large compared to the size of the short-time volume increase caused by the pressure change (which was the case in the transient model plots presented above), the time for onset of maximum protective effect is mainly a function of the washout time.

As a simplified approach, the time for initial volume changes can be considered to be governed by our short-time limiting equation and the time for onset of the protective effect governed by our long-time limiting equation. The relevance of the transient model to the steady-state lung water function curve is diagrammed in Figure 6-12. Assuming the system starts in the state represented by point (A), rapid changes in pressure would cause movement along line AB. As time passed, the system would move along line BC until eventually the steady state point (C) is reached. The effect is that measurements made after a pressure elevation but before steady-state exists would tend to underestimate the transition point pressure. That is, a lung water function curve created using such measurements would have a knee shifted to the left. In light of our time constant of 20 minutes for protein washout, a delay of 40 minutes between the time of pressure elevation and of lung water measurements should be sufficient to allow the assumption of steady-state.

Figure 6-12: Transient Behavior of Water Function Curve



6.6.3 Clinical implications

An observation having intriguing clinical implications concerns the behavior of the C_c perturbation study. Its clinical implications result because a typical treatment for acute edema is the administration of protein. Our model shows that, after a step increase in capillary protein concentration, there occurs a fairly rapid decrease in interstitial water followed by a very slow rise. Such a behavior is desirable because it provides an effective acute treatment and allows sufficient time to implement more chronic treatments such as diuresis.

But our limiting model shows that the length of effectiveness is highly dependent on ω . This dependence is, of course, evident on intuitive grounds. After all, if the membrane is highly leaky to protein, there would not be much use for a treatment that depends on the existence of a protein concentration difference. But our model shows that the recovery time is not dependent on L_p . Edema caused by increased permeability to water with no change in protein permeability would be a perfect candidate for this type of treatment.

A second clinical implication of this model concerns the issue discussed in the previous section. The protective effect was shown to be slow of onset. This would mean that sudden changes in pulmonary vascular pressure might be predicted to cause edema which would gradually decrease over a period of 20 minutes or so as the protein protective mechanism gradually came into play.

6.6.4 Characteristic system parameters

An observation from the model results presented above is that the response to a change in ω is far different from that caused by a change in L_p . This is significant because it shows once again that a single parameter or index may not be sufficient to describe the intrinsic state of the lungs. Pathologies that change one parameter may have a different time course than if they change the other. Further, the time course of reaction to changes such as an increase in P_c is affected differently depending on the values of the other system parameters. Thus, with our simple models, changes in ω have no effect on initial water transient and changes in G_1 have a second order effect (through J_{v1}) on the protein transients.

6.7 Summary

In this chapter we presented a model for lung water system transient behavior created by adding accumulation terms for water and protein to the basic steady-state lumped model of Chapter 4. This model was first characterized using a numerical solution with the results presented in the form of plots of the time sequence of system events after a step change in each of the various system parameters. These results were then used to direct the derivation of three simplified models for limiting behavior and were also compared to existing experimental data.

From this work, we conclude that the nature of the steady-state behavior predicted in previous chapters must be modified if measurements are made before steady-state is reached. Measurements made soon after a pressure increase would tend to produce a lung water function curve shifted to the left. Response times for changes in the various system parameters varied from minutes to hours with water tending to equilibrate quickly and protein taking much longer. The model predicts an interesting behavior for increased C_c where after an initial rapid water decline, equilibration to the much higher steady-state water volume is greatly prolonged by a period of hours. This has interesting clinical implications. This model also predicts that the transient response characteristics depend on L_p , ω , and σ in different ways indicating that a single parameter may not be sufficient to characterize the transient response of the lung water system.

This concludes our modeling. In the next chapter, we will discuss in detail the implications of this work in terms of measurements of lung water as well as provide an overall summary of our work.

Chapter 7

GENERAL DISCUSSION AND CONCLUSIONS

The work reported in this thesis started originally as an effort to measure "permeability" of the lung. Specifically, we were interested in using an indicator-dilution tracer technique to measure the 'PS' product (generalized permeability) in the lung and thereby differentiate between "high pressure edema" and "capillary leak" edema. In the course of this work, it became apparent that the term, "permeability", as used by lung physiologists is not a very well defined word. The term is used to refer to both water permeability as well as protein permeability. But more often, it has simply been used as a term to describe the water state of the lung.

It became clear that before any reasonable measurement of "permeability" could be devised, the concepts of lung water dynamics had to be more carefully defined. A better understanding of the system being measured was needed. The orientation of the thesis thus evolved into a study of the basic concepts of lung water dynamics.

An appropriate way to begin this concluding chapter is to restate the basic goals of our modeling effort. The two goals were to create a framework for interpreting measurements of the lung water state and to create a clinically oriented model of the pulmonary edema process. .

Reviewing, in the second chapter we presented general background and defined concepts needed for our modeling efforts. In Chapter 3, the framework for the basic model was assembled. In Chapters 4 and 5, we presented steady-state forms of the model and in Chapter 6, a transient

form. We conclude this thesis by discussing the appropriateness of the particular modeling approach taken and by reemphasizing the relevance of these models to measurements and to clinical utilization.

A topic that combines the issues of measurements, clinical relevance, and modeling is the topic of tracers. Tracers are the focus of the first section of this chapter. The second section focuses on the suitability of our modeling approach by considering both its important assumptions and possible alternate approaches. In the third section, we present some of the significant results and implications of our modeling efforts. Next we consider areas that are indicated for future study. Finally, we consider and summarize the major points of this thesis.

7.1 Tracers and Lung Water Dynamics

A clinically oriented model of lung water dynamics is of little use if it cannot be correlated to clinical situations. To serve such a purpose, one needs clinically practical measurements. Pulmonary lymphatic cannulation, discussed in previous chapters, is only appropriate for use with research animals. In searching for measurements that might be available for application in the clinical setting, the various uses of tracers stand out. Tracers provide the best promise for converting our lung water model from a research tool to an approach useful for improving patient care. In fact, as stated above, such measurements served as the initial impetus for this research. In this section, we discuss tracers in terms of our previous discussion of lung water and in terms of our lung water models.

7.1.1 The utilization of tracers

7.1.1.1 Tracer background

The behavior of a tracer itself is usually not of direct interest. Rather, its use is as a probe. One use is to assess the behavior of some particular molecule. For example, tritiated water is used as a tracer to determine total lung water. Tracers may also be used to assess the performance of some particular component of the system. As an example, labeled urea is used as a tracer to study the permeability characteristics of the capillary membrane [35].

No matter the protocol, the utilization of tracers remains the same. The tracer is added to the system and its observed behavior used to give information about the system.

There are problems in interpreting the meaning of a given tracer's behavior. While the interest may lie in measuring microscopic parameters, a tracer measurement is by its nature a macroscopic measurement. The tracer measurement not only involves some weighted average of the behavior of many functional subunits, but reflects the behavior of non-functional units as well. In the case of water dynamics, the blood distribution network, not considered in the water dynamics model, has a profound effect on indicator-dilution tracer behavior. Also, when using a tracer to study a system component, the tracer's behavior may be sensitive to more than one of the component's descriptive parameters. For example, a tracer used to evaluate capillary permeability may be sensitive both to capillary tracer permeability (ω_t) and to tracer reflection coefficient (σ_t).

7.1.1.2 The use of indices to characterize tracer behavior

Even a good tracer will be influenced by many factors other than just the parameter of interest. For this reason, one usually characterizes the tracer's behavior by deriving a quantity we call an index of function. The concept of indices is very important to tracer studies (as well as other biological measurements). An index is some quantity derivable from a measurement of tracer behavior that is felt to be correlated to the physical parameter of interest. As an example, the mean transit time of an indicator-dilution injection of tritiated water is used as an "index" of total lung water content.

Once found, there are two ways in which an index might be used. It might be used to derive a numerical value for the sought parameter. On the other hand, no attempt may be made to do further processing on the index. In this case it is used as a global assessment of the lung. Indices used for this purpose we term clinical indices. Through statistical studies, they are correlated with symptoms, diseases, optimal treatments, and expected outcome.

7.1.1.3 The use of models in tracer index interpretation

When trying to use a tracer index to extract a numerical value for a system parameter, some form of model must be employed. Such a model has two features: 1.) it predicts tracer behavior (and tracer index behavior) and 2.) it has the sought parameter as one of its model parameters. Of course there will be other parameters in the model. The model is utilized by an inversion procedure whereby, given the model output, the sought parameter which represents a model "input" is extracted.

7.1.2 Indicator-dilution: a tracer utilization example

Indicator-dilution provides a perfect example for demonstrating the concepts of tracer utilization. Urea is used as a tracer for measuring lung capillary "permeability". It is injected in a bolus fashion into the blood entering the lung. The concentration of urea is measured continuously in the outflow stream. The result of this procedure is a concentration versus time curve of urea which must then be correlated in some way with capillary "permeability".

There are many models that attempt to make this correlation. The most popular derives an index from the curve known as the tracer "extraction" which is formed from the ratio of urea concentration to the concentration of a vascular limited tracer. The model relates extraction to urea permeability through a simple approach that assumes an axially distributed capillary and an infinite interstitium [13].

A more complex approach is to solve the coupled partial differential equations that describe the axially distributed, radially lumped, finite interstitium volume Krogh model in which there is zero axial diffusion and infinite radial diffusion in both capillary and interstitium [80, 26, 108]. The solution is generally found for an impulse input and is of the form of a tracer concentration versus time curve. The permeability index is derived by fitting this solution to the data. Here the tracer index is implicit in the shape of the curve. The question in both this and the previous case is in how the derived index might be related to lung water dynamics. How are these indices related to the "propensity for water accumulation"?

7.1.3 Implications for lung water modeling

7.1.3.1 Tracers used to measure component properties

A common application of tracers, particularly of the indicator-dilution type, is to attach a value to membrane "permeability". One problem in this effort is in choosing a suitable model. The magnitude of this problem is attested to by the number of models, often contradictory, that have been developed to extract permeability from experimental tracer behavior. Unfortunately, there is often little basis for choosing one over another and no good way of testing the accuracy of any particular model.

A second issue is that the tracer used for membrane analysis is almost never one of the two substances of importance in lung water dynamics: water and protein. It is assumed that an index derived from the behavior of a tracer such as urea is sufficient to characterize the capillary membrane. Yet even the simplest Kedem and Katchalsky and pore models indicate the need for at least two characteristic parameters. Deriving a single "urea permeability" value is less than satisfactory if one needs to know both hydraulic permeability and protein permeability as is the case for lung water "intrinsic state" measurements.

7.1.3.2 Use of traces to assess system behavior

Often, the values derived from tracer behavior such as urea permeability are intended to be used as an assessment of lung water state. It is important to recognize the steps implicit in the act of employing a tracer-concentration curve to provide information about state of the lung water system. First, a tracer model is used to extract a component property from the tracer curve. Then a water model is used to interpret

this property in terms of lung water behavior. Two models are involved. Both need to be accurate. Some features may be common to both models. But other model features are unique to one or the other. For example, indicator-dilution analysis procedures universally employ distributed models because tracer concentration changes occur in the same time frame as capillary transit. Changes in water occur much more slowly and, as shown in chapter 5, can be reasonably treated with lumped models.

In applying tracer data to characterize the lung water system, both models must be accurate to obtain meaningful information. This fact restricts the usefulness of tracers as tools for validating our models. In effect, such usage would represent an attempt to simultaneously validate our model and the tracer model employed. It is partially for this reason that no attempt was made in this thesis to compare our model to tracer data.

An interesting outgrowth of this discussion is that, analyzing tracer data by deriving a component parameter value may not be the best way to utilize tracers for assessing lung water state. It might be better to abridge the middle step and use tracer data to derive values for system parameters which represent features common to both tracer and water behavior. Specifically, an appropriate application of tracers might be to directly derive values for the α , β , and γ parameters of Chapter 4 or even the dimensionless variables given in that chapter such as C^* . This possibility has not been considered by others. It is difficult to see how it might be accomplished but it certainly deserves exploration given the system parameter's simplifying nature.

7.2 Suitability of Our Modeling Approach

7.2.1 Alternate Approaches

There are two areas of alternative approaches to be considered. First one needs to consider whether the added complexity introduced by an integrated approach gives benefits that make it worth the effort. Secondly, one must consider the suitability of the specific way in which we implemented our model.

7.2.1.1 The integrated approach

The almost universally used approach is to explain lung water dynamics solely in terms of the capillary membrane. The advantages of taking an integrated approach are the following: First, and most importantly, only an integrated approach can hope to adequately treat a dynamic system. The various forces and membrane properties may be measured in a static situation but the lung is not a static system. Variations in one force tend to influence other forces and possibly the system parameters. One needs a systems approach to hope to understand how the various components interact.

Secondly, the water related behavior of the lungs can be complex at times. Models of the membrane have been becoming increasingly more complex to try to account for this behavior. However, if more than one component is included in the system, the complexity can be shared among them. Studying the complex system can then consist of studying its much less complex parts. Thirdly, although it is realized that the lung does not respond instantly to system changes, the membrane-only approach does not have the capability for demonstrating anything but instantaneous

behavior.

7.2.1.2 Model implementation: selection of components

Any model is a simplification of the real situation. As was made clear in the first three chapters, the physical lung is a complex structure. In creating our model, we elected to include the membrane, a volume, and a mechanism for draining the volume independently from the membrane. This approach neglected the multi-compartment structure of the lung. The interplay of these compartments could be a very important factor in lung water dynamics. More information is needed before a model considering this interplay can be selected as superior to ours. Specifically, experiments are needed to determine how the state variables of each compartment such as pressure and volume change in relationship to one another with general system changes.

Our model considers the behavior of a single subunit to be representative of the behavior of the whole lung. But it might be that the interplay of the functional subunits is a very important factor in lung water dynamics. Perhaps, for example, the interstitiums of adjacent subunits might interact (this is somewhat analogous to the two-segment case treated in Chapter 5). Certainly gravity is a factor, meaning that the subunits at the top of the lung behave differently from the subunits at the bottom of the lung. It is important to find out experimentally both how easy it is for adjacent functional subunits to interact and how the behavior of the individual subunits is weighted in making up the average behavior of the lung. This might possibly be done by looking at simultaneous behavior of different lobes.

7.2.1.3 Model implementation: characterization of components

We selected simple, physically reasonable models for the behavior of each of the components of our system. This was done with the realization that the behavior of the system model might have been different had we selected different component models. In some cases, a different choice would not have significantly affected our results. For example, the use of the pore model to describe the membrane would not have added anything other than to decrease the degrees of freedom of our system by one.

Other choices were more critical. Particularly critical was the choice of the model describing the behavior of the lymphatic. Perhaps the lymphatic has a much more active role in water dynamics than we credit it with. The lymphatic might even act as an active control element with sensors of interstitial pressure or volume modulating its function in more than a simple proportional relationship. The lymphatic might be sensitive to the past history of the interstitial water state. Such behavior would drastically modify the behavior of our system model. At this point there is not enough information to argue for one behavior over another. Experiments are needed both to see exactly what controls lymphatic pumping and to determine whether this might be an important mechanism for modulating the water state of the lungs.

7.3 Suggestions for Future Work

There are several areas that deserve more work. The most important relate to the lung water function curve. Work is needed to explore the relationship between our predicted lung water function curves and experimentally derived curves. It should be verified that experimental

curves do indeed agree well with the general shape of those predicted by our model. It should also be determined whether component parameter variations produce changes in the experimental curves similar to the changes predicted by our model. Both of these steps would insure the general usefulness of our approach.

The non-dimensional form of our model provides one point of orientation for experiments. This form predicts a fairly rigid structure for lung behavior which can be tested if the dimensionless variables can be derived. In practice, one would attempt to fit lung water function curve data to possible model curves by adjusting the three system parameters, α , β , and γ . The closeness of fit would be one test of the model. Perturbations on the system that change the experimental curve could then be used to determine the effect of such perturbations on each of the system parameters.

The Prichard model provides another point of orientation for experiments. The differences between the behavior predicted by their model and the behavior predicted by our model must be resolved. Such experiments would provide information on the relative importance of possible protective effects other than protein dilution. For example, their model indicates that changing L_p does not change the slope of the curve at high pressures. Such a result would only occur if the membrane resistance to water flow were not important at high pressures in which case lymphatic saturation may be a reality.

Other areas appropriate for future study can be divided into three major categories. The first category consists of studies designed to explore the proper basic structure for a lung water systems model. We

assumed a single compartment interstitium. It is not entirely clear that this is the right approach. It is difficult to see how one might experimentally explore the advisability of this assumption. But it is reasonable to make simple models which represent feasible behaviors of various multi-interstitial compartment models. Doing this would make a model that would agree more closely with observed anatomical structure than our model does.

The second additional category of potential areas of future work are studies of the appropriate models to be used to describe the behavior of individual system components. Particularly key here is to determine if another description of lymphatic behavior is reasonable and what type of system behavior such a description would predict. Some of these efforts could take the form of modeling. However, it is vital that existing data on the lymphatic be carefully scrutinized and possible new experiments formulated in order to settle the important question of whether the lymphatic provides an active or a passive role in lung water dynamics.

A third area for future study is in the area of measurements. The work of this thesis indicates that multiple parameters may be needed to characterize the water state of the lung. Tracers must be explored in greater detail to see whether, either by judicious selection of tracers or by improvements in tracer models, multiple lung indices can be extracted from lung tracer experiments. Work is also needed to more carefully define exactly how the derived tracer indices relate to the fundamental system physical parameters.

7.4 Significant Results and Implications of Our Model

7.4.1 General results

The important result of our lumped steady-state modeling effort is that we were able to define a simple model which nevertheless accurately predicts the two-part form of the lung water function curve. This curve represents the clinically appropriate method for conveying the lung water state. Based on our model, seven component parameters are needed to characterize the intrinsic water state of the lungs. But the model also showed that these can be condensed into a group of three parameters. This is still more than the single parameter used when the lung water state is characterized with a single "permeability" parameter. The inference is that a single measurement is not sufficient to characterize the water state of the lungs. The model can be condensed further into a dimensionless form. But in this case, the dimensionless parameter-variable combinations that represent the system's input and output may not be easily measured.

The shape of the lung water function curve can be adequately explained considering only the protein protective effect. No non-linear components are needed to explain the existence of the knee. Our transition region did occur, however, at a slightly lower pressure than that reported from experimental results. This difference might be explained by a positive lymphatic pressure, P_1 . It might also be explained by admitting that there is indeed non-linear behavior in either the interstitial compliance or the lymphatic pump.

Besides the three membrane parameters that exist in our model, there are four other parameters representing the state of the interstitium and

the lymphatic. A particularly important parameter turns out to be G_1 . It controls lung water directly through its control of P_i and indirectly by influencing J_v . Precious little is known about this parameter. Our model indicates that its measurement should be a top priority.

Our results shed some additional light on the lymphatic cannulation experiments. Interpreting data from such experiments by assuming that limiting high flux exists is most likely to be suitable when the animal is near normal conditions. Very little change is needed in either L_p or ω to extend the pressure at which limiting behavior can be assumed far beyond any physiologically obtainable pressure. Further, our two-segment modeling showed that conclusions based on analysis of cannulation data may be significantly in error if the system is not lumped.

Our transient modeling efforts showed that the time course for water volume and water flow changes is on the order of a couple of minutes whereas the time course of protein flow and concentration changes is on the order of 20 minutes. Measurements made after several hours can be reasonably said to be in steady-state, except after an infusion of protein which is treated as a special case. If steady-state is not yet reached when a "steady-state" measurement is made, erroneous conclusions might result in which the protective effect of protein is underestimated.

7.4.2 Clinical relevance

The lung water function curve shows explicitly how lung water responds to changes in pulmonary vascular pressure and our model shows how the lung water function curve responds to change in the system. It also shows that changes in component parameters can have quite different effects on the clinical edema state depending on the region of the curve

the system is operating. We showed that the clinical usefulness of the model does not depend on the condition that the underlying system is lumped. We showed that measurements made a fairly short time after a system change (>30 minutes) can usually be interpreted properly in terms of a steady-state description but measurement made before this time might underestimate the magnitude of the protein protective effect. We also showed that certain clinical treatments, such as plasma protein administration, may have their beneficial effects greatly prolonged.

Our model indicates that a single measurement is not sufficient to completely characterize the water state of the lung. In terms of component parameters, all seven influence the model and should be known. However, we showed that in the steady-state, three derived "system" parameters are sufficient to characterize the lung water function curve. This indicates that three measurements should be sufficient to characterize the water state of the lung: either α , β , and γ or some combination of the three. These relate directly to system behavior and thus can be measured by appropriate measurements made on the lung water behavior of the lung. The results of such measurements can be presented in condensed form by non-dimensionalizing the variables. In this case, all information can be presented in a single plot.

When a clinician talks about "permeability", he or she is usually talking about the general state of the capillary membrane. In our model, three parameters characterize the membrane and changes in each parameter has greatly different effects, both in the steady-state case and in the transient case. This has not been well considered by others. Staub admits that, theoretically, independent changes may occur in the membrane that have different effects on lung water. However he states that,

speaking practically, "all known permeability edemas cause an increase in both water and protein flow" [91]

We have the following response to this statement. First, while the membrane parameters may change simultaneously, the relative magnitudes of the changes may differ from disease to disease. Secondly, while L_p and ω are related to membrane surface area, σ is not. It would thus be easy to change independently two membrane parameters simply by changing membrane surface area. This could occur without membrane "permeability" changes. Finally, a person in severe permeability edema is always observed to have plenty of both protein and water in the interstitium making the issue of whether hydraulic or protein permeability change is greater a moot point. However, there is also clinical interest in the stages leading up to end-stage edema. In this case, the person may respond differently to treatment depending on whether a change in L_p or a change in ω is the primary defect. Here, it is useful to be able to differentiate between the two.

7.5 Conclusions

In this thesis, we set out to create a clinically oriented model to interpret water related measurements of the lung. The problem inherent in this effort has been that no similarly oriented model exists which could serve as a foundation for this work. The models of the lung that do exist have different orientations. We were thus forced to lay our own groundwork, not only providing the specific details used in the model, but also defining and creating the general concepts needed to interpret the model. The concepts of "lung water function curve", "propensity for water

accumulation'', and ''indices of intrinsic lung water function'' all appear for the first time in this thesis. The creation of this foundation and the definition of such concepts represents as much a contribution as the model itself.

As stated at the beginning of this chapter, the work reported by this thesis was initiated to provide a basis for measurements of ''permeability''. This task has been accomplished. Although all of the details of lung water dynamics are certainly not contained in our model, a reasonable foundation has been created. Lung physiologist and clinicians can now use this foundation both to organize thought concerning lung water and to guide the search for better lung measurements.

REFERENCES

- [1] Anderson, J.L. and J.A. Quinn.
Restricted transport in small pores: A model for steric exclusion and Hindered Particle Motion.
Biophys. J. 14:130-149, 1979.
- [2] Apelblat, A., A. Katzir-Katchalsky, and A. Silberberg.
A mathematical analysis of capillary-tissue fluid exchange.
Biorheology 11:1-49, 1974.
- [3] Bean, C.P.
The physic of porous membranes - neutral pores.
In G. Eisenman (editor), Membranes: Vol. I, Macroscopic Systems and Models, pages 1-54. Marcel Dekker, New York, 1972.
- [4] Bhattacharya, J. and N.C. Staub.
Direct measurement of microvascular pressure in the isolated perfused dog lung.
Science 210:327-328, 1980.
- [5] Blake, L.H. and N.C. Staub.
Pulmonary vascular transport in sheep: A mathematical model.
Microvas. Res. 12:197-220, 1976.
- [6] Blake, L.H.
Mathematical modeling of steady state fluid and protein exchange in lung.
In N.C. Staub (editor), Lung Water and Solute Exchange, pages 99-128. Marcel Dekker, New York, 1978.
- [7] Bloom, W. and D.W. Fawcett.
A Textbook of Histology.
W.B. Saunders, Philadelphia, 1975, pages 743-765, chapter 30.
- [8] Boyd, R.D.H., J.R. Hill, R.W. Humphreys, I.C.S. Normand, E.O.R. Reynolds, and L.B. Strang.
Permeability of lung capillary to macromolecules in foetal and newborn lambs and sheep.
J. Physiol (Lond.) 201:567-588, 1969.
- [9] Brigham, K.L., and J.D. Snell.
In vivo assessment of pulmonary vascular integrity in experimental pulmonary edema.
The J. of Clin. Invest. 52:2041-2052, 1973.
- [10] Brigham, K.L.
Lung edema due to increased vascular permeability.
In N.C. Staub (editor), Lung Water and Solute Exchange, pages 235-276. Marcel Dekker, New York, 1978.
- [11] Brigham, K.L.
Pulmonary edema: cardiac and noncardiac.
Amer. J. Surg 138:361-367, 1979.

- [12] Cobbold, A., B. Folkow, I. Kjellmer, and S. Mellander.
Nervous and local chemical control of pre-capillary sphincter in skeletal muscle as measured by changes in filtration coefficient.
Acta Physiol. Scand. 57:180-192, 1963.
- [13] Crone, C.
The permeability of capillaries in various organs as determined by use of the 'indicator dilution' method.
Acta Physiol. Scand. 58:292-305, 1963.
- [14] Crone, C.
Capillary permeability - techniques and problems.
In C. Crone and N.A. Lassen (editors), Capillary Permeability, pages 15-31. Academic Press, New York, 1970.
- [15] Deen, W.M.
Personal communication, 1982.
- [16] Diem, K., editor.
Documenta Geigy, Scientific Tables.
Geigy Pharmaceuticals, Ardsley, New York, 1962.
- [17] Erdmann, III, J.A., T.R. Vaughan, K.L. Brigham, W.C. Woolverton, and N.C. Stauv.
Effect of increased vascular pressure on lung fluid balance in unanesthetized sheep.
Circ. Res. 37:271, 1975.
- [18] Ferry, J.D.
Ultrafilter membranes and ultrafiltration.
Chem. Rev. 18(3):373, 1936.
- [19] Fishman, A.P.
Pulmonary edema: the water-exchanging function of the lung.
Circulation 46:390-408, 1972.
- [20] Fung, Y.C. and S.S. Sorbin.
Theory of sheet flow in lung alveoli.
J. Appl. Phys. 26:472-488, 1969.
- [21] Gaar, K.A., Jr., A.E. Taylor, L.J. Owens, and A.C. Guyton.
Effect of capillary pressure and plasma protein on development of pulmonary edema.
Am. J. Phys. 213(1):79-82, 1967.
- [22] Gehr, P., J.M.J. Bachofen, and E.R. Weibel.
The normal lung: ultrastructure and morphometric estimation of diffusion capacity.
Resp. Physiol. 32:121-140, 1978.
- [23] Gil, J.
Edema formation in the lung: Quantitative morphological methods.
Bull. Physio-path. Resp. 7:1075-1094, 1971.

- [24] Gil, J.
Lung interstitium, vascular and alveolar membranes.
In N.C. Staub (editor), Lung Water and Solute Exchange, pages 49-73.
Marcel Dekker, New York, 1978.
- [25] Gil, J. and J.M. McNiff.
Interstitial cells at the boundary between alveolar and
extra- alveolar connective tissue in the lungs.
J. Ultra. Res. 76(2):149-157, 1981.
- [26] Goresky, C.A., W.H.Ziegler, and G.G. Bach.
Capillary exchange modeling -- barrier-limited and flow-limited
distribution.
Circ. Res. 27:739-764, 1970.
- [27] Gump, F.E.
Lung fluid and solute compartments.
In N.C. Staub (editor), Lung Water and Solute Exchange, pages 75-95.
Marcel Dekker, New York, 1978.
- [28] Guntheroth W.G., D.L. Luchtel, and I. Kawabori.
Pulmonary microcirculation: Tubules rather than sheet and post.
J. Appl. Phys. 53(2):510-515, 1982.
- [29] Guyton, A.C., and A.W. Lindsey.
Effect of elevated left atrial pressure and decreased plasma
proteing concentration on the development of pulmonary edema.
Circ. Res. 7(7):649-657, 1959.
- [30] Guyton, A.C.
Textbook of Medical Physiology.
W.B. Saunders Company, Philadelphia, 1971.
- [31] Guyton, A.C., A.E. Taylor, and H.J. Harris.
Circulatory Physiology II: Dynamics and Control of the Body Fluids.
W.B. Saunders, Philadelphia, 1975, pages 73-74.
- [32] Guyton, A.C., A.E. Taylor, and H.J. Harris.
Circulatory Physiology II: Dynamics and Control of the Body Fluids.
W.B. Saunders, Philadelphia, 1975, pages 27-52.
- [33] Guyton, A.C. and B.J. Barber.
The energetics of lymph formation.
Lymphology 13:173-176, 1980.
- [34] Halmagyi, D.F.J.
Role of lymphatics in the genesis of 'shock lung': A hypothesis.
In N.C. Staub (editor), Lung Water and Solute Exchange, pages
423-436. Marcel Dekker, New York, 1978.

- [35] Harris, T.R., R.D. Rowlett, and K.L. Brigham.
The identification of pulmonary capillary permeability from multiple-indicator data: Effects of increased capillary pressure and alloxan treatment in the dog.
Microvasc. Res. 12:177-196, 1976.
- [36] Harris, T.H.
Lung microvascular permeability: transport theory and measurement methods.
In Cooney, D.O. (editor), Advances in Biomedical Engineering, Part 1, . Marcel Dekker, New York, 1980.
- [37] Harris, T.R. and R.J. Roselli.
A theoretical model of protein, fluid and small molecule transport in the lung.
J. Appl. Physiol. 50(1):1-14, 1981.
- [38] Haunso, S., W.P. Paaske, P. Sejrsen, and O. Amtorp.
Capillary permeability in canine myocardium as determined by bolus injection, residue detection.
Acta Physiol. Scand. 108:389-397, 1980.
- [39] Horsfield, K.
Morphometry of the small pulmonary arteries in man.
Circ. Res. 42(5):593-597, 1978.
- [40] Hughes, J.M.B., J.B. Glazier, J.E. Maloney and J.B. West.
Effect of extra-alveolar vessels on the distribution of blood flow in the dog lung.
J. Appl. Physiol. 25:462, 1968.
- [41] Iliff, L.D., R.E. Green, J.M.B. Hughes.
Effects of interstitial oedema on distribution of ventilation and perfusion in isolated lungs.
J. Appl. Physiol. 33, 1972.
- [42] Isselbacher, K.J., R.D. Adams, E. Braunwald, R.G. Petersdorf and, J.D. Wilson.
Harrison's Principles of Internal Medicine.
Mcgraw-Hill, New York, 1980, page A-2.
- [43] Iverson, P. and E.H. Johansen.
Pathogenese und Resorption von Trans- und Exudaten in der Pleura.
Klin. Wochenschr. 8:1311-1312, 1929.
- [44] Karliner, J.S.
Noncardiogenic forms of pulmonary edema.
Circulation 56:212-215, 1972.
- [45] Karnovsky, M.J.
The ultrastructural basis of capillary permeability studied with peroxidase as a tracer.
J. Cell. Biol. 35:213-236, 1967.

- [46] Karnovsky, M.J.
The ultrastructural basis of transcapillary exchange.
J. Gen. Physiol. 52:64s-95s, 1968.
- [47] Katchalsky, A. and P.F. Curran.
Nonequilibrium Thermodynamics in Biophysics.
Harvard Univ. Press, Cambridge, Ma., 1965.
- [48] Katz, M.A.
Capillary filtration measurement by strain gauge: II. Effects of
mannitol infusion.
Amer. J. Physiol. 232:H361-H367, 1977.
- [49] Katz, M.A.
Increased hydrostatic capillary pressure increases reflection
coefficient in canine hindquarters (abstract).
Microvasc. Res. 21:247, 1981.
- [50] Katz, M.A.
System analysis of vascular membrane water and protein transport:
General methods and application to canine hindquarters.
Microvasc. Res. 23:31-55, 1982.
- [51] Kedem, O. and A. Katchalsky.
Thermodynamic analysis of the permeability of biological membranes
to non-electrolytes.
Biochim. Biophys. Act. 27:229-246, 1958.
- [52] Kedem, O. and A. Katchalsky.
A physical interpretation of the phenomenological coefficients of
membrane permeability.
J. Gen. Physiol. 45:143-179, 1961.
- [53] Kedem, O. and A. Katchalsky.
Permeability of composite membranes. Part 1: Electric current,
volume flow, and flow of solute through membranes.
Trans. Faraday Soc. 59:1918-1930, 1963.
- [54] Kedem, O. and A. Katchalsky.
Permeability of composite membranes. Part 2: Parallel elements.
Trans. Faraday Soc. 59:1931-1940, 1963.
- [55] Kedem, O. and A. Katchalsky.
Permeability of Composite Membranes. Part 3: Series array of
elements.
Trans. Faraday Soc. 59:1941-1954, 1963.
- [56] Kirkwood, J.G.
Transport of ions through biological membranes from the
standpoint of irreversible thermodynamics.
In T. Clarke (editor), Ion Transport Across Membranes, pages 119.
Academic Press, New York, 1954.

- [57] Krogh, A.
The number and distribution of capillaries in muscles with calculations of the oxygen pressure head necessary for supplying the tissue.
J. Physiol. 52:391-415, 1919.
- [58] Laider, K.J. and K.E. Shuler.
The mechanisms and the kinetic laws for diffusion through membranes.
J. Chem. Phys. 17:851-857, 1949.
- [59] Landis M.E. and J.R. Pappenheimer.
Exchange of substances through capillary walls.
In W.F. Hamilton and P. Dow (editors), Handbook of Physiology, Sect. 2, Vol. 2: Circulation, chapter 29, pages 961-1034. Amer. Physiol. Society, Washington, 1963.
- [60] Lassen, N.A., H.H. Parving, and N. Rossing.
Filtration as the main mechanism of overall transcapillary protein escape from the plasma.
Microvasc. Res. 7:i-iv, 1974.
- [61] Laver, M.B. and W.G. Austen.
Disorders of the lungs, pleura, and chest wall: III. Lung function: physiologic considerations applicable to surgery.
In D.C. Sabiston Jr. (editor), Davis-Christopher Textbook of Surgery, chapter 55, pages 2019-2046. W.B. Saunders, Philadelphia', 1977.
- [62] Levitt, D.G.
General continuum analysis of transport through pores: 1. Proof of Onsager's reciprocity postulate for uniform pores.
Biophys. J. 15(6):553-563, 1975.
- [63] Low, F.N.
Lung Interstitium: Development, morphology, fluid content.
In N.C. Staub (editor), Lung Water and Solute Exchange, pages 17-48. Marcel Dekker, New York, 1978.
- [64] Miller, W.S.
The Lung.
Charles C. Thomas, Springfield, Ill., 1947.
- [65] Pappenheimer, J.R. and A. Soto-Rivera.
Effective osmotic pressure of the plasma proteins and other quantities associated with the capillary circulation in the hind limbs of cats and dogs.
Amer. J. Physiol. 152:471-491, 1948.
- [66] Pappenheimer J.R., E.M. Renkin, and L.M. Borrero.
Filtration, diffusion and molecular sieving through peripheral capillary membranes: A contribution to the pore theory of capillary permeability.
Amer. J. Physiol. 167:12-46, 1951.

- [67] Parker, R.E., R.J. Roselli, T.R. Harris, and K.L. Brigham.
Effects of graded increases in pulmonary vascular pressures on lung
fluid balance in unanesthetized sheep.
Circ. Res. 49:1164-1172, 1981.
- [68] Pearce, M.L. and M.J. Wong.
Interstitial pressure and compliance changes in experimental
pulmonary oedema in the dog.
In C. Giuntini (editor), Central Haemodynamics and Gas Exchange, .
Minerva Medica, Torino, Italy, 1971.
- [69] Perl, W.
Convection and permeation of albumin between plasma and
interstitium.
Microvas. Res. 10:83-94, 1975.
- [70] Pietra, G.G. and A.P. Fishman.
Bronchial edema.
In N.C. Staub (editor), Lung Water and Solute Exchange, pages
407-421. Marcel Dekker, New York, 1978.
- [71] Prichard, J.S., B. Rajagopalan, and G.de J. Lee.
Experimental and theoretical studies on the aetiology of adult
respiratory distress syndrome.
Herz 2(6):449-458, 1977.
- [72] Prockop, D.J.
Collagen, Elastin, and Proteoglycans: Matrix for fluid accumulation
in the lung.
In A.P. Fishman and E.M. Renkin (editors), Pulmonary Edema, pages
125-136. American Physiological Society, Bethesda, Maryland,
1979.
- [73] Reid, L.
Structural and functional reappraisal of the pulmonary artery
system.
The Sci. Basis of Med. Ann. Rev. 289-307, 1968.
- [74] Renkin, E.M.
Filtrations, diffusion, and molecular sieving through porous
cellulose membranes.
J. Gen. Physiol. 38:225-243, 1954.
- [75] Renkin, E.M.
Multiple pathways of capillary permeability.
Circ. Res. 41(6):735, 1977.
- [76] Renkin, E.M.
Lymph as a measure of the composition of interstitial fluid.
In A.P. Fishman and E.M. Renkin (editors), Pulmonary Edema, pages
145-159. Amer. Physiol. Society, Bethesda, Md., 1979.

- [77] Robin, E.D., C.E. Cross, and R. Zelis.
Pulmonary Edema (first of two parts).
New Engl. J. Med. 288(5):240-246, 1973.
- [78] Robin, E.D., C.E. Cross, and R. Zelis.
Pulmonary edema (second of two parts).
New Engl. J. Med. 288(6):292-304, 1973.
- [79] Salathe, E.P. and K.N. An.
A mathematical analysis of fluid movement across capillary walls.
Microvasc. Res. 11:1-23, 1976.
- [80] Sangren, W.C. and C.W. Sheppard.
Mathematical derivation of the exchange of a labeled substance
between a liquid flowing in a vessel and an external compartment.
Bull. Math. Biophys. 15:387, 1953.
- [81] Schmidt, G.W.
A mathematical theory of capillary exchange as a function of tissue
structure.
Bull. Math. Biophys. 14:229-263, 1952.
- [82] Schneeberger-Keeley, E.E. and M.J. Karnovsky.
The ultrastructural basis of alveolar-capillary membrane
permeability to peroxidase used as a tracer.
J. Cell Biol. 37:781-793, 1968.
- [83] Smaje, L., B.W. Zweifach, and M. Intaglietta.
Micropressure and capillary filtration coefficients in single
vessels of the cremaster muscle of the rat.
Microvasc. Res. 2:96-110, 1970.
- [84] Solomon, A.K.
Characterization of biological membranes by equivalent pores.
J. Gen. Physiol. 51:335-363s, 1968.
- [85] Spiegler, K.S.
Transport processes in ionic membranes.
Trans. Faraday Soc. 54:1408-1428, 1958.
- [86] Starling E.H.
The influence of mechanical factors on lymph production.
J. Physiol. 16:224-267, 1894.
- [87] Starling, E.H.
On the absorption of fluids from the connective tissue spaces.
J. Physiol. 19:312-326, 1895-96.
- [88] Staub, N.C.
Steady state pulmonary transvascular water filtration in
unanesthetized sheep.
Circ. Res. 28/29 (Suppl. 1):I-135-139, 1971.

- [89] Staub, N.C.
Pulmonary edema.
Physiol. Reviews 54(3):678, 1974.
- [90] Staub, N.C.
Panel Discussion of ion and water transport in lung.
In Porter, R. and M. O'Connor (editors), Lung Liquids - Ciba Foundation Symposium 38, . Elsevier-Excerpta Medical-North Holland, New York, 1976.
- [91] Staub, N.C.
Lung fluid and solute exchange.
In N.C. Staub (editor), Lung Water and Solute Exchange, pages 3-16.
Marcel Dekker, New York, 1978.
- [92] Staub, N.C.
Pulmonary edema due to increased microvascular permeability to fluid and protein.
Circ. Res. 43(2):143-151, 1978.
- [93] Staub, N.C.
Fluid accumulation in the lungs.
In A.P. Fishman and E.M. Renkin (editors), Pulmonary Edema, pages 113-124. American Physiological Society, Bethesda, Md., 1979.
- [94] Staub, N.C.
The pathogenesis of pulmonary edema.
Prog. in Card. Dis. 23(1):53-80, 1980.
- [95] Staverman, A.J.
The theory of measurement of osmotic pressure.
Rec. Trav. Chim 70:344, 1951.
- [96] Stedman.
Stedman's Medical Dictionary.
Williams and Wilkins Company, Baltimore, 1976.
- [97] Szidon, J.P., G.G. Pietra, and A.P. Fishman.
The alveolar-capillary membrane and pulmonary edema.
N. E. J. Med. 286:1200, 1972.
- [98] Taylor, A.T., D.N. Granger, and R.A. Brace.
Analysis of lymphatic protein flux data: I. Estimation of the reflection coefficient and permeability surface area product for total protein.
Microvasc. Res. 13:297-313, 1977.
- [99] Taylor, A.E. and R.E. Drake.
Fluid and protein movement across the pulmonary microcirculation.
In N.C. Staub (editor), Lung Water and Solute Exchange, pages 129-166. Marcel Dekker, New York, 1978.

- [100] Taylor, A.E.
Capillary fluid filtration: Starling forces and lymph flow.
Circ. Res. 49(3), 1981.
- [101] Warwick, R. and P.L. Williams.
Gray s Anatomy, 35th British Ed.
W.B. Saunders, Philadelphia, 1973, pages 1196-1204.
- [102] R.C. Weast, editor.
Handbook of Chemistry and Physics.
The Chemical Rubber Company, Cleveland, Ohio, 1971.
- [103] Weibel, E.R. and H. Bachofen.
Structural design of the alveolar septum and fluid exchange.
In A.P. Fishman and E.M. Renkin (editors), Pulmonary Edema, pages
1-20. American Physiological Society, Bethesda, Md., 1979.
- [104] F.M. White.
Fluid Mechanics.
McGraw Hill, New York, 1979.
- [105] Wolfe, W.G.
Disorders of the lungs, pleura, and chest wall: II. Anatomy.
In D.C. Sabiston Jr. (editor), Davis-Christopher Textbook of
Surgery, chapter 55, pages 2009-2018. W.B. Saunders,
Philadelphia", 1977.
- [106] Woolverton, W.C., K.L. Brigham, and N.C. Staub.
Effects of positive pressure breathing on lung lymph-flow and water
content in sheep.
Circ. Res. 42(4):550-557, 1978.
- [107] Zapol, W.M., M.T. Snider, and R.C. Schneider.
Extracorporeal membrane oxygenation for acute respiratory failure.
Anesthesiology 46(4), 1977.
- [108] Ziegler W.H. and C.A. Goresky.
Transcapillary exchange in the working left ventricle of the dog.
Circ. Res. 29:181-207, 1971.